A LABORATORY MODEL STUDY ON SETTLEMENT REDUCTION OF STONE COLUMNS IN SOFT CLAY

A THESIS SUBMITTED TO
THE GRADUATE SCHOOL OF NATURAL AND APPLIED SCIENCES
OF
MIDDLE EAST TECHNICAL UNIVERSITY

BY

MEHMET EMRAH SÜNNETCİOĞLU

IN PARTIAL FULFILLMENT OF THE REQUIREMENTS
FOR
THE DEGREE OF MASTER OF SCIENCE
IN
CIVIL ENGINEERING

AUGUST 2012

Approval of the thesis:

A LABORATORY MODEL STUDY ON SETTLEMENT REDUCTION OF STONE COLUMNS IN SOFT CLAY

submitted by **MEHMET EMRAH SÜNNETCİOĞLU** in partial fulfillment of the requirements for the degree of **Master of Science in Civil Engineering Department, Middle East Technical University** by,

Prof. Dr. Canan Özgen _____
Dean, Graduate School of **Natural and Applied Sciences**

Prof. Dr. Güney Özcebe _____
Head of Department, **Civil Engineering Dept., METU**

Prof. Dr. Mehmet Ufuk Ergun _____
Supervisor, **Civil Engineering Dept., METU**

Examining Committee Members:

Prof. Dr. Sadık Bakır _____
Civil Engineering Dept., METU

Prof. Dr. Mehmet Ufuk Ergun _____
Civil Engineering Dept., METU

Assist. Prof. Dr. Nejan Huvaj Sarıhan _____
Civil Engineering Dept., METU

Inst. Dr. N. Kartal Toker _____
Civil Engineering Dept., METU

A. Mengüç Ünver, M. Sc. Civil Engineer _____
ARGEM Geotechnical Eng. Consult. Co. Ltd.

Date: 16.08.2012

I hereby declare that all information in this document has been obtained and presented in accordance with academic rules and ethical conduct. I also declare that, as required by these rules and conduct, I have fully cited and referenced all material and results that are not original to this work.

Name, Last Name : MEHMET EMRAH SÜNNETCİOĞLU

Signature :

ABSTRACT

A LABORATORY MODEL STUDY ON SETTLEMENT REDUCTION EFFECT OF STONE COLUMNS IN SOFT CLAY

Sünnetcioğlu, Mehmet Emrah

M.Sc., Department of Civil Engineering

Supervisor: Prof. Dr. Mehmet Ufuk Ergun

August 2012, 177 pages

An experimental study was conducted in order to examine settlement reduction ratios of footing supported by both floating and end bearing type of stone columns. For the floating types, tests were done with varying column lengths of one and two widths of footing ($L = B, 2B$).

Tests were conducted in 200 mm* 200 mm* 200 mm cubic loading tanks. The reinforcement effect was achieved by the installation of four stone columns with 20 mm diameter under 70 mm* 70mm model footing. Parameters such as area replacement ratio (a_s), loading plate dimensions, consolidation and vertical pressures applied, and the relative density (D_R) of the granular column were kept constant, the column length (L) was set as the only variable in the experimental tests conducted. In the tests, footing settlements together with subsurface settlements at depths equal to footing width (B) and two times the footing width ($2B$) were measured by specially designed telltales.

The settlement reduction ratios both at surface and subsurface were evaluated in order to determine the effect of column length on settlement improvement. It has been found out that as the column length increases the settlement reduction ratios decrease for all depth intervals. However, there exists a threshold column length ($L = 2B$), beyond which the composite ground demonstrates little settlement improvement.

Keywords: Granular Column, Stone Column, Settlement Reduction Ratio, Model Study, Footing, Floating Column, End Bearing Column

ÖZ

YUMUŞAK KİLDE TAŞ KOLONLARIN OTURMA AZALTICI ETKİSİNİN LABORATUVAR MODEL ÇALIŞMALARI İLE İNCELENMESİ

Sünnetcioğlu, Mehmet Emrah

Yüksek Lisans, İnşaat Mühendisliği Bölümü

Tez Yöneticisi: Prof. Dr. Mehmet Ufuk Ergun

Ağustos 2012, 177 sayfa

Uç ve yüzen tip taş kolonlar tarafından desteklenen temellerin oturma azaltma oranlarını incelemek amacı ile deneysel bir çalışma gerçekleştirilmiştir. Yüzen tip taş kolonlar için, deneyler temel ve temel genişliğinin iki katına eşit kolon boylarında $(L = B, 2B)$ gerçekleştirilmiştir.

Deneyler, 200 mm* 200 mm* 200 mm boyutlarındaki kübik yükleme tanklarında gerçekleştirilmiştir. Güçlendirme etkisi 20 mm çapındaki dört adet taş kolonun, 70 mm* 70 mm model temel altına yüklenmesi ile elde edilmiştir. Alan değişim oranı (a_s), yükleme plakası boyutları, konsolidasyon yükü, temele uygulanan düşey basınç ve granüler kolonun relatif sıkılığı (D_R) gibi parametreler sabit tutulurken, deneysel testlerdeki tek değişken olarak kolon boyu (L) belirlenmiştir. Deneylerde temel oturmaları ile temel genişliğine (B) eşit ve temel genişliğinin iki katına eşit $(2B)$ derinliklerdeki yüzey altı oturmaları özel olarak tasarlanan oturma ölçme çubuklarıyla ölçülmüştür.

Kolon boyunun oturma iyileştirmesi üzerine olan etkisini belirleyebilmek amacıyla yüzey ve yüzey altı oturma azaltma oranları değerlendirilmiştir. Taş

kolon boyunun artırıldığı sürece oturma azaltma oranlarının tüm derinlik aralıklarında düştüğü gözlemlenmiştir. Ancak, kolon boyu için bir eşik değerinin $(L = 2B)$ bulunduğu ve bu değerden uzun kolon boylarında az oranda oturma iyileştirmesi elde edildiği görülmüştür.

Anahtar Kelimeler: Granüler Kolon, Taş Kolon, Oturma Azaltma Oranı, Model Çalışması, Temel, Yüzen Tip Taş Kolon, Uç Tipi Taş Kolon

To My Parents...

ACKNOWLEDGEMENTS

I would like to state that I am grateful to my advisor **Prof. Dr. Mehmet Ufuk ERGUN** for his contributions, support from the initial to final level, who influenced and reshaped my career, future plans and expectations by his perfectionism, motivation of achievement and positive reinforcements.

I would also like to thank to my teacher **Inst. Dr. Kartal TOKER** for his guidance in writing the experimental setup and test procedure chapter.

I owe my deepest graditute to my dear mom, **Zehra Sema SÜNNETÇİOĞLU** and to my dear dad, **Turhan SÜNNETÇİOĞLU** for their patience, endless support, interest and encouragement. This study could not be completed without you. I am so grateful to you.

I am also grateful to my dear aunt, **Seral LEVENTLER** for her encouragement, positive motivation and endless support in hard times.

I am indebted to my dear sister, **Hande KARAKAHYA** and my dear brother in-law, **Murat KARAKAHYA** for all their guidance and moral support. Thanks a lot for all the precious and meaningful times you allocated for me.

I would like to thank to my grandmother, **Hayriye UZUNOĞLU** for all her best wishes.

I am heartily thankful to my grandfather, **Abdullah UZUNOĞLU**. Rest in peace.

I would like to thank to **Mr. Ali BAL** and **Mr. Mustafa YALÇIN** for their assistance and help during experiments.

I would like to show my graditute to **Zeynep ÇEKİNMEZ** and **Davood TALEFIROUZ (Aydın)** for their help, support and great friendship.

I wish to thank to my friends, **Okan KÖKSALAN, Cemre YARDIM** for their support.

I would also like to thank to my brother **Tuğrul Cem BIÇAK** for his motivation.

I would also like to thank **Mr. Sina KİZİROĞLU**, chief of **Research and Development Department of General Directorate of Highways**, for supplying dial gauges.

I am also grateful to **Faik Usta**, **ERBAY MAKİNA** for manufacturing the cubic loading tanks, telltales, and pre-bored plates, and **Mutlu MERDİN**, **HIDRO MEGA** for the maintenance of the pneumatic system.

I would like to thank **KALE MADEN End. Ham. San. ve Tic. A.Ş.** for the provision of kaolin clay used in the experiments.

Finally, I would like to express my greatest gratitude to **MUSTAFA KEMAL ATATÜRK**, and **all the martyrs** for all the things they provide us.

TABLE OF CONTENTS

LIST OF FIGURES

FIGURES

LIST OF TABLES

TABLES

CHAPTER 1

INTRODUCTION

1.1 General

Barksdale and Bachus (1983) state that increasing value of land, increasing need to develop marginal land and increased cost of conventional design methods, post-construction maintenance expenses and environmental constraints make the ground improvement techniques even significant and economically feasible.

Van Impe (1989) points out that, ground improvement techniques were used even for the Babyloan temples, moreover wood, bamboo or straw were used by the Chinese for soil improvement more than 3000 years ago. Among all the ground improvement techniques the desired one must be chosen in order to solve the corresponding problem. These techniques can be listed as;

i) Piles

ii) Preloading

iii) Sand drains

iv) Replacing the soft soils

v) Jet Grouting

vi) Cement Grouting

vii) Compaction Grouting

viii) Soil fracturing

ix) Lime and lime/cement columns

x) In situ soil mixing

xi) Deep Vibro Techniques

xii) Dynamic compaction

xiii) Stone Columns

According to Moseley and Kirsch (2004), all these techniques aim to improve the related soil characteristics matching the desired results of a project. The proper selection of the ground improvement technique in the design at an early stage, reveals which foundation can be chosen and this often results in more economically feasible solutions. As a consequence of technological developments and increasing awareness of the economical and environmental benefits of these modern methods, ground improvement methods maintains its development.

Ambily (2007) states that out of these several improvement techniques available, stone columns have been widely used to increase the bearing capacity and to reduce consolidation settlements.

Stone column technique which is also called as vibro-replacement technique is a part of the vibratory compaction techniques. Priebe (1995) states that this widely used ground improvement technique improves the cohesive soil with the installation of load bearing columns made of coarse grained backfill material.

Ambily (2007) states that stone columns has successfully been used for the structures for low rise buildings, liquid storage tanks, earthen embankments, abutments, etc., which can tolerate relatively large settlements.

Shahu (2000) emphasizes that due to their higher strength and stiffness compared to the surrounding soft soil, granular columns, also called as sand columns or stone columns, takes on the greater portion of the vertically applied loads.

Stone Columns perform three functions;

i) Reduce settlements by reinforcing the soil

ii) Mobilize drag rapidly during initial stages of construction

iii) Acts as drains and accelerate construction (Datye, 1982)

The stone columns were first employed in Europe in the 1830s and have been used there extensively since the late 1950s. Bearing capacity increase of 150-300% values and settlement reduction of 30-80 % values were proven to be obtained by this ground improvement technique. (Priebe, 1995) Likewise, Bergado et. al (1984) found that the ultimate bearing capacity was to 3 to 4 times greater than that of the untreated ground.

Craig et. al. (1997) states that diameters of the stone and sand columns varies from 0.60 m to 2.0 m. When sand column piles are constructed on land, diameter values are usually less than 1.0 m, however if they are for reclamation purposes, diameters are larger with a spacing of 1.20 m to 3.0 m. Shahu and Reddy (2011) state that stone columns are usually constructed with particle sizes of D=25-50 mm and have diameters varying between d=0,6-1.0 m. Wood et al (2000) emphasizes that d/D ratio varies between 12-40.

The column diameter and the column spacing depends on the desired improvement, the method of installation and the sensitivity of the in situ soil. Square and the rectangular grid patterns with center-to-center spacing of 1.50 m to 3.50 m are used. (Munfakh et. al., 1987)

Juran et. al. (1991) emphasizes that area replacement ratio (as), the group effect, the mechanical properties of the granular column and the untreated soil, the loading process and rate, the radial drainage of the columns are several parameters affecting the bearing capacity and settlement behaviour of the improved soil.

1.2 Scope of the Study

Various settlement theories for settlement estimation of soils improved with granular columns have been proposed so far, most of which accept the unit cell concept. These methods are generally empirical, semi-empirical, analytical and moreover valid for end-bearing types of columns, except the method proposed by Priebe (2005).

In spite of the wide use of stone columns, scarce data are available on model tests on groups of floating stone columns. Hughes and Withers (1974) states that model tests in the past are applied to a single, end bearing column to represent unit cell behaviour.

Due to the above-mentioned reasons, this laboratory model study on the settlement reduction effect of stone columns in soft clay, aims to contribute to the settlement behavior of the treated soil with a group of both floating and end bearing types of stone columns. Four columns in a square pattern under square footing were used for the purpose of the improvement of the soil. A constant vertical pressure was applied to the footing. Both footing settlements and subsurface settlements at several depths along the columns were measured at constant time intervals. For the determination of the settlement reduction effect of granular columns, tests were also applied to the unimproved soil, moreover

the corresponding subsurface and footing settlements were measured also for these tests.

CHAPTER 2

LITERATURE REVIEW

2.1 Introduction

Studies have done so far show that stone column installation as a ground improvement technique has been successfully applied to increase the bearing capacity, to reduce the total and differential settlements, to reduce the liquefaction potential of sands, to increase the slope stability and to increase the consolidation rate of settlement. Among all the other techniques granular columns are widely used and preferred due to economical considerations. Ambily et. Al., 2007)

Datye (1982) represents the methods of installation of stone columns in three main groups;

i) Vibro compaction by wet process using vibroflot equipment which compacts by vibrations in horizontal direction.

ii) Vibro compaction using powerful vibrators attached to the casing with a bottom flap, the vibrations being in vertical direction.

iii) Stone and sand placed in cased boreholes and compacted by a heavy hammer.

Figure 2.1, Figure 2.2, and Figure 2.3 show typical construction procedures.

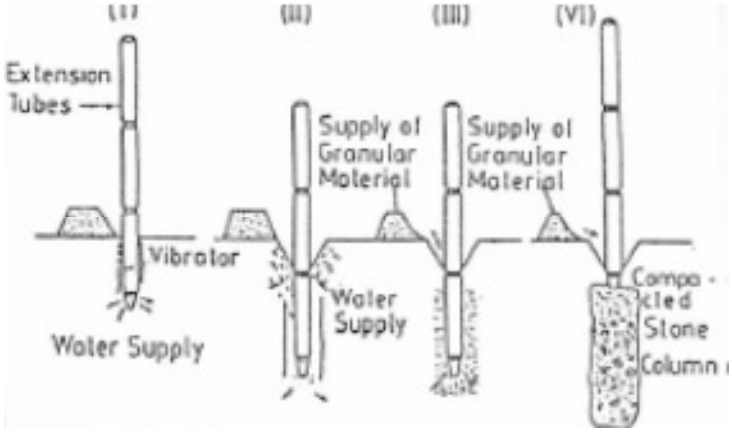

Figure 2.1 Vibroflotation Equipment and Process (Datye, 1982)

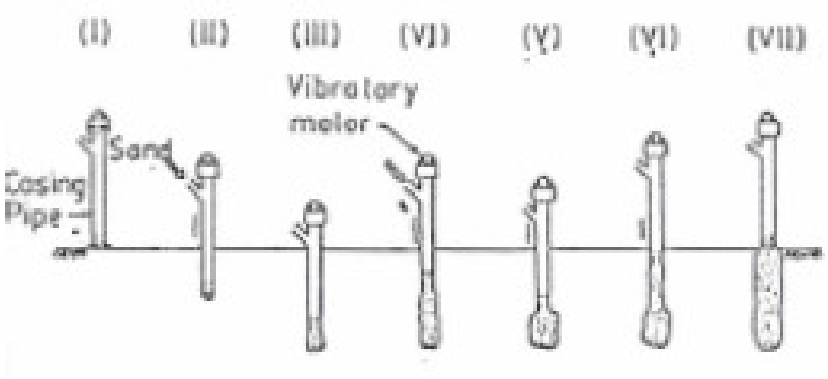

Figure 2.2 Construction of compaction piles by the composer system (Datye, 1982)

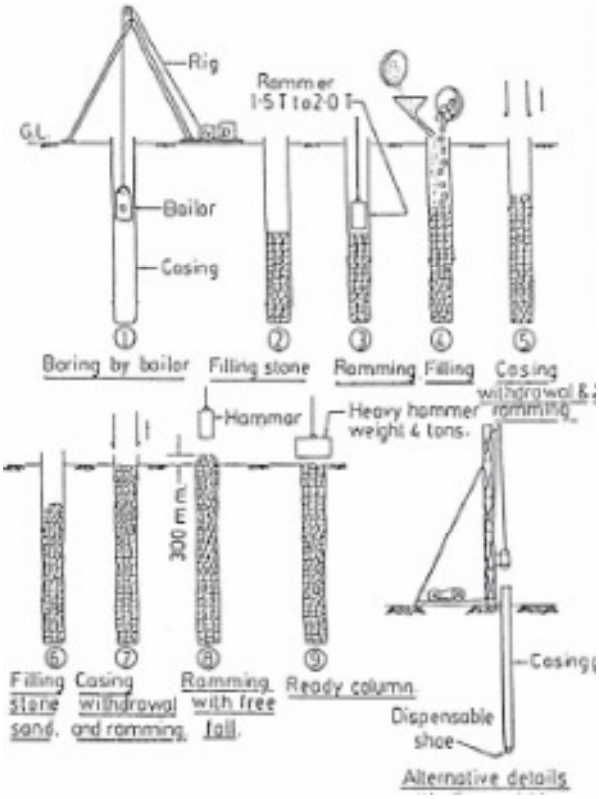

Figure 2.3 Installation methods stone columns through cased bore holes (Datye, 1982)

2.1.1 Situations Where The Use of Stone Columns Is Advantageous

Datye (1982) states that one of the most beneficial property of stone columns is their adaptation potential to the load which prevents the failure of the foundation. Moreover, the drainage paths, the stone columns provide accelerates the consolidation process and the drag forces on columns act immediately.

Datye (1982) emphasizes that in order to realize the efficiency of stone columns, it is vital to use structural systems which can compensate the predicted settlements.

Stone columns consisting of compacted granular material in long cylindrical holes provide economical solutions for low-rise buildings, liquid storage tanks, abutments, embankments, where relatively large settlements are permissible. (Shahu, 2011)

Datye (1982) considers that the use of stone columns with pre-load fills leads to more economical solutions, since the final factor of safety would be very high.

Stone column method is largely used in thick soft clay deposits where strength and consolidation characteristics are critical. (Ambily, 2007)

2.2 Comparison of Stone Column, Pile Foundation, Lime Column and Preloading

Due to its ability to adapt to the applied load, i.e. the ability to release the stress when deforming, the stone columns are more advantageous than pile foundations. In addition to this, stone columns can be much shorter than pile foundations, since stone columns can be made floating which allows the sufficient load transfer. In areas where pile foundations are subjected to negative skin friction, stone column alternative would be more favorable since the foundation over stone columns can bear large drag forces without failure. (Datye, 1982)

Since the stone columns act as drainage path, the lime column system may not consolidate as fast as the stone column system. However, the availability of

equipments affects the economy of lime columns or deep mixing methods. The stone column installation can be done by equipments which can be used for other operations, whereas special equipments needed for lime column installation. Another drawback is the need of suitable gradation for lime. (Datye, 1982)

The availability of the fill material, difficulty of imposing the required vertical stress for small areas, time availability are the major disadvantages of conventional preloading method when compared to stone column method. (Datye, 1982)

2.3 Applicability Criteria Of Stone Column

The main feature to estimate the compactibility is the grain size distribution of the soil and particularly the content of fines. Figure 2.4 shows a grain size diagram with a shaded zone. (Priebe, 1993)

Priebe (2005) stated that within the guidelines published in 1976 by German Institution Forschungsgesellsshaft für das Straßenwesen for the application of deep vibratory compaction techniques, this method was restricted to soils with a shear strength, c_u, of at least 15kN/m^2 to 25kN/m^2.

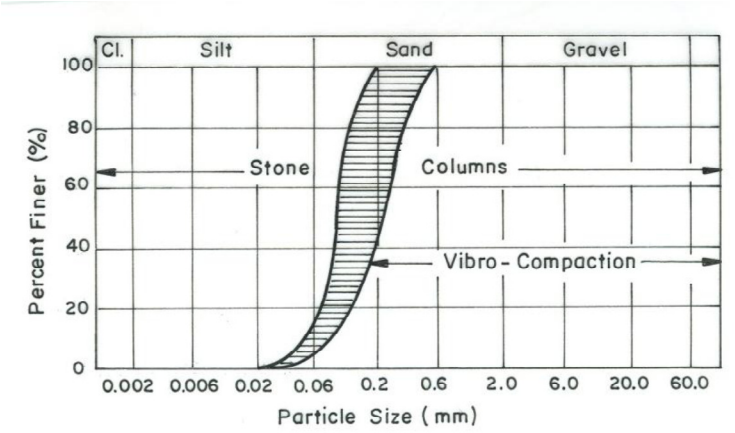

Figure 2.4 Application ranges of deep vibratory compaction technique (Priebe, 1993)

2.4 Unit Cell Idealization

2.4.1 Equivalent Diameter

Bachus and Barksdale (1983) state that for the simplicity of settlement and stability analyses, association of stone column and tributary area of surrounding soft soil is useful. (Figs. 2.5, 2.6) Bachus and Barksdale (1983) also state that approximation of equivalent circle with same total area can be done even if the tributary area of hexagonal shape.

For an equilateral triangular pattern of stone columns the equivalent circle has an effective diameter of;

$$De = 1.05\, s \qquad (2.1)$$

And for a square grid;

$$De = 1.13\ s \tag{2.2}$$

Where;

s: spacing of the columns

The resulting equivalent cylinder of material having a diameter D_e enclosing the tributary soil and one column is known as the *unit cell*. (Bachus and Barksdale, 1983)

2.4.2 Area Replacement Ratio

Area replacement ratio is defined by Barksdale and Bachus (1983) as the fraction of soil tributary to the stone column replaced by the stone:

$$a_s = \frac{A_s}{A} \tag{2.3}$$

Where;

$a_{s:}$ area replacement ratio

$A_{s:}$ area of the stone column

A: the total area within the unit cell

The area replacement ratio, a_s, can be expressed in terms of the diameter and spacing of the stone columns as follows:

$$a_s = C_1 \left(\frac{D}{s}\right)^2 \tag{2.4}$$

Where:

D: diameter of the compacted stone column

S: center-to-center spacing of the stone columns

C_1: a constant dependent upon the pattern of stone columns used; for a square pattern $C_1 = \pi/4$ and for an equilateral triangular pattern $C_1 = \pi/(2\sqrt{3})$.

For an equilateral triangular pattern of stone columns the area replacement ratio is then;

$$A_s = 0.907 \left(\frac{D}{s}\right)^2 \tag{2.5}$$

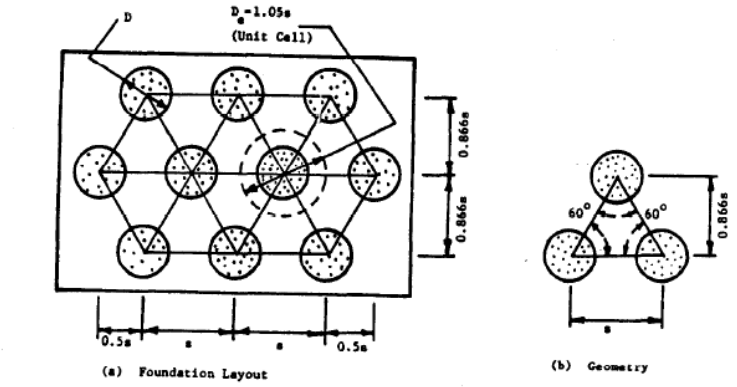

Figure 2.5 Equilateral triangular pattern of stone columns (Barksdale and Bachus, 1983)

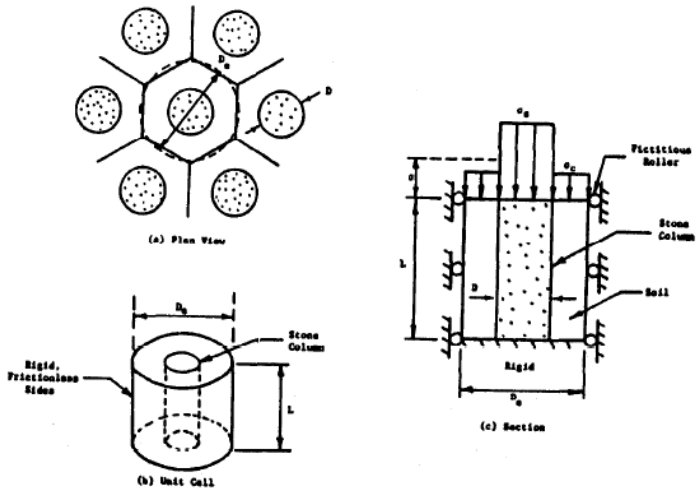

Figure 2.6 Unit cell idealization (Barksdale and Bachus, 1983)

2.4.3 Extended Unit Cell Concept

Many settlement theories discussed in this review assumes the unit cell concept to be valid.

Barksdale and Bachus (1983) state that each individual column may be treated as unit cell by the assumption of an infinitely large group of stone columns uniformly loaded over the area. Barksdale and Bachus (1983) also state that lateral deformations are not permitted across unit cell boundaries and the shear stresses on the outside boundaries, due to the symmetry of load and geometry. In consideration of these assumptions Barksdale and Bachus (1983) emphasize that uniform vertical loading applied over the unit cell must stay on inside the unit cell, however the stress distribution within the unit cell between the granular column and the surrounding soil changes with depth.

The unit cell can be physically modeled as a cylindrical-shaped container having a frictionless, rigid exterior wall symmetrically located around the stone column. (Fig. 2.6c) (Barksdale and Bachus,1983)

2.4.4 Stress Concentration Ratio

Barksdale and Bachus (1983) state that due to the higher stiffness of the granular column the vertical stress applied concentrates on the column. Moreover, the vertical settlement of the stone column and surrounding soil is assumed approximately to be the same.

Stress concentration factor, n is defined as;

$$n = \frac{\sigma_s}{\sigma_c} \tag{2.6}$$

where:

σ_s: stress in the stone column

σ_c : stress in the surrounding cohesive soil

For the equilibrium of vertical forces within the unit cell the average stress σ equals:

$$\sigma = \sigma_s * a_s + \sigma_c (1 - a_s) \quad (2.7)$$

$$\sigma_c = \frac{\sigma}{[1 + (n-1)a_s]} = \mu_c \sigma \quad (2.8)$$

and

$$\sigma_s = n\sigma[1 + (n-1)a_s] = \mu_s \sigma \quad (2.9)$$

where

μ_c : ratio of stress in the clay

μ_s : ratio of stress in the stone column

σ= average stress over the tributary area

Barksdale and Bachus (1983) state that these formulations (2.8 & 2.9) can be valid to determine the stresses in the clay and the stone column if a reasonable stress concentration factor is assumed based on previous measurements.

Barksdale and Bachus (1983) state that for both settlement and stability analyses the above mentioned equations are enormously helpful.

The assumptions made in the derivation of these equations are:

- The extended unit cell concept is valid,
- Statics is satisfied,
- The value of stress concentration is either known or can be estimated. (Barksdale and Bachus, 1983)

Barksdale and Bachus (1983) state that even for the cases where the extended unit cell concept is not valid, the equations 2.8 & 2.9 appears to give satisfactory results, probably because the vertical stress changes slightly with the horizontal distance. The accuracy of this approach is directly related to the number of stone columns in the group. Barksdale and Bachus (1983) also emphasize that the accuracy of this approach decreases when the number of stone columns decrease.

2.5 Settlement of the Composite Ground

2.5.1 Settlement Reduction Ratio

The settlement reduction ratio is defined as; (Bergado et.al., 1991)

$$\beta = \frac{S_t}{S_0} \tag{2.10}$$

Where;

S_t: Settlement of the composite ground

S_0: Settlement of the unimproved ground

The settlement reduction ratio is also expressed as a function of the area replacement ratio, a_s, angle of internal friction of the granular materials, φ_s, stress concentration factor, n and etc. Fig 2.7 shows relationships between the settlement reduction ratio and the aforementioned parameters based on different methods. (Bergado et al., 1991)

According to the equilibrium method, the settlement estimation, S, of the composite ground is ;

$$S = m_v * (\mu_c * \sigma) * H \tag{2.11}$$

Where;

m_v: modulus of volume compressibility

H : thickness of layer

Whereas the settlement S_0 of clayey soil can be calculated by the following equation: (Aboshi et. al., 1991)

$$S_0 = m_v * \sigma * H \tag{2.12}$$

Where;

m_v : modulus of volume compressibility

H : thickness of the layer

Substituting equations 2.11 and 2.12 into equation 2.10; (Aboshi et. Al., 1991)

$$\beta = \frac{S_t}{S_0} = \mu_c = 1/\ [1 + (n-1)a_s] \qquad (2.13)$$

On the other hand, Aboshi et. al. (1979) notes that, equation 2.13 overestimates the settlement, as the area replacement ratio becomes far greater than 0.30, since the replacement effect is neglected by equation 2.13.

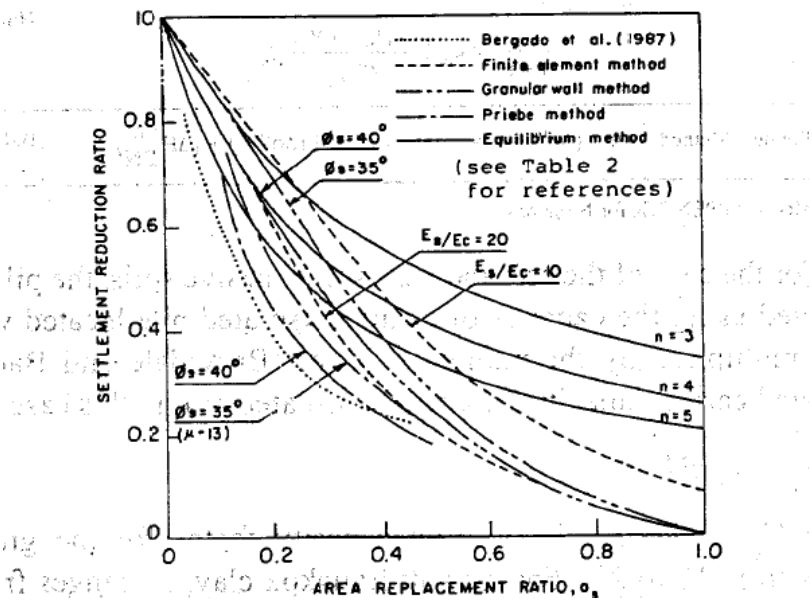

Figure 2.7 Comparison of estimating settlement reduction of improved ground (after Aboshi and Suematsu, 1985) (Bergado et. Al., 1991)

2.5.2 Settlement Theories

Datye (1982) states that the settlement analysis may be evaluated in two main categories (Figure 2.8 and 2.9);

- The case when the column does not yield
- The case when the column has yielded

Elastic theory can be used for the first case on the other hand, equilibrium theory with the combination of conventional settlement estimation methods would be used for the stone column yielded case.

Datye (1982) recognizes that extended settlement reductions for the cases of stone columns which yielded over a part of its length, are not clearly given in the available theories. Moreover, Datye (1982) points out that there is scarce information about the construction operation effect on the yield load estimation parameters.

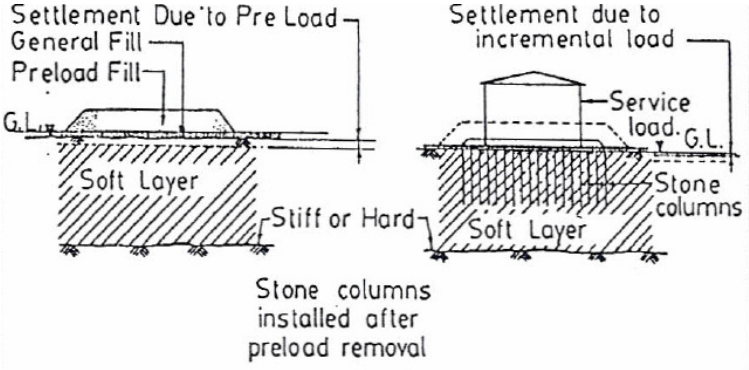

Figure 2.8 Case 1 Stone column not yielded (Datye, 1982)

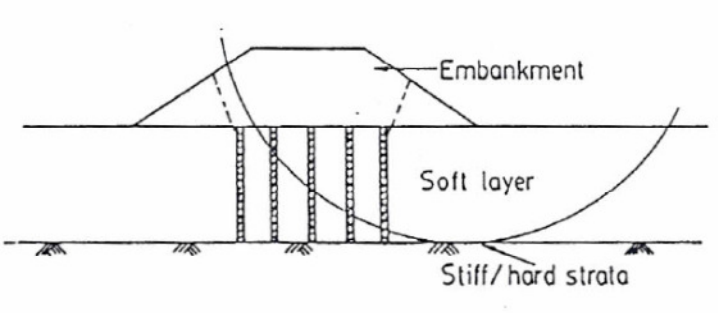

Figure 2.9 Case 2 Stone column yielded (Stability critical) (Datye, 1982)

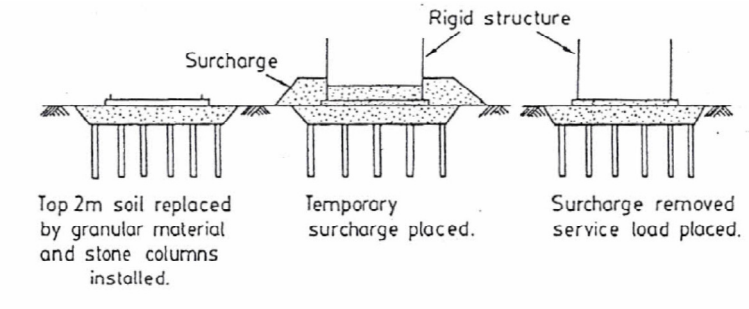

Figure 2.10 Case 2 Stone column yielded during non critical condition (Datye, 1982)

2.5.2.1 Equilibrium Method

The equilibrium method is used in Japanese practice to estimate the settlements of a ground treated by sand compaction piles. However, this method also gives realistic results for the stone column improved grounds. For the application of this simple approach, stress concentration factor, n, must be estimated using previous site measurements and past experiences. In order to be on the safe side

it is better to use a conservatively low stress concentration factor. Accordingly the estimated settlement reduction will be safer. (Barksdale and Bachus, 1983)

The assumptions considered in the equilibrium method are;

- The extended unit cell concept is valid,
- Sum of the forces carried by the stone and the soil equals to the total vertical load applied to the unit cell,
- No relative replacements between the soil and the stone column,
- Along the length of the stone column uniform vertical stress distribution exists. (Barksdale and Bachus, 1983)

Due to the applied vertical stress the change of stress in the clay;

$$\sigma_c = \mu_c * \sigma \tag{2.14}$$

Where;

σ: the average applied stress

From conventional one dimensional consolidation theory;

$$S_t = \left(\frac{C_c}{1+e_0}\right) log_{10}\left(\frac{\overline{\sigma_0} + \sigma_c}{\overline{\sigma_0}}\right) * H \tag{2.15}$$

where:

S_t: primary consolidation settlement occurring over a distance H of stone column treated ground,

H: vertical height of stone column treated ground over which settlements are being calculated,

$\overline{\sigma_0}$: average initial effective stress in the clay layer,

σ_c: change in stress in the clay layer due to externally applied loading,

C_c: compression index from one-dimensional consolidation test,

e_0: initial void ratio.

For normally consolidated clay the ratio of settlements of stone column treated ground to untreated ground;

$$\frac{S_t}{S} = \frac{\log_{10}\left(\frac{\overline{\sigma_0} + \mu_c\,\sigma}{\overline{\sigma_0}}\right)}{\log_{10}\left(\frac{\overline{\sigma_0} + \sigma}{\overline{\sigma_0}}\right)} \qquad (2.16)$$

As it can be seen from this equation, the level of improvement depends on;

- stress concentration factor, n,
- the initial effective stress in clay, $\overline{\sigma_0}$, and
- the magnitude of the applied stress, σ.

According to equation 2.16, if the other parameters kept constant, a greater reduction in settlement is obtained, since the average $\overline{\sigma_0}$ increases with column

length and for smaller applied stress increments. For very large $\overline{\sigma_0}$ and very small applied stresses, σ, the settlement ratio approaches;

$$\frac{St}{S} = \frac{1}{1 + (n-1)a_s} = \mu_c \qquad (2.17)$$

Equation 2.17 is shown graphically on Figure 2.11 which gives higher estimates of the expected ground improvement.

In spite of the fact that this method overestimates the improvement, it is practical and very useful for the preliminary design stage. (Barksdale and Bachus, 1983)

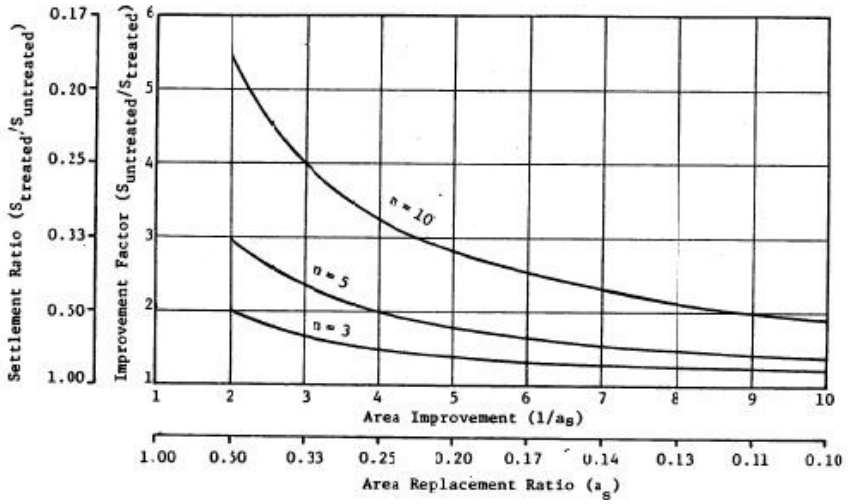

Figure 2.11 Maximum Reduction in Settlement that can be obtained using stone columns- equilibrium Method Of Analysis. (Barkdale and Bachus, 1983)

2.5.2.2 Priebe Method

This method also uses the unit cell idealization model. The Stone column is assumed to show plastic behavior while the soil within the unit cell is assumed to show elastic behavior. The column material is assumed to be incompressible, as a result, vertical shortening of the stone column shows the change of volume within the soil, i.e. any settlement results in the bulging of the column. Other assumptions made in the analysis are;

- Equal vertical settlement of the stone and soil
- Uniform stresses in two materials
- Bulk densities of both the column and the soil are neglected which means the initial pressure difference between the columns and soil depends only on the foundation load distribution.
- The column is based on a rigid layer (End Bearing)

By taking into consideration of the all above mentioned assumptions and the further assumption of taking the coefficient of earth pressure K=1 the following equation of basic improvement factor $\boldsymbol{n_0}$ is derived;

$$n_0 = 1 + \frac{A_c}{A} * \left[\frac{\frac{1}{2} + f(\mu_s, \frac{A_c}{A})}{K_{aC} * f(\mu_s, \frac{A_c}{A})} - 1 \right] \tag{2.18}$$

$$f\left(\mu_s, \frac{A_c}{A}\right) = \frac{(1-\mu_s) * \left(1 - \frac{A_c}{A}\right)}{1 - 2\mu_s + \frac{A_c}{A}} \tag{2.19}$$

$$\mathrm{K_{aC}} = \tan^2\left(45 - \frac{\varphi_c}{2}\right) \tag{2.20}$$

μ_s=1/3 assumption results in a simple expression;

$$n_0 = 1 + \frac{A_c}{A} * \left[\frac{5 - \frac{A_c}{A}}{4 * K_{ac} * \left(1 - \frac{A_c}{A}\right)} - 1 \right] \tag{2.21}$$

The design relationship developed by Priebe is given in Fig. 2.12.

This method also proposes a settlement prediction by the following equation.

$$s_\infty = p.\frac{d}{D_s.n_2} \tag{2.22}$$

Where;

$$n_2 = f_d * n_1 \tag{2.23}$$

n_2: the final improvement value obtained by considering the bulk density effects of both the column and soil

n_1: reduced improvement factor derived by taking into consideration the compressibility of the column material, and calculated by equation 2.24;

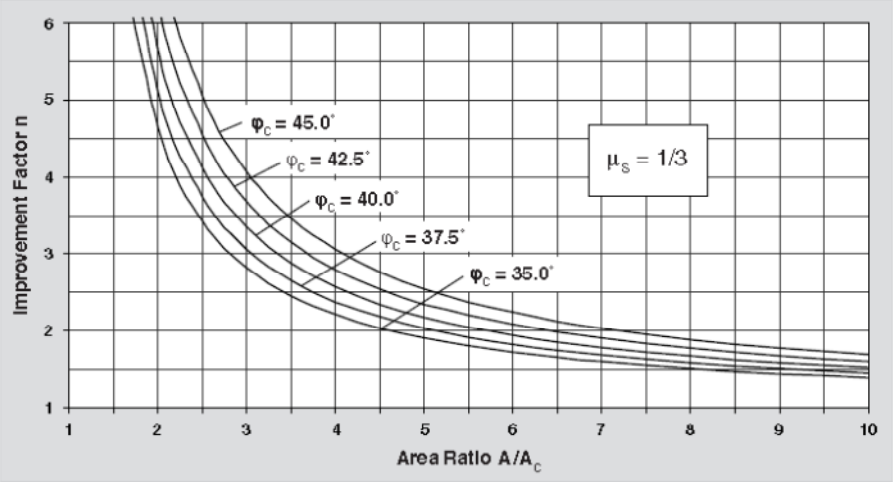

Figure 2.12 Design Chart for vibro replacement (Priebe, 1995)

$$n_1 = 1 + \frac{\overline{A_c}}{A}.\left[\frac{\frac{1}{2} + f\left(\mu_s, \frac{\overline{A_c}}{A}\right)}{K_{ac}.f\left(\mu_s, \frac{\overline{A_c}}{A}\right)} - 1\right] \tag{2.24}$$

Where;

$$\frac{\overline{A_c}}{A} = \frac{1}{\frac{A}{A_c} + \Delta\left(\frac{A}{A_c}\right)} \tag{2.25}$$

and

$$\Delta\left(\frac{A}{A_c}\right) = \frac{1}{\left(\frac{A_c}{A}\right)_1} \tag{2.26}$$

$$f_d = \frac{1}{\left[1 - y.\sum\frac{\gamma_s.\Delta d}{p}\right]} \tag{2.27}$$

f_d: depth factor determined from the simplified diagram in Figure 2.13 by the help of influence factor y.

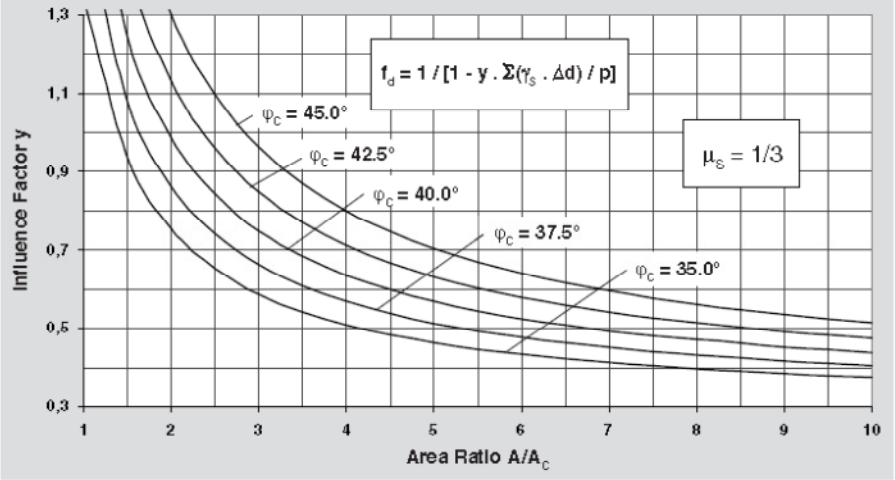

Figure 2.13 Determination of the depth factor (Priebe, 1995)

Figure 2.14 and Figure 2.15 give the settlement ratios ($s/s\infty$) versus depth-diameter ratios (d/D) of both single and strip footings for various numbers of stone columns.

"$s\infty$" value used in equation 2.22 and figures 2.14 and 2.15 represents the total settlement of an unlimited column grid below an unlimited load area (*Unit cell concept*), whereas the "s" value represents the actual settlement.

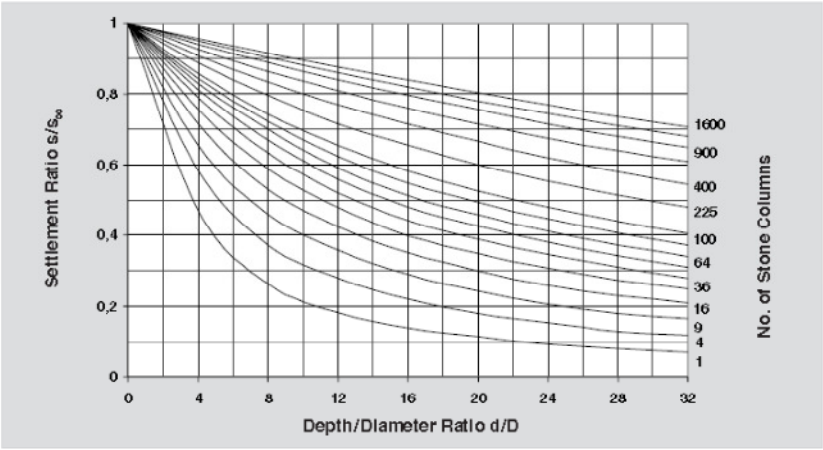

Figure 2.14 Settlement of single footings (Priebe, 1995)

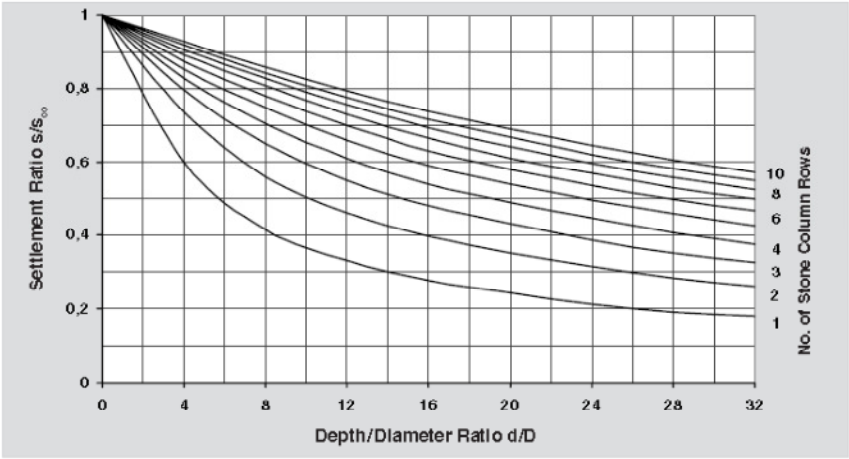

Figure 2.15 Settlement of strip footings (Priebe, 1995)

2.5.2.3 Greenwood Method

Empirical curves as a function of stone column spacing and settlement reduction, for the estimation of consolidation settlements of clay reinforced by granular columns are presented by Greenwood (1970) and shown in Figure 2.16. By these

curves Greenwood (1970) neglects the immediate settlements and shear displacements and assumes that columns are resting on a firm stratum (end bearing).

Bachus and Barkdale (1983) replotted these curves as a function of area ratio and improvement factor and superimposed the equilibrium method curve for comparison. (Figure 2.17)

Barksdale and Bachus (1983) states that Greenwood's suggested improvement factors for firm soils and for $0{,}15 \leq a_s \leq 0{,}35$ improvement factors seem to be high. Moreover, if the stiffness of the soil increases with respect to the one of the granular column, the stress concentration, n decreases.

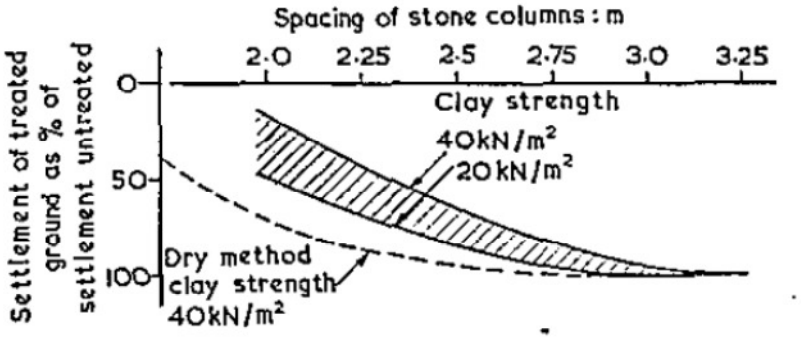

Figure 2.16 Settlement diagram for stone columns in uniform soft clay (Greenwood, 1970)

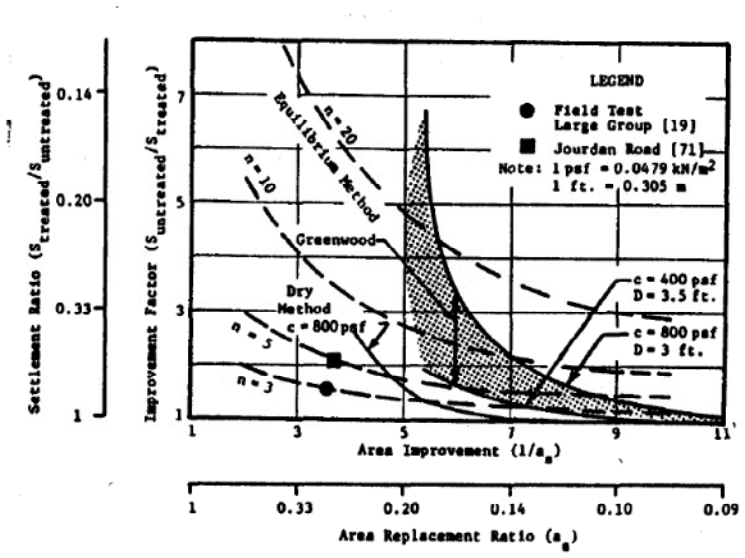

Figure 2.17 Comparison of Greenwood and equilibrium methods for predicting settlement of stone column reinforced soil (Barksdale and Bachus, 1983)

2.5.2.4 Incremental Method

Incremental method was proposed by Goughnour and Bayuk. Within this approach the unit cell concept with an incremental, iterative, elastic-plastic solution is used. (Barksdale and Bachus, 1983)

Incremental method offers a solution by dividing the unit cell into small horizontal increments, for which all variables are assumed to be constant, and the vertical strain with vertical and radial stresses are calculated iteratively.

$$s = \sum_{i=1}^{m} s_i \tag{2.28}$$

$$s_i = 2H_i(2\delta_{ri}/d_p) \tag{2.29}$$

Where;

H_i: Thickness of i^{th} layer

$2\delta_{ri}/d_p$: Radial strain of i^{th} layer

d_p: Diameter of the column

Goughnour (1983) states that the failure (plastic flow within the columns) will not occur if the vertical load applied is not higher than the confining pressure provided by in-situ soil, whereas the failure (bulging) will take place when the applied load is higher than the confining pressure. Yielding of the column first takes place at the top portion, since the confining pressure increases with depth. In other words, Goughnour (1983) states that the column material assumed to be incompressible and assumed to show both elastic and plastic behavior whereas the soil confining the unit cell is assumed to behave as it is stated in the Terzaghi's Theory of Consolidation. Barksdale and Bachus (1983) states that the granular column shows elastic behavior if the applied vertical stress is relatively small. However, for usual design stresses, the lateral failure (bulging) of the column occurs showing plastic behavior. By the incompressibility assumption of the granular column, all volume change occurs in the clay.

Moreover, Goughnour (1983) argues that Elasticity theory is sufficient for the settlement estimation of the soils which are relatively incompressible, and in free draining. On the other hand, for fine grained soils showing large time-dependent volume deformations, the stress distribution between the soil and the column is much more complicated.

A further assumption of this approach is that the vertical, radial and tangential stresses at the soil-column interface are principal stresses meaning that no shear

stresses are generated on the vertical boundary between the stone column and the soil. Goughnour (1983) proves that if the vertical load applied only to the stone column, relative motion between the column and the soil resulting from the vertical motion of the column would generate shear stresses along the periphery of the stone column. Therefore the largest load would be at the top of the column. More commonly vertical loading is applied to both the column and the in-situ soil so that equal vertical deformations occur. Due to the relative incompressibility of the stone column, the surrounding soil supplies all the volume change which results from the vertical and radial strains.

By this approach the vertical strain equals the vertical stress increment divided by the modulus of elasticity for the elastic analysis which is a conservative value. However, in case of plastic analysis the vertical stress in the column equals the radial stress in the clay at the interface times the coefficient of passive pressure of the stone.

Barksdale and Bachus (1983) believe that a programmable calculator or a computer is needed for the direct solution of equations. However use of design curves offered by Goughnour (1983) makes this method easy to apply.

2.5.2.5 Elastic Continuum Approach

Mattes and Poulos (1969) propose a method for the calculation of single granular pile. Mattes and Poulos (1969) state that major part of vertical deformation is immediate pseudo-elastic settlements, because of the fact that the vertical stress is exerted on the column by isolated footings. Moreover, Mattes and Poulos (1969) substitute effective stress modulus for undrained soil modulus, which

shows a 10% difference in the settlement. Mattes and Poulos (1969) propose the following equation for the settlement calculation;

$$s = \left(\frac{P}{E_s * L}\right) * I_p \tag{2.30}$$

Where;

P: total load on the column

L: column length

I_p: influence factor based on the geometry of the column and the pile stiffness factor

2.5.2.6 Finite Element Method

Shahu and Reddy (2011) prepared three-dimensional finite element models and the analysis is conducted by the ABAQUS software. The material properties of the clayey soil defined by modified Cam-clay model, whereas the stone columns and mat are defined by Mohr Coulomb's elastic-perfectly plastic model.

Shahu and Reddy (2011) conclude that the bending of the column increases at the edges of the pattern, moreover the central columns shows almost no bending. However, settlement is higher at the central columns, and decreases while moving away from the center. Likewise, top portion of the column shows maximum vertical deformation and while going downward the deformation decreases.

Shahu and Reddy (2011) emphasize that due to the mesh convergence issues, uncertainties in the model parameters, and improperness of granular material model, imprecise results may be obtained by the finite element analysis.

Ambiliy and Gandhi (2004) also conducted a finite element analysis based on an axisymmetric analysis using Mohr-Coulomb's criterion for clay and stones, with the help of a package named PLAXIS.

Barksdale et. al. (1984) state the following for the Finite Element Method: The Finite element method considers both radial and vertical compression of in-situ soil, both elastic and plastic behavior, and the effect of increased soil-confining pressure with depth. This approach makes the problem much more easier to consider the changing soil parameters and stress levels with depth.

2.5.2.7 Analytical Method Proposed By Balaam and Booker (1981)

Balaam and Booker (1981) also derived an analytic solution for the settlement analysis of rigid rafts supported by stone columns using the elastic theory. Figure 2.18 shows the definition of the problem of a large number of end bearing granular column and clay system underlying a smooth rigid raft. The unit cell idealization is again valid that each column and surrounding soil system behaves the same as those neighboring.

Domain of influence term mentioned by Balaam and Booker (1981) refers to the representative area surrounding the stone column and used for the simplification of analysis. Again the effective diameter parameter (d_e) mentioned before in the unit cell concept was used.

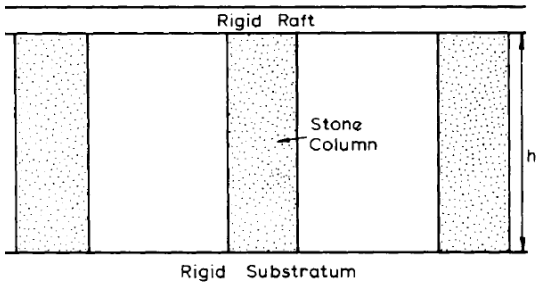

Figure 2.18 Problem definition (Balaam and Booker, 1981)

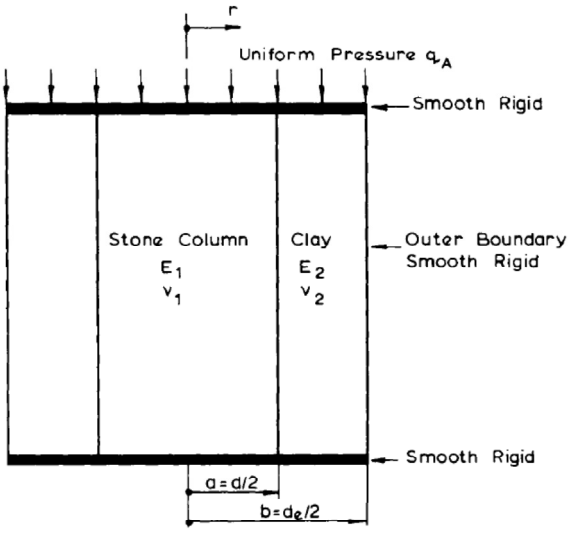

Figure 2.19 Definition of terms for analysis of equivalent cylindrical unit (Balaam and Booker, 1981)

Figure 2.19 shows a cylindrical body representing the simplified problem of the compression analysis between smooth (the raft) and rough (the substratum) plates with the lateral restriction of a smooth rigid wall in which the elastic Young's moduli E_1, E_2 and Poisson's ratios ν_1, ν_2 were used for the

approximation of behaviors of both the column and the soil. (Balaam and Booker, 1981)

Balaam and Booker (1981) state that the solution is dependent upon five dimensionless parameters; a/b, h/b, E_1/E_2. Finite element analysis is conducted in order to assign representative values for these parameters, and the following decisions reached;

Vertical displacements varied almost linearly from zero at the base to a maximum value at the surface. Uniformity of vertical strains on each horizontal slice is obtained.

In general small shear stresses were developed along the substratum. The assumption of substratum being perfectly rough or perfectly smooth has neutral effect on the field quantities far from the substratum. (Balaam and Booker, 1981)

Table 2.1 shows the analytic solution C. Balaam and Booker (1981) consider that due to smooth base assumption the obtained solutions are independent of the parameter h/b. Poissons ratio of the stone column is taken as $\nu_1 = 0{,}3$ and granular material used to construct the column assumed to deform under drained conditions.

Figure 2.20 shows the diagram of a/b versus $\varepsilon_z/(q_a\, m_{v2})$ for $E_1/E_2 = 10, 20, 30, 40$ and $v_1 = v_2 = 0{,}3$. The parameter $\varepsilon_z/(q_a\, m_{v2})$ is the ratio of settlement of the raft on the treated site to that on the untreated site, i.e. reduction in the settlement. As it can be seen from the diagram if $a/b = 0$, there is no improvement, on the other hand if $a/b = 1$, which means that the clay is replaced by granular columns, settlement reduction equals the ratio of compressibilities of the granular material and clay.

Figure 2.21 shows the diagram of vertical strain to a vertical strain corresponding to $v_2 = 0{,}3$ against different Poisson's ratios, v_2. A correction factor

corresponding to the specific v_2 value to be applied to the value obtained from Figure 2.20 can be chosen from Figure 2.21.

In order to calculate the undrained and the total final settlements the equations in Table 2.1 and Figures 2.20 and 2.21 can be used.

Table 2.1 Analytic Solution C (Balaam and Booker, 1981)

	Region 1 (Stone Column)	Region 2 (Clay)
ε_z	ε	$\left[F\frac{a^2}{r}\frac{(b^2-r^2)}{(b^2-a^2}\right]\varepsilon$
u_r	$Fr\varepsilon$	$\left[\lambda_2+\frac{2a^2F}{b^2-a^2}\right]\varepsilon$
σ_r	$[\lambda_1-2(\lambda_1+G_1)F]\varepsilon$	$\left[\lambda_2+\frac{2a^2F}{b^2-a^2}(\lambda_2+G_2+G_2\frac{b^2}{r^2}\right]\varepsilon$
σ_θ	$[\lambda_1-2(\lambda_1+G_1)F]\varepsilon$	$\left[\lambda_2+\frac{2a^2F}{b^2-a^2}(\lambda_2+G_2-G_2\frac{b^2}{r^2}\right]\varepsilon$
σ_z	$[\lambda_1+2G_1-2\lambda_1F]\varepsilon$	$\left[\lambda_1+2G_2+2\lambda_2\frac{Fa^2}{b^2-a^2}\right]\varepsilon$

Where;

$$\lambda = \frac{\nu E}{(1-2\nu)(1+\nu)} \tag{2.31}$$

$$G = \frac{E}{2(1+\nu)} \tag{2.32}$$

$$F = \frac{(\lambda_1 - \lambda_2) * (b^2 - a^2)}{2a^2(\lambda_2 + G_2 - \lambda_1 - G_1) + b^2(\lambda_1 + G_1 + G_2)} \tag{2.33}$$

and

$$a = \frac{d}{2} \tag{2.34}$$

$$b = \frac{d_e}{2} \tag{2.35}$$

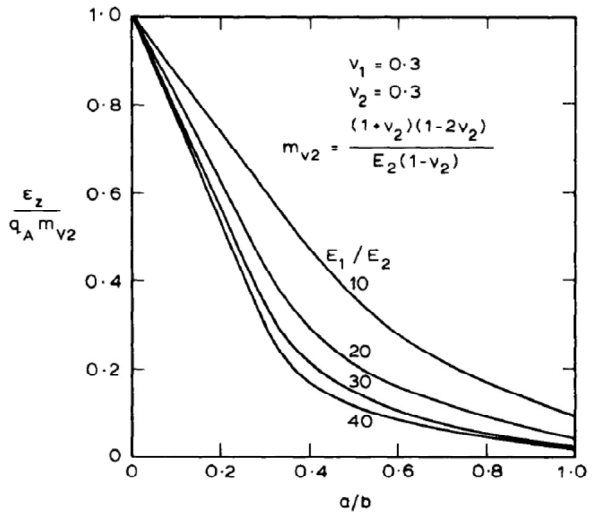

Figure 2.20 Vertical strain of pile-soil unit with varying spacing (Balaam and Booker, 1981)

Balaam and Booker (1981) recognize that the results of the analysis reveals the higher significance of consolidation settlement than the initial undrained settlement.

By an increase in the rigidity of the raft, the vertical stress increases in the stone column. Figure 2.22 shows the relation between the vertical stress, σ_z, in the stone column and the E_1/E_2 ratio for $v_1 = v_2 = 0{,}3$. As it can be seen from the Figure 2.22, for a certain value of the ratio b/a, the stress concentration ratio rapidly increases as the E_1/E_2 ratio increases which indicates the efficiency of using rigid columns rather than perfectly flexible raft.

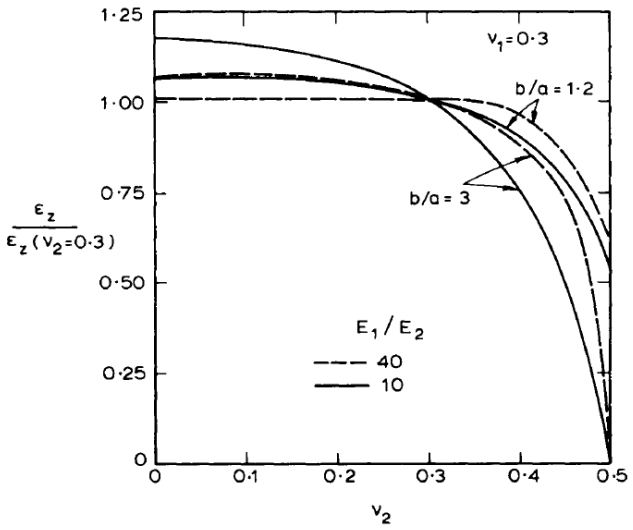

Figure 2.21 Ratio of strains for calculating settlements for complete range of Poisson's ratio (Balaam and Booker,1981)

Balaam and Booker (1981) emphasize that although the results of this analysis indicate that the column takes much more vertical stress than the surrounding soil, the condition when the load initially applied shows a different behavior.

Since the clay is in undrained condition, it is stiffer than the column material and behaves as an incompressible material and takes the higher percent of the vertical load. As the radial flow of the pore water in the clay through the column takes place, the stiffness of the surrounding soil decreases resulting in higher contact stresses on the stone columns. This phenomenon is illustrated by Figure 2.23. In consideration of Figure 2.23 Balaam and Booker (1981) state that the moment and shear distributions in raft foundations change as consolidation takes place. The initial moments and shears are expected to be smaller in the undrained condition with respect to those values in the drained condition.

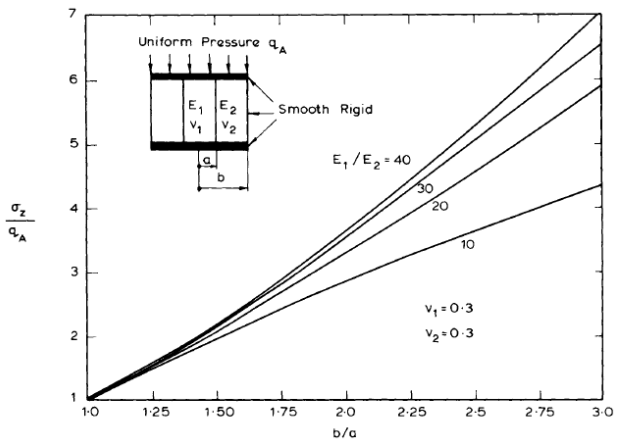

Figure 2.22 Variation of vertical stress in stone column with b/a (Balaam and Booker,1981)

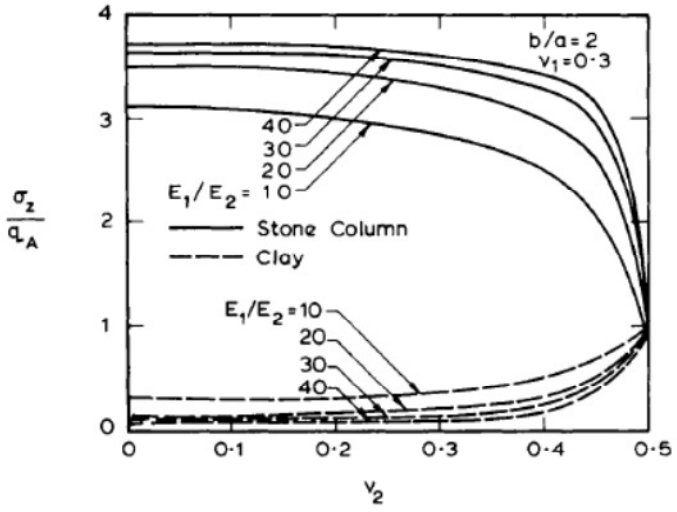

Figure 2.23 Variation of vertical stresses with Poisson's ratio of clay (Balaam and Booker, 1981)

2.5.2.8 Priebe's Method For Floating Stone Columns

The last restricting condition of the Priebe's method (1995) is not satisfied for the floating types of stone columns. Priebe (2005) discusses the floating stone column concept.

According to Priebe (2005), for the floating case of columns it is apparent that the balancing of stress and strain takes place either in the upper treated zone or in the untreated zone below.

2.5.2.8.1 Balance of Stress In The Upper Treated Zone

Priebe (2005) assumes that the treated depth is divided into a zone, for which the distributed vertical pressures maintain constant, and a transitional zone, for which the vertical pressures in the column linearly decrease, whereas the

pressures in the soil linearly increase by disregarding the unit weights of both the column and the soil, till the value of uniformly distributed value, p is reached (Figure 2.24).

The stress is distributed with the proportional load on the columns, m' above the transition zone.

Where;

$$m' = (n-1)/n$$

Which is the reduced value of "m" presented by Priebe (1995)

$$m = (n - 1 + \overline{A_c/A})/n$$

Figure 2.25 shows the reduced (m') and not reduced (m) proportional load of the columns.

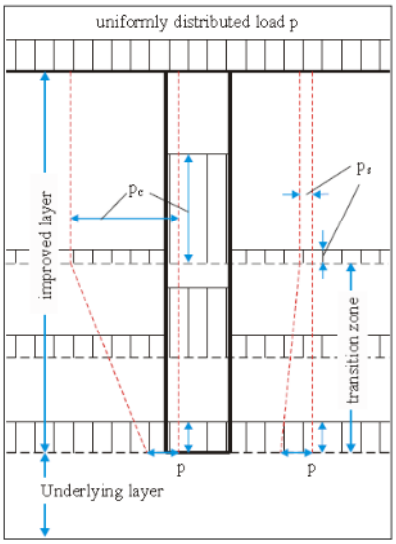

Figure 2.24 Vertical stress distribution with stress equalization in the upper treated layer (Priebe, 2005)

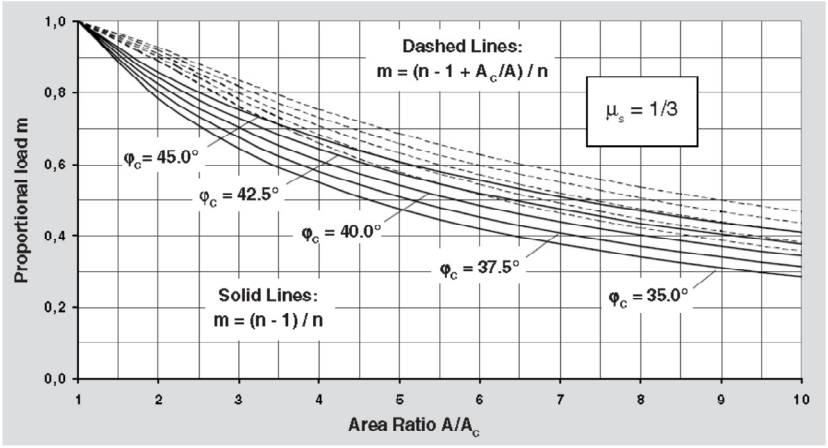

Figure 2.25 Proportional load on stone columns (Priebe, 1995)

A transfer of differential load, ΔP is assumed to occur from the column to the soil by shear resistances, R. " ΔP" and "R" are stated by the following formulations;

$$\Delta P = p * A * \left(m' - \frac{A_c}{A}\right) = p * A \left(\frac{n-1}{n} - \frac{A_c}{A}\right) \tag{2.36}$$

$$R = \pi * dia_{column} * (c_s + F) \tag{2.37}$$

Where;

c_s: cohesion of the soil

F: friction in the soil resulting from the lateral support of the soil and its friction angle, ϕ_s

Priebe (2005) argues that it is too conservative to determine the lateral support only from the proportional external load on the soil between the columns, p_s, whereas assumed value of K=1 is doubtful, else total weight of the soil should be taken into consideration.

By the assumption of linearly increasing improvement the height of the transitional zone equals;

$$h = \frac{\Delta P}{R} \tag{2.38}$$

However, Priebe (2005) indicates that the settlement of the transition zone must be calculated with a reduced average improvement factor n', which equals;

$$n' = \frac{1 + n}{2} \tag{2.39}$$

Priebe (2005) argues that the use of this approach is unfavorable due to the unclarity in the values regarding the shear resistance.

2.5.2.8.2 Balance of Stress In The Untreated Zone

Priebe (2005) assumes that the transfer of load is occurred along the depth of the treated layer i.e., vertical pressures remain constant within the length of the stone column with this case (Figure 2.26).

A comparison of the depression caused by a single column in the underlying soil with circular footing settlement, is proposed by Priebe (2005). Footing

settlement is calculated by using the proportional vertical load of the stone column, furthermore by using the depth where the pressure equals the uniformly distributed load, p value, is proposed by Priebe (2005).

Priebe (2005) states that both the above mentioned approaches overestimate the settlements which is in some certain cases not acceptable.

Priebe (2005) claims that for the first approach, inaccuracy arises from the growing stiffness of the untreated zone whereas, for the second approach inaccuracy arises from the increasing initial stiffness of the treated layer.

Inaccuracy in the second approach can be eliminated easily by limiting the punching to a value the treated layer without improvement will allow.

$$s'_p = \frac{s_p * s_0}{s_p + s_0} \tag{2.40}$$

Where;

s_p: calculated punching value

s_0: settlement of the treated layers without improvement

s'_p: reduced punching value

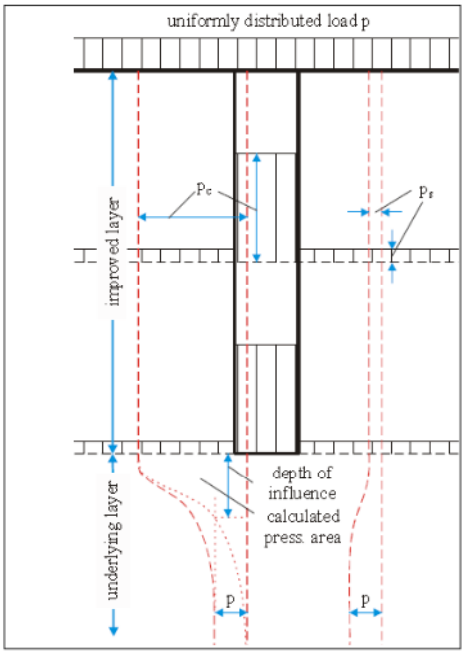

Figure 2.26 Vertical stress distribution with stress equalization in the substratum (Priebe, 2005)

Priebe (2005) recognizes that the second approach is easier to implement and gives more accurate estimations comparing with the first approach. Moreover, according to Priebe (2005), the settlement calculations include three main parts including;

- Settlement of the treated soil
- Additional settlement by punching into the untreated stratum.
- Settlement of all layers below the treated layer

Thus;

$$s = s_u + s'_p + s_i \qquad (2.41)$$

Where;

s_u: calculated settlement of upper treated soil

s_i: calculated settlement of layers below the treated zone (settlement of the untreated layers)

2.5.2.9 Granular Wall Method

Van Impe and De Beer (1983) proposed a simple method for improving effect calculation of the soil reinforced with stone columns by considering the following two cases;

- Deformation of columns at constant volume (limit of equilibrium)
- Elastic deformation of columns

For the first case the corresponding computation procedure is as follows;

i) Stone walls with equivalent area represent stone columns to simply solve the problem.

$$d_f = \frac{\pi D^2}{4a} \tag{2.42}$$

Where;

d_f: The equivalent thickness of the stone wall

D: Diameter of the stone column

a: The smallest distance center to center (Figure 2.27)

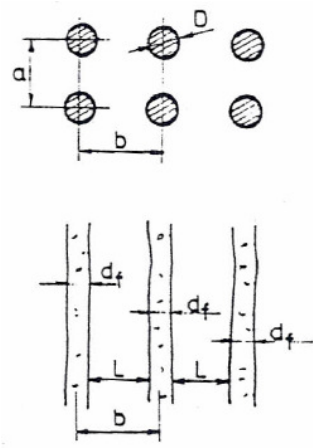

Figure 2.27 Equivalent thickness (Van Impe and De Beer, 1983)

ii) The shear stresses generated between column and clay are neglected.

iii) Unit weights of both the soil and the column material are neglected.

iv) The substratum beneath the soft soil is assumed to be undeformable.

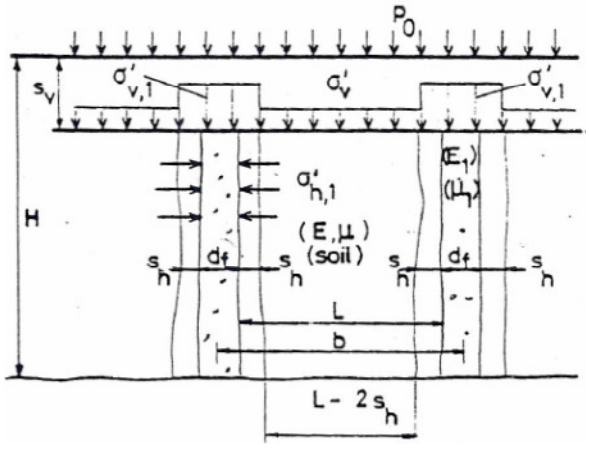

Figure 2.28 Equivalent thickness (Van Impe and De Beer, 1983)

For the above geometry (Figure 2.28) the equivalent thickness;

$$d_f . H = (d_f + 2s_h)(H - s_v) \tag{2.43}$$

Where;

s_v: Vertical settlement of the stone wall which is equal to the settlement of clay

s_h: the horizontal deformation of the stone which is equal to the horizontal deformation of the column

H: the initial stone wall height

$$s_v = \frac{H}{E} * (1 - \mu^2) . \left(\sigma'_v - \frac{\mu}{1 - \mu} * \sigma'_h\right) \tag{2.44}$$

$$s_h = \frac{L}{2E} * (1 - \mu^2) * \left(\sigma'_h - \frac{\mu}{1 - \mu} * \sigma'_v\right) \tag{2.45}$$

From the vertical equilibrium condition;

$$p_0 * b = \left(d_f * 2s_h\right) * \sigma'_{v,1} * (L - 2s_h) * \sigma'_v \tag{2.46}$$

Where;

p_0:The mean unit load transferred to the soil

b: horizontal center-to-center distance of stone walls

$\sigma'_{v,1}$: effective vertical stress in the granular material

L: distance between the lateral faces of adjoining stone walls (Van Impe and De Beer,1983)

From the limit equilibrium of stone wall material condition and neglecting the cohesion of the stone wall material,

$$\sigma'_{v,1} = \sigma'_{h,1} \tan^2\left(\frac{\pi}{4} + \frac{\varphi_1}{2}\right) \tag{2.47}$$

Where;

φ_1: angle of shearing resistance of stone wall material

$\sigma'_{h,1}$: horizontal effective stress in the lateral contact face wall-clay

$$\sigma'_{h,1} = \sigma'_h \tag{2.48}$$

The modulus of elasticity is obtained from the oedometer modulus by the following conversion;

$$E = (1 + \mu) * \frac{1 - 2\mu}{1 - \mu} * E_{oed} \tag{2.49}$$

Dimensionless parameter, ;

$$\alpha = \frac{\pi D^2}{4ab} = \frac{d_f}{b} = 1 - \frac{L}{b} \tag{2.50}$$

Moreover, assigning;

$$\tan^2\left(\frac{\pi}{4} + \frac{\varphi_1}{2}\right) = \lambda_{u,1} \tag{2.51}$$

The following equations are obtained;

$$\frac{s_v}{H} = \frac{2\left(\frac{s_h}{\alpha b}\right)}{1 + 2\left(\frac{s_h}{\alpha b}\right)} \tag{2.52}$$

$$\frac{\sigma_v'}{P_0} = \frac{2}{(1+\mu)(1-2\mu)} * \left[\frac{1-\mu}{1 + 2\left(\frac{s_h}{\alpha b}\right)} + \mu\frac{\alpha}{1-\alpha}\right]\frac{E * s_h}{\alpha b P_0} \tag{2.53}$$

$$\frac{\sigma_h'}{P_0} = \frac{2}{(1+\mu)(1-2\mu)} * \left[\frac{\mu}{1 + 2\left(\frac{s_h}{\alpha b}\right)} + (1-\mu)\frac{\alpha}{1-\alpha}\right]\frac{E * s_h}{\alpha b P_0} \tag{2.54}$$

$$\frac{1}{\alpha} = \left[1 + 2\frac{s_h}{\alpha b}\right]\frac{\sigma_h'}{P_0}\lambda_{p,1} + \left[\frac{1-\alpha}{\alpha} - 2\frac{s_h}{\alpha b}\right]\frac{\sigma_v'}{P_0} \tag{2.55}$$

$$\frac{8\alpha}{1-\alpha}\left[\lambda_{p,s}(1-\mu)-\mu\right]\left(\frac{s_h}{\alpha b}\right)^3 + 4\left[(1-\mu)\left(\frac{2\alpha}{1-\alpha}\lambda_{p,1}-1\right)+\mu\left(\lambda_{p,1}+\frac{1-2\alpha}{1-\alpha}\right)\right]\left(\frac{s_h}{\alpha b}\right)^2 + 2\left[(1-\mu)(\frac{\alpha}{1-\alpha}\lambda_{p,1}+\frac{\alpha}{1-\alpha}+\mu\left(\lambda_{p,1}+1\right)-\frac{P_0}{E}(1-2\mu)(1+\mu)\frac{1}{\alpha}\right]\frac{s_h}{\alpha b}-\frac{P_0}{E}(1-2\mu)(1+\mu)\frac{1}{\alpha}=0 \qquad (2.56)$$

For the known values of parameters $\alpha, \lambda_{p,1}, P_0/E$, the horizontal relative deformation s_h/b can be calculated from the above equation.

By using the s_h/b value calculated from equation, s_v/H, σ_v'/P_0, σ_h'/P_0 values can be deduced from the above equations.

Van Impe and De Beer (1983) define the following parameters for the representation of the improvement effect on the settlement behavior;

$$m = \frac{F_1}{F_{tot}} = \alpha\left(\frac{\sigma'_{v,1}}{P_0}+2\frac{s_h}{\alpha b}\right) \qquad (2.57)$$

$$\beta = \frac{s_v}{s_{v,0}} \qquad (2.58)$$

Where;

F_1: the vertical load transferred to the stone column

F_{tot}: the total vertical load on the area $a * b$

s_v: the vertical settlement of the composite clay-stone column structure.

$s_{v,0}$: the vertical settlement of the unimproved soil

Figure 2.29 and 2.30 show the curves of m and β values respectively.

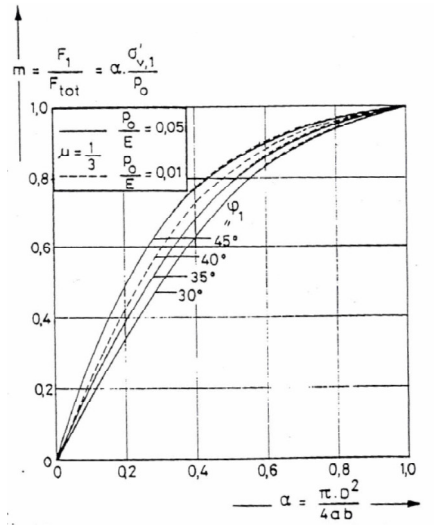

Figure 2.29 m values (Van Impe and De Beer,1983)

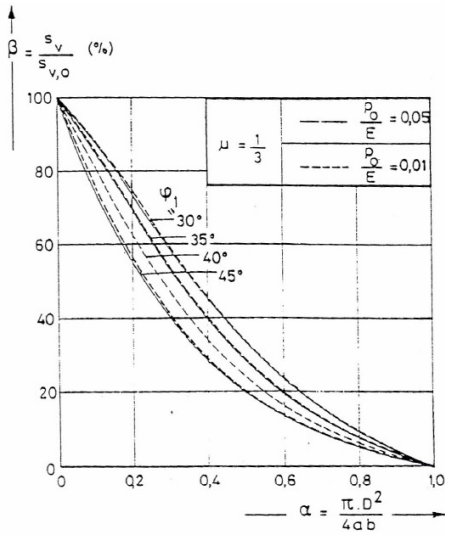

Figure 2.30 β values (Van Impe and De Beer, 1983)

2.6 Model Tests For Settlement Measurement

2.6.1 General

Black et al. (2011) state that numerous factors control the effectiveness and performance of stone column technique (Figure 2.31). These factors include the column length to diameter ratio (L/D), the area replacement ratio, (a_s), the column spacing (s), the stiffness of the column and the surrounding soft soil (E_c and E_s), the stress ratio of the column and the soil (σ_{vc}/σ_{vs}), the number of columns beneath the footing and the method of installation.

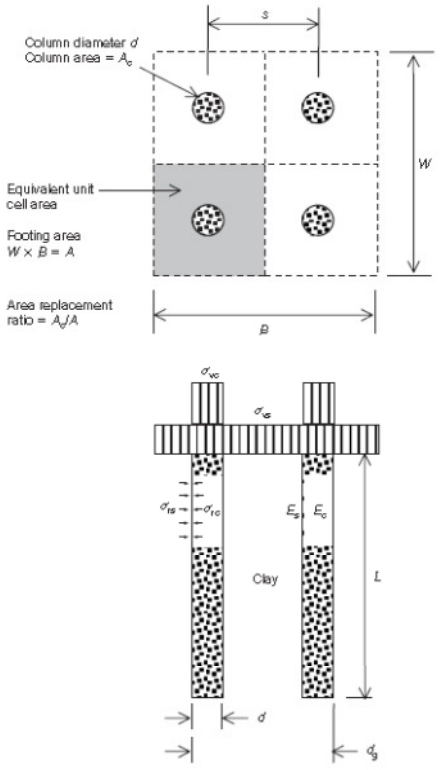

Figure 2.31 Key factors affecting granular columns performance (Black et al., 2011)

2.6.2 Material Properties

Shahu and Reddy (2011) state that stone columns are usually constructed with particle sizes of D=25-50 mm and have diameters varying between d=0,6-1.0 m. Wood et al (2000) emphasizes that d/D ratio varies between 12-40.

Shahu and Reddy (2011) used granular material which has d/D ratios ranging from 13 to 59 for stone column construction in their model tests. 50% relative density is used for most of the tests conducted, however 80% relative density used for a few tests. Shahu and Reddy (2011) emphasizes that for a relative density value of 80%, it is very difficult to guarantee a uniform stone column diameter.

Properties of clay and sand used in the models tests conducted by Ambily (2004) are tabulated in Table 2.2 and Table 2.3.

Table 2.2 Properties of the clay used in the models tests conducted by Ambily (2004)

Type of clay	CH
Specific gravity	2.492
Liquid limit	52%
Plastic limit	21%
Plasticity index	31%
Clay content	25%
Silt content	45%
Max dry density	16.63 kN/m^3
Optimum moisture content	19.25%

Table 2.3 Properties of the sand used in the models tests conducted by Ambily (2004)

Angle of internal friction	42°
Size	2-10 mm
Uniformity coefficient	2
Modulus of elasticity	48000 kPa

Ambiliy (2004) states that clay slurries are prepared at varying water contents of 25%, 30%, and 35%.

McKelvey (2004) states that the by preparing the kaolin at a water content 1.5 times its liquid limit, inherent soil structuring can be avoided. However kaolin was prepared at a water content 1.35 times its liquid limit. Initial consolidation pressure of 140 kPa is applied which lasted for 8 days. After the completion of preconsolidation stage the pressure was reduced to zero.

McKelvey (2004) used two different materials for soft clay representation, which are transparent clay and the commercially available kaolin. Transparent clay is used for the examination of failure mechanisms and deformation characteristics of the granular columns, whereas the kaolin slurry is used for examining the load-deformation characteristics of the composite soil. However, uniformly graded fine sand is used for the both types of clays. The coefficient of consolidation, c_v is reported to vary between 0.8-1.2 m^2/year, and the coefficient of compressibility m_v ranged between 1.3-3.4 m^2/MN. Moreover, the slope of the compression line, C_c is found out to be 4.8, which is relatively high when compared with that of kaolin. Unconsolidated undrained (UU) triaxial tests were carried out for shear strength determination, and they were found to be 15 kPa, 22 kPa and 31 kPa for the consolidation pressures of 75 kPa, 100kPa and 150 kPa. The angle of frictions of both the transparent clay and the sand used for

granular column are found out to be 34°. However McKelvey (2004) states that the difference between angles of friction of the sand and soft soil is usually 10°-15° in full scale engineering practice. Figure 2.32 shows the void ratio-effective stress relationship of transparent clay used by McKelvey (2004). Figure 2.33 shows the relationship between the undrained shear strength and one dimensional consolidation pressure for transparent clay and kaolin.

The results of the vane shear tests carried out at the center of the clay bed prepared by Ambily (2004) are shown in table 2.4.

Table 2.4 Test Program (Ambily, 2004)

s/d	w (%)	S_u (kPa)	Loading condition	
			Entire area	Column alone
2	25	30	✓	✓
2	30	12	✓	✓
2	35	6.5	✓	✓
3	30	12	✓	✓
4	30	12	✓	✓

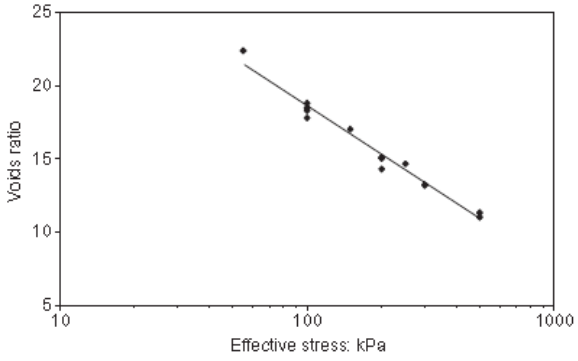

Figure 2.32 Relationship between voids ratio and σ_v' for transparent clay (McKelvey, 2004)

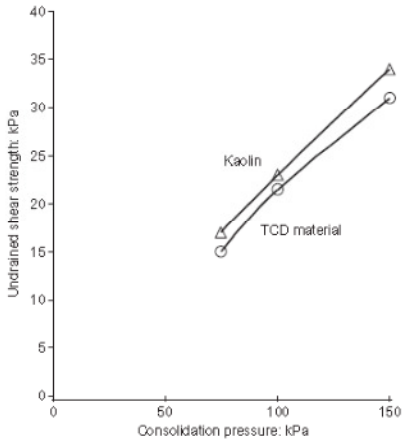

Figure 2.33 Relationship between undrained shear strength and one dimensional consolidation pressure for transparent material and kaolin (McKelvey, 2004)

McKelvey (2004) emphasizes that the density of the granular columns considerably effect the composite soil performance. As the density of the column increases the stiffness also increases, and moreover forming process of the granular columns will also affect the soil column interaction.

Christoulas (2000) emphasizes that the void ratios of the undisturbed samples taken from clay at the end of consolidation stage varies between 1.30 and 1.45, and saturated unit weights varies between 16.2 to 16.9 kN/m^3.

The parameters of the kaolin used for the model tests conducted by Christoulas (2000) are as follows:

Liquid limit= 47-52%

Plastic limit= 35-40%

Plasticity index= 10-12%

Clay fraction= 23-27%

Christoulas (2000) emphasizes that prior to stone column installation, after the end of consolidation stage, in situ vane shear tests and unconsolidated undrained triaxial tests were carried out for shear strength determination. The results of vane shear tests came out to be between 38-45 kPa, whereas the results of unconsolidated undrained triaxial tests came out to be 50-60 kPa. The friction angle was found to be between 39-44°.

Granular material with a mean diameter of d_{50}=6-8 mm and a maximum diameter of d_{max}=20 mm which approximately equals 1/3 of the prototype size of aggregates in practice, was used to construct the stone columns in the model study carried out by Christoulas (2000).

Table 2.5 represents the material properties of the study done by Black et al. (2011).

Table 2.5 Material properties (Black et al., 2011)

Material	Property	Value
Clay: Speswhite kaolin clay	Particle size: μm	< 63
	Liquid limit: %	68
	Plastic limit: %	34
	Plasticity index: %	34
	Modulus of elasticity, E': kN/m^2	4
	Friction angle, ϕ: degrees	22
	Undrained shear strength: kN/m^2	35
	Compression index, C_c	0·47
	Swelling index, C_s	0·12
Basalt aggregate: crushed basalt, uniformly graded	Particle size: mm	1·18–2·36
	Modulus of elasticity, E': kN/m^2	30
	Friction angle, ϕ: degrees	43

2.6.3 Model Dimensions and Test Setups

Figure 2.34 illustrates the loading arrangement of the model study conducted by Malarvizhi and Ilamparuthi (2004).

Figure 2.35 illustrates the schematic view of stone column foundation implemented by Shahu and Reddy (2011).

Figures 2.36 and 2.37 illustrate the type and layout of the instrumentation used to monitor the loading tests. (Christoulas, 2000)

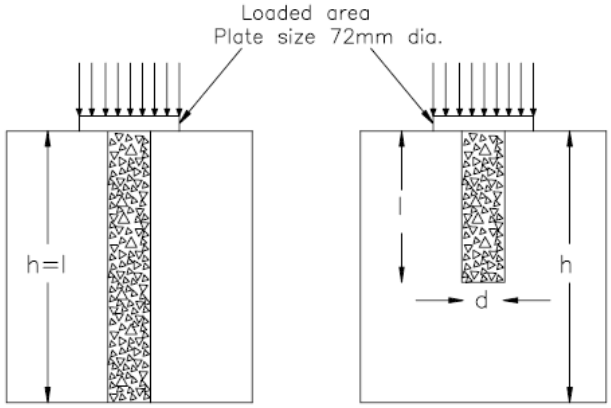

Figure 2.34 Loading of the composite bed (Malarvizhi and Ilamparuthi, 2004)

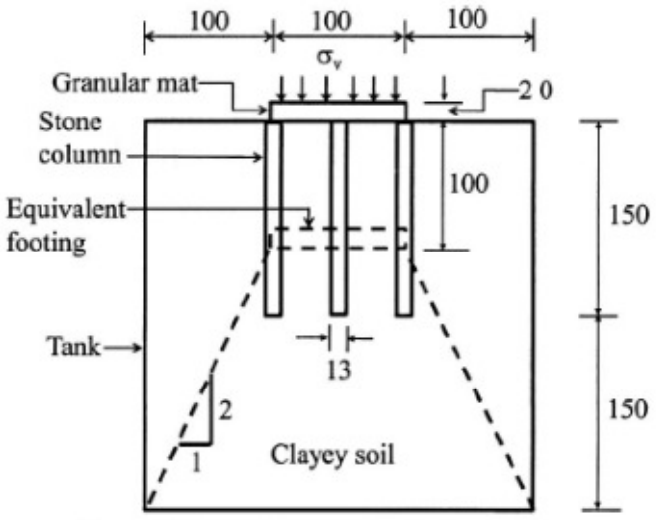

Figure 2.35 Schematic view of Stone column foundation (Shahu and Reddy, 2011)

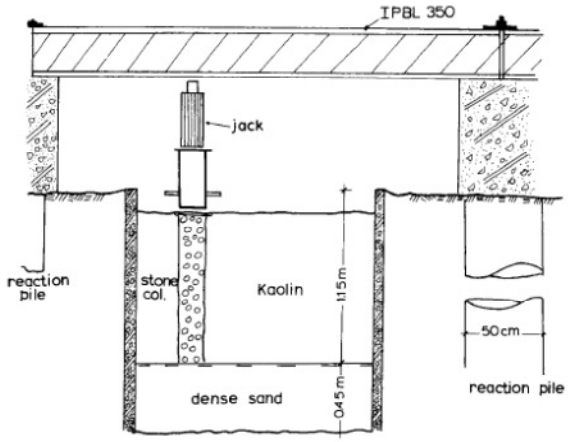

Figure 2.36 Cross section of test pit with the stone column and the load application system (Christoulas, 2000)

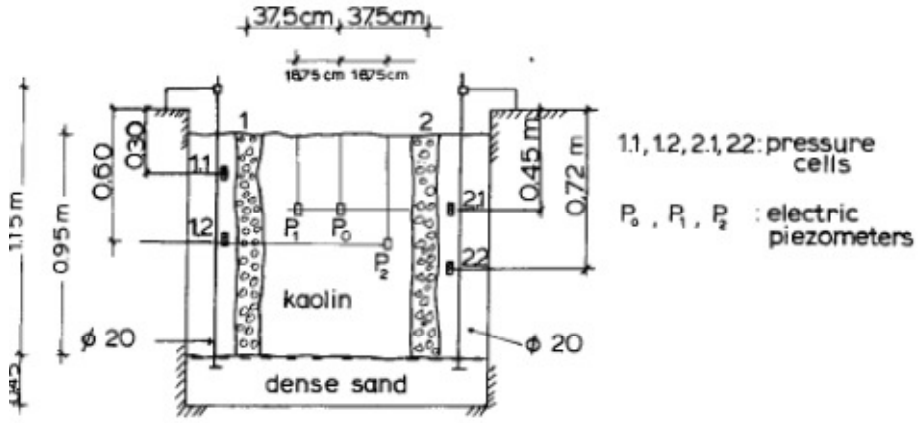

Figure 2.37 Cross section of two model stone columns and instrumentation layout (Christoulas, 2000)

2.6.4 Test Procedures and Test Schedules

Shahu and Reddy (2011) state that the consolidation takes 20-25 days for completion, and after consolidation clay was unloaded for stone column and mat foundation installation. 60 kPa pressure was used for most cases for the consolidation of kaolinite type of clay and poorly graded sand with loosest and densest unit weights of 12,93 kN/m^3 and 15,75 kN/m^3 was used as the granular material. The undrained shear strengths of the clay were found out to be between 7 and 9 kPa by laboratory vane shear tests with a vane diameter of 12 mm.

Details of the model tests conducted by McKelvey (2004) and Black et al. (2011) are given in Table 2.6 and Table 2.7.

Christoulas (2000) states that kaolin was first mixed with water to obtain a water content of 50% which is higher than the liquid limit, and then it was consolidated at 126 kPa in order to simulate the in situ-soil conditions.

Christoulas (2000) also states that the side walls of pit were covered with geotextile filter for the acceleration of drainage during consolidation stage.

Table 2.6 Parameters in model tests (McKelvey, 2004)

Test	Clay type	Footing	No. of cols	d: mm	L: mm	t: mm	p_c: kPa	c_u: kPa	A_s: %	L/d
TS-01	TCD	Circular	3	25	150	50	85	17·5	23	6
TS-02	TCD	Circular	3	25	250	50	130	27·2	23	10
TS-03	TCD	Strip	3	25	150	35	100	21·5	40	6
TS-04	TCD	Strip	3	25	250	35	100	20·5	40	10
TS-11	Kaolin	Pad	4	25	250	43	142	32	24	10
TS-12	Kaolin	Pad	0	–	–	–	142	32	0	–
TS-13	Kaolin	Pad	4	25	250	43	142	32	24	10
TS-14	Kaolin	Pad	4	25	150	43	142	32	24	6

Table 2.7 Test schedule (Black et al., 2011)

Test	Column configuration	Column length, L: mm	Column diameter, d: mm	Area replacement ratio, A_s: %	L/d ratio	
TS-01	Unreinforced	N/A	N/A	N/A	N/A	
TS-02	Isolated	125	25	17	5·0	
TS-03	Isolated	250	25	17	10·0	
TS-04	Isolated	400	25	17	16·0	
TS-05	Isolated	125	32	28	3·9	
TS-06	Isolated	250	32	28	7·8	
TS-07	Isolated	400	32	28	12·5	
TS-08	Isolated	125	38	40	3·3	
TS-09	Isolated	250	38	40	6·6	
TS-10	Isolated	400	38	40	10·5	
TS-11	Group	250	18 × 3	40	13·8	4·1*
TS-12	Group	400	18 × 3	28	22·2	6·6*
TS-13	Group	250	22 × 3	28	11·3	4·1*
TS-14	Group	400	22 × 3	40	18·1	6·6*

*Calculated using L/d_g, where d_g = group diameter.

2.6.5 Test Results and Discussions

Shahu and Reddy (2011) used initial effective geostatic stress, p_i' as foundation parameter for normalization, instead of c_u. Likewise, the settlement is normalized by the column length.

Shahu and Reddy (2011) state that the following parameters influence the settlement behavior of the stone column group foundation;

$$\delta = f\left(\sigma_v, s, l, d, p_i', p_p', \lambda, \kappa, M, E_s, N\right) \tag{2.59}$$

Where;

δ: settlement of footing

σ_v: applied vertical stress on the footing

s: spacing of columns

l: length of column

d:diameter of column

p_i': initial mean effective geostatic stress

p_p': mean effective pre-consolidation stress

λ: slope of the virgin consolidation line

κ: slope of the unloading-reloading line

M: critical state ratio

E_s: secant modulus

N: number of columns

Shahu and Reddy (2011) state that the abovementioned parameters were nondimensionalized by Buckingham's theorem of dimensional analysis as:

$$\frac{\delta}{l} = f\left(\frac{\sigma_v}{p_i'}, A_r, \frac{l}{d}, R, \frac{E_s * \lambda}{p_i'}, M, N\right) \tag{2.60}$$

Where;

A_r: Area ratio

R: overconsolidation ratio

$$A_r = \left(\frac{\pi}{4}\right)\left(\frac{d}{s}\right)^2 \tag{2.61}$$

$$R = \frac{p_p'}{p_i'} \tag{2.62}$$

$$\kappa \approx \frac{\lambda}{5} \tag{2.63}$$

Results of the experimental model study conducted by Wood (2000) illustrated in Figures 2.38-2.41, which give the normalized footing load versus normalized footing settlement behavior by variable area ratio values, A_s for short and long columns, and column length. Wood (2000) states that as the area ratio increases, the stiffness and thus the strength also increases. Moreover, Wood (2000) states that there exists a certain point up to which the column length is relevant. No

further advantage is obtained by increasing the column length beyond that point.

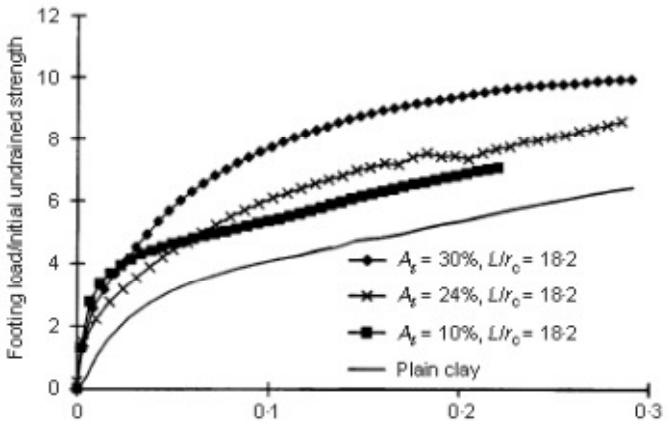

Figure 2.38 Normalized load-settlement results for model footings; variation of area ratio (short columns) (Wood, 2000)

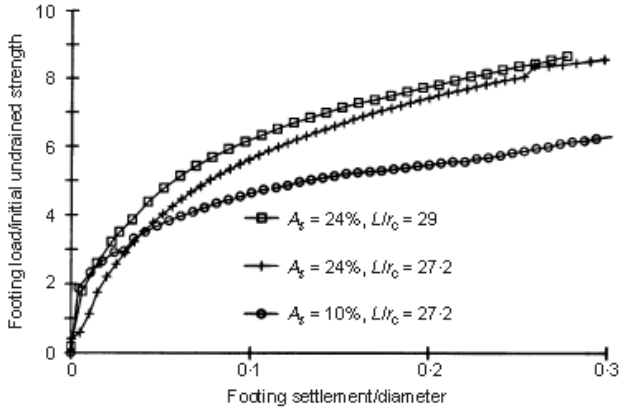

Figure 2.39 Normalized load-settlement results for model footings; variation of area ratio (long columns) (Wood, 2000)

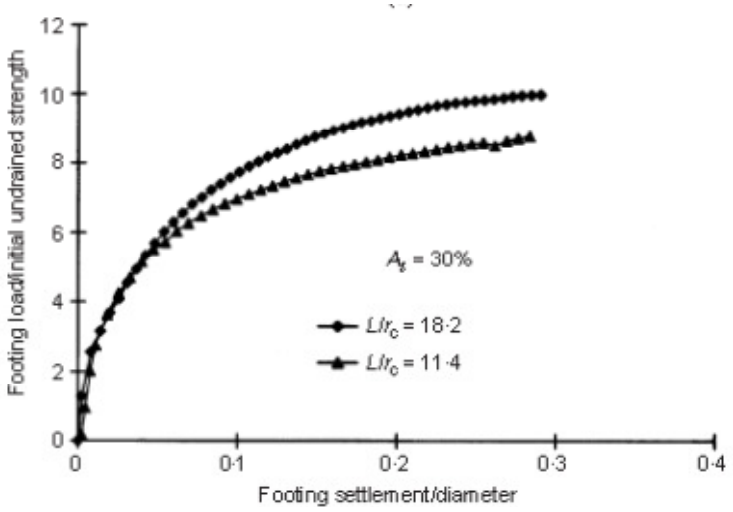

Figure 2.40 Normalized load-settlement results for model footings; variation of column length (short columns) (Wood, 2000)

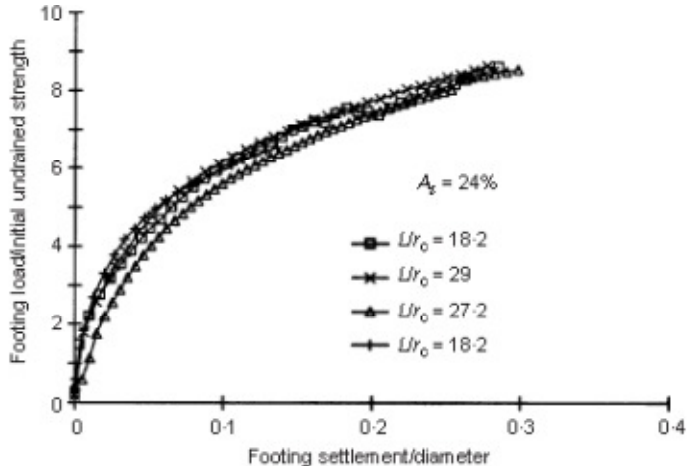

Figure 2.41 Normalized load-settlement results for model footings; variation of column length (long columns) (Wood, 2000)

Shahu and Reddy (2011) state that as the normalized vertical stress, $\frac{\sigma_v}{p_i'}$ increases the settlement nonlinearly increases up to a certain critical stress level for both ratios of $\frac{l}{d} = 7.7$ and $\frac{l}{d} = 11{,}54$. After this critical vertical stress value failure occurs resulting in excessive settlement which has been used to define the normalized failure stress, P_{max}/p'_i. Moreover, as it can be seen from Figures 2.42, 2.43 and 2.44 for a constant vertical stress applied, the settlement decreases and failure stress increases as the area ratio increases, since the stiffness of the foundation increases with increasing area ratio.

As seen on the Figures 2.45, 2.46, and 2.47 at constant normalized vertical stress, as the normalized column length increases, the failure stress increases and the normalized settlement decreases.

Figure 2.48 shows that for constant normalized vertical stress, the normalized settlement increases as the moisture content of the sand increases.

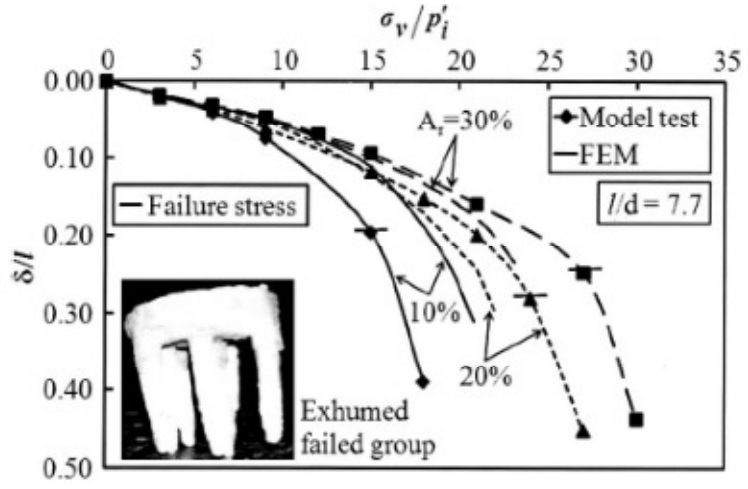

Figure 2.42 Comparison of finite element and model test results for 13 mm diameter columns with different area ratios for $l/d = 7.7$ (Shahu and Reddy, 2011)

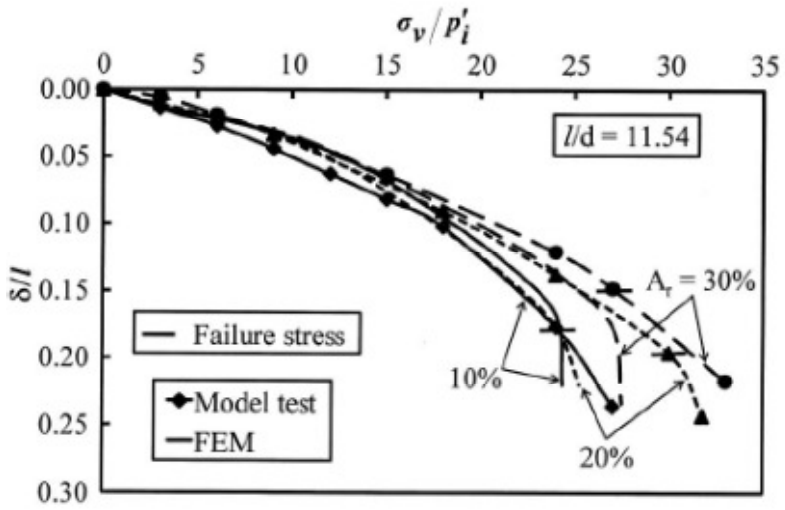

Figure 2.43 Comparison of finite element and model test results for 13 mm diameter columns with different area ratios for $l/d = 11{,}54$ (Shahu and Reddy, 2011)

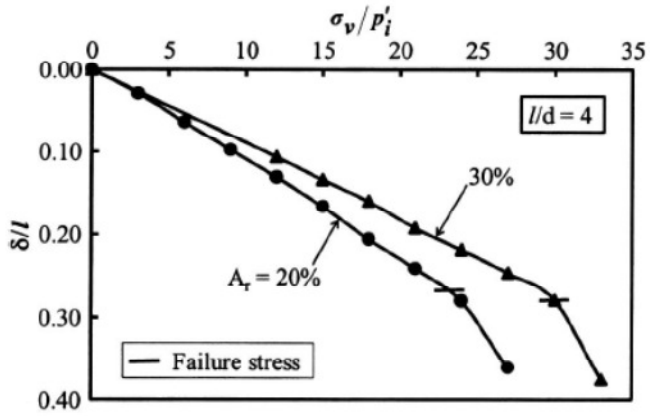

Figure 2.44 Normalized vertical stress versus settlement relationship for $l/d = 4$ (Shahu and Reddy, 2011)

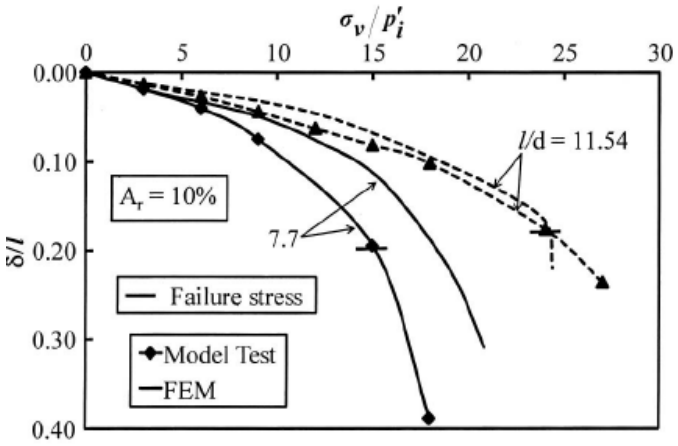

Figure 2.45 Comparison of finite element and model test results for different l/d ratios ($A_r = 10\%$) (Shahu and Reddy, 2011)

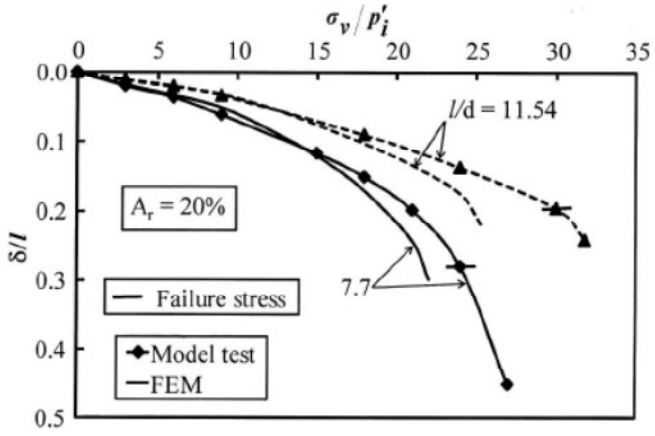

Figure 2.46 Comparison of finite element and model test results for different l/d ratios ($A_r = 20\%$) (Shahu and Reddy, 2011)

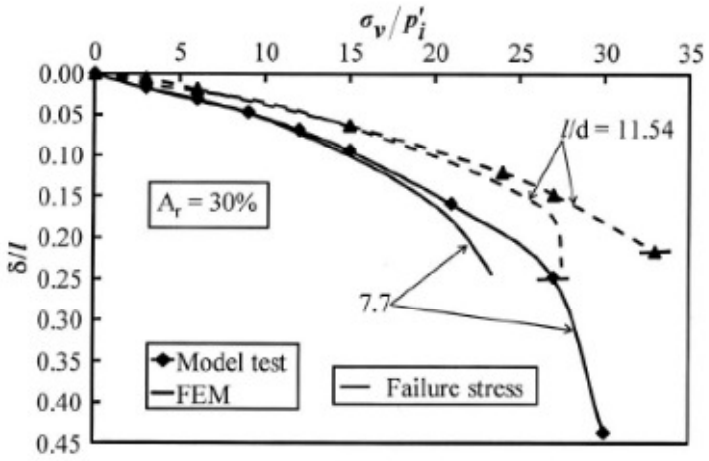

Figure 2.47 Comparison of finite element and model test results for different l/d ratios ($A_r = 30\%$) (Shahu and Reddy, 2011)

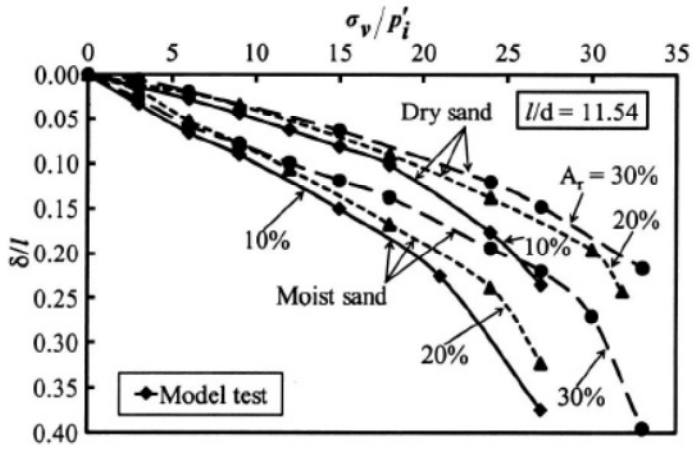

Figure 2.48 Effect of sand moisture condition on stress-settlement relationship (Shahu and Reddy, 2011)

Figure 2.49 illustrates that as the area ratio increases, the normalized settlement value decreases. However, the settlement reduction is a lot larger when the area ratio increases from 10% to 20% than the ratio increases from 20% to 30%.

Figure 2.50 illustrates that as the relative density of stone columns increases, the stiffness of the column group increases which results in a decrease in the settlement. Shahu and Reddy (2011) conclude that this settlement reduction effect due to the relative density increase is negligible at low applied vertical stress levels, however it is considerable near failure stress levels.

Shahu and Reddy (2011) state that as the overconsolidation ratio, R increases, the stiffness of the clay bed increases which results in an increase in the stiffness of the column group, thus decrease in the settlement (Fig. 2.51).

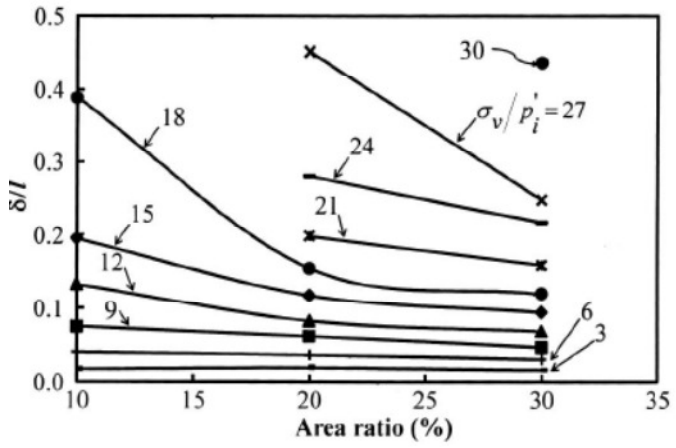

Figure 2.49 Normalized settlement versus area ratio relationship for different applied vertical stress for l =100 mm (d=13 mm; p_p'=60 kPa ; D_r=50%; and dry sand) (Shahu and Reddy, 2011)

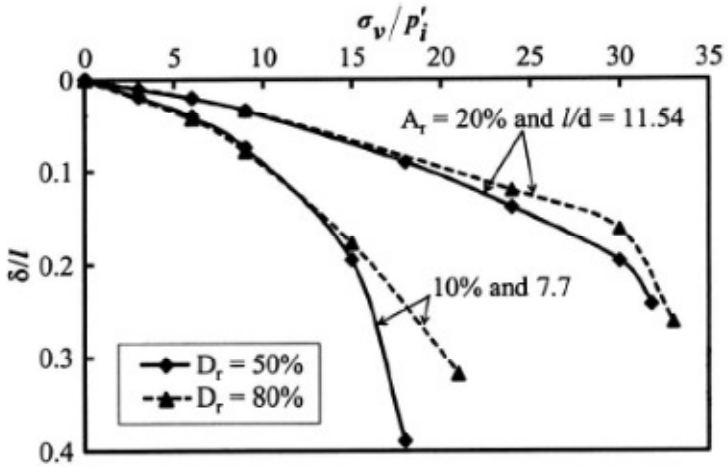

Figure 2.50 Settlement versus vertical stress relationship for different relative density of sand for A_r=10% and l=100 mm; and for A_r=20% and l=150 mm (d=13mm, dry sand)(Shahu and Reddy, 2011)

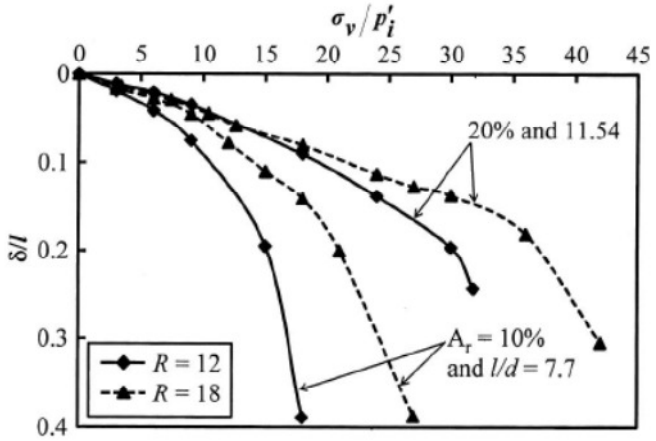

Figure 2.51 Settlement versus vertical stress relationship for different R(overconsolidation ratio) for A_r=10% and l= 100 mm; and A_r=20% and l=150 mm (d=13mm, D_r=50%, dry sand)(Shahu and Reddy, 2011)

Figures 2.52-2.54 illustrate the relationship between bearing pressure and settlement for A_s= 17%, A_s= 28%, A_s= 40% at H_c/H_s ratios of 0.31, 0.62, 1.0. (H_c and H_s are the column length and the sample height respectively) H_c/H_s=1.0 represents end bearing (fully penetrating) column whereas H_c/H_s< 1.0 represents floating columns. (Black et al., 2011) The relevant settlement values and the settlement improvement factors are given in Table 2.8.

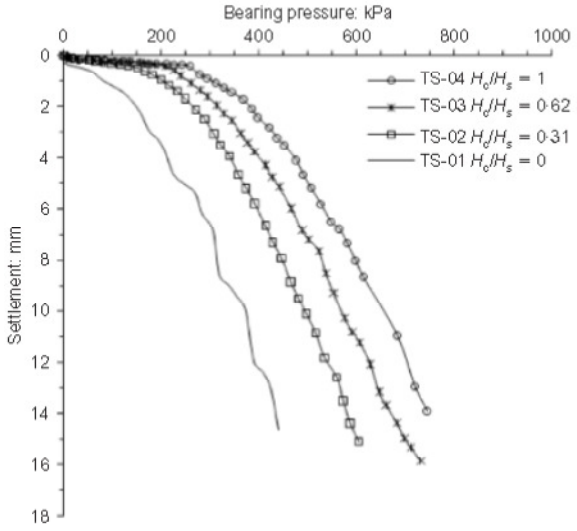

Figure 2.52 Footing pressure–settlement response of sample reinforced with columns of various area replacement and H_c/H_s ratios; A_s= 17% (Black et al., 2011)

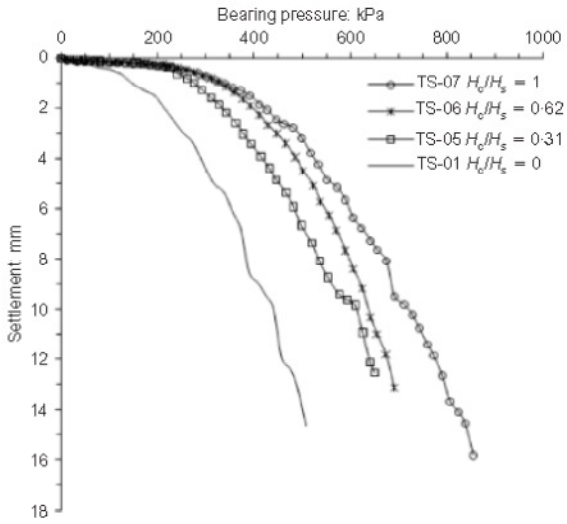

Figure 2.53 Footing pressure–settlement response of sample reinforced with columns of various area replacement and H_c/H_s ratios; A_s=28% (Black et al., 2011)

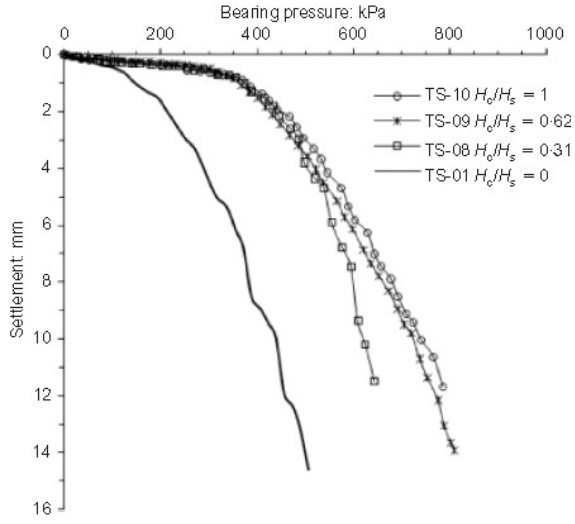

Figure 2.54 Footing pressure–settlement response of sample reinforced with columns of various area replacement and H_c/H_s ratios; A_s =40% (Black et al., 2011)

In Figures 2.55 and 2.56, it is illustrated by Black et al. (2011) that settlement improvement factors are plotted against L/d ratio for all values of A_s (L and d are the column length and the column diameter respectively). Black et al. (2011) state that as L/d ratio increases stress improvement factor, n also increases which is illustrated in Figure 2.56. However, at lower A_s values of 17% and 28% increasing L/d ratio beyond 8-10 presents little improvement. On the other hand increasing L/d ratio beyond 8, presents better improvement for A_s=40%, however rate of increase also tends to diminish for this area ratio. In Figure 2.55, Black et al. (2011) plotted the settlement improvement factors with respect to area replacement ratio. Black et al. (2011) also state that as illustrated in Figure 2.56, as area replacement ratio increases the settlement improvement factor also increases, however predominantly for floating columns there exists a threshold A_s value between 30% and 40%.

Table 2.8 Settlement improvement factor during foundation loading (Black et al., 2011)

Test no.	Settlement: mm	Improvement factor, n
TS-01	1·50	1·00
TS-02	0·40	3·75
TS-03	0·28	5·36
TS-04	0·26	5·77
TS-05	0·23	6·49
TS-06	0·22	6·82
TS-07	0·21	7·14
TS-08	0·29	5·24
TS-09	0·23	6·52
TS-10	0·20	7·50

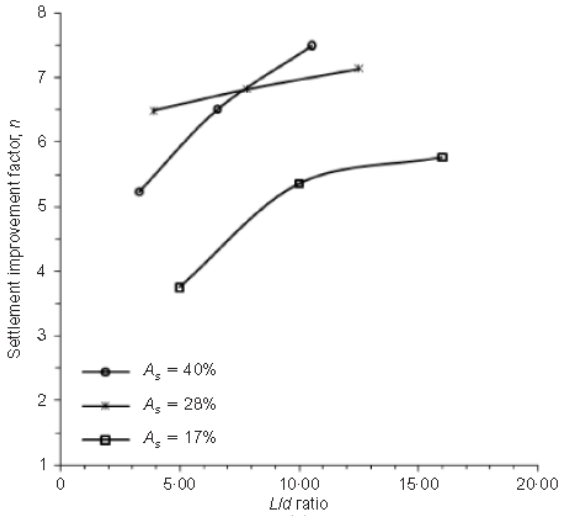

Figure 2.55 Settlement improvement factor plotted against A_s ratio (Black et al., 2011)

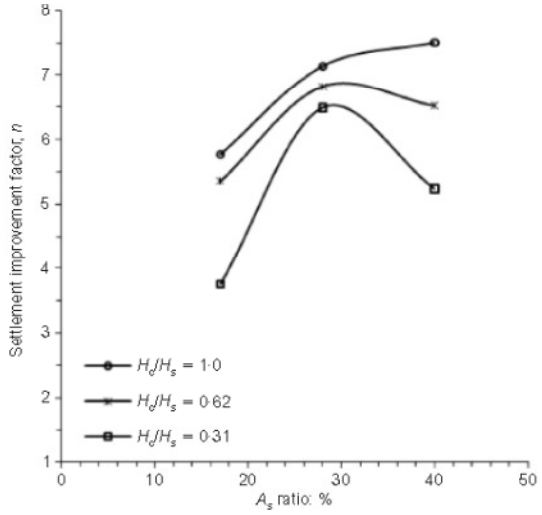

Figure 2.56 Settlement improvement factor plotted against L/d ratio (Black et al., 2011)

Figures 2.57-2.60 illustrate pressure-settlement behavior for small group of three columns, comparing with the single column of the same area replacement value and column length. Black et al. (2011) state that the performance of the single column is higher than that of the corresponding group, which is more considerable when the column is of floating type.

Black et al. (2011) conclude that by the installation of shorter columns (L/d <6) at higher replacement ratios or longer columns (L/d >6) at relatively lower area replacement ratios, settlement can equally be controlled.

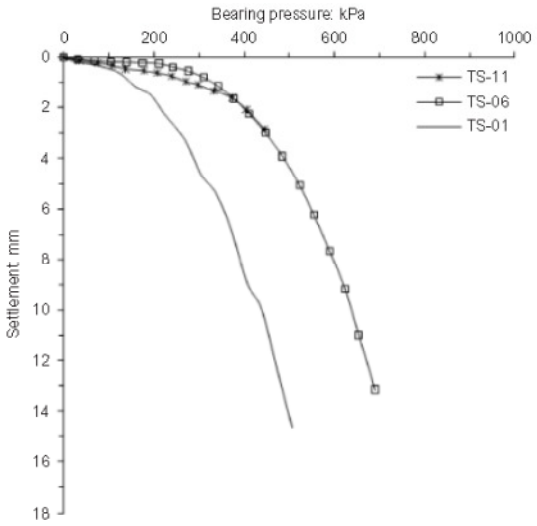

Figure 2.57 Small-group performance compared with isolated column; A_s= 28%, H_c/H_s= 0.62 (Black et al., 2011)

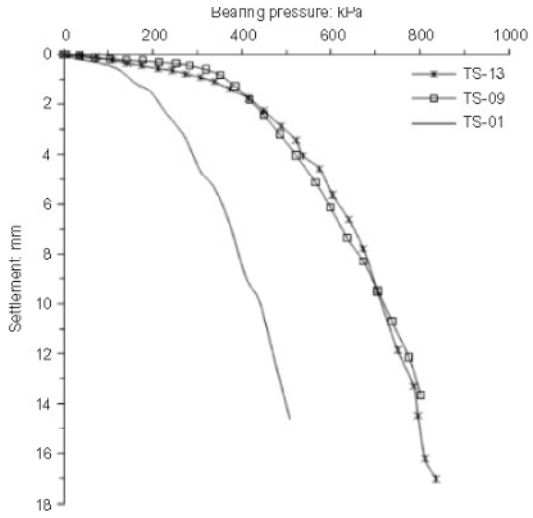

Figure 2.58 Small-group performance compared with isolated column; A_s= 28%, H_c/H_s=1.0 (Black et al., 2011)

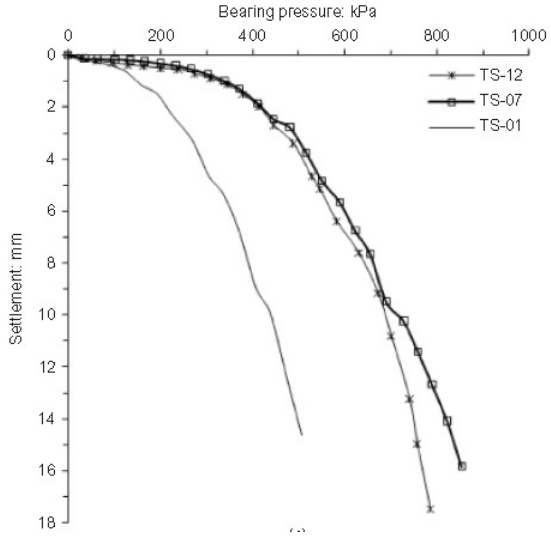

Figure 2.59 Small-group performance compared with isolated column; As= 40%, H_c/H_s=0.62 (Black et al., 2011)

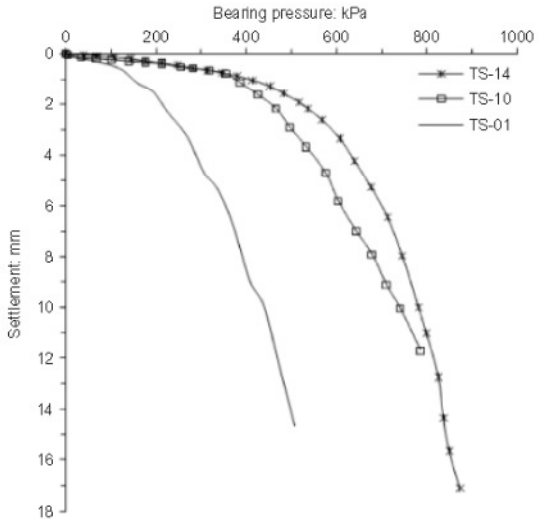

Figure 2.60 Small-group performance compared with isolated column; A_s= 40%, H_c/H_s=1.0 (Black et al., 2011)

Malarvizhi and Ilamparuthi (2004) state that the rate of increase of resistance decreases with settlement. Malarvizhi and Ilamparuthi (2004) also state that treated ground shows more brittle behavior when compared with the untreated one. Following the bulging, the settlement increases rapidly. Figure 2.61 represents the load-settlement behavior of stone columns for varying l/d ratios.

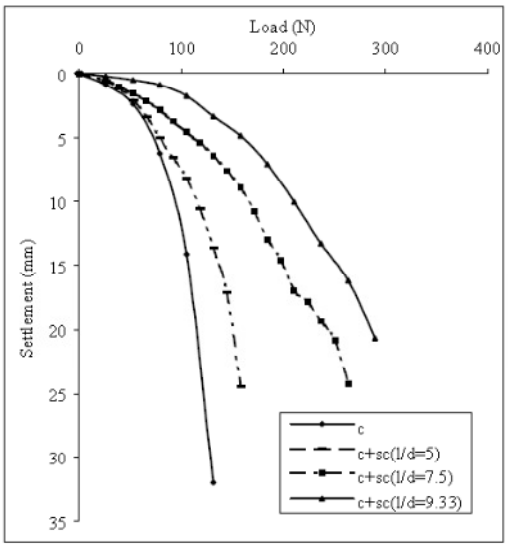

Figure 2.61 Load vs Settlement Curve of Stone Columns having different l/d ratios (Malarvizhi and Ilamparuthi, 2004)

Where;

"c" refers to loading the claybed alone.

"$c + s_c$" refers loading the stone column stabilized bed

Figure 2.62 compares the results of the finite element analysis and model tests carried out by Ambily (2004).

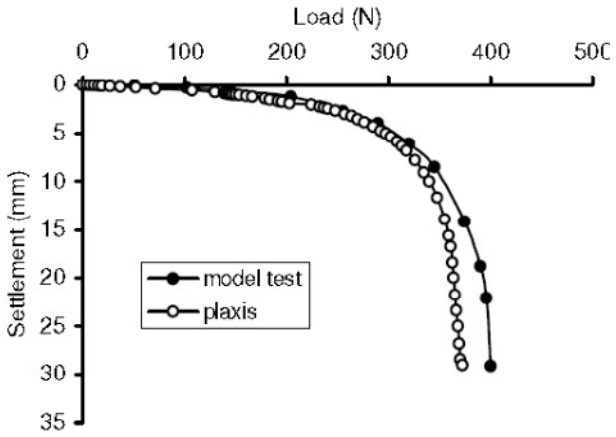

Figure 2.62 Validation of Plaxis (Ambily, 2004)

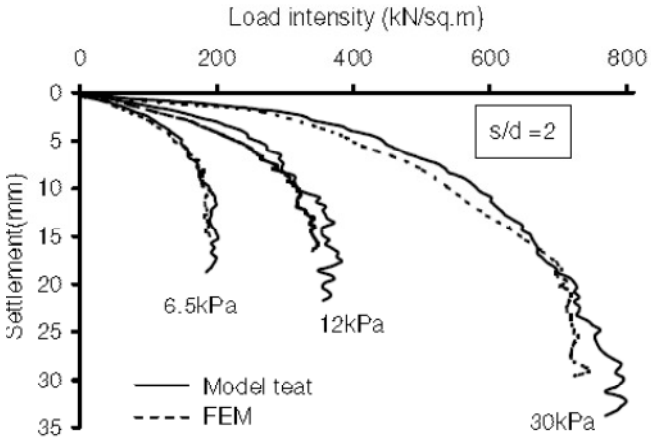

Figure 2.63 Load – settlement curves at different shear strength; column area alone loaded (Ambily, 2004)

Figures 2.63 and 2.65 show the load-settlement behavior for different shear strengths, and the same space to diameter ratio of 2, whereas Figure 2.64 and

2.66 show the load-settlement behavior for different s/d ratios with same shear strength of 12 kPa. (Ambily, 2004)

Ambily (2004) concludes that s/d ratio of 4 compared to the load settlement for s/d ratio of 2 and 3, does not show considerable improvement.

Figures 2.67 and 2.68 show load-displacement relationships of model tests conducted by McKelvey (2004) for circular and strip footing tests on transparent (TCD) clay. The footing pressure is normalized by consolidation pressure for the illustration.

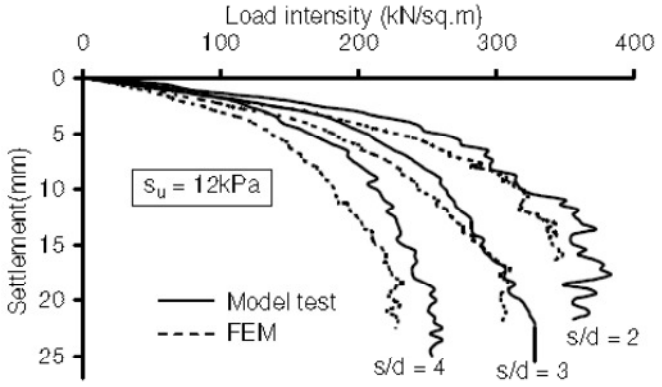

Figure 2.64 Load – settlement curves for different s/d ratios; column area alone loaded (Ambily, 2004)

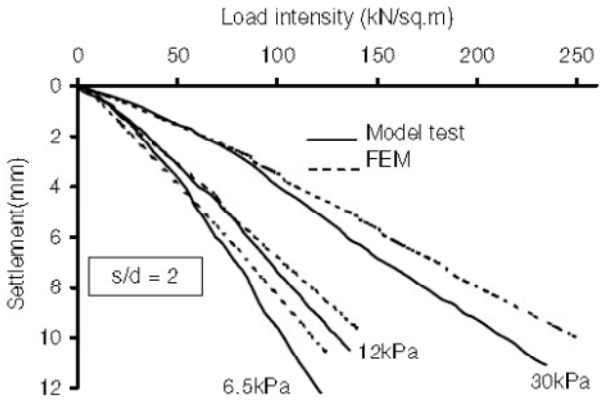

Figure 2.65 Load –settlement curves for different shear strength; entire area loaded (Ambily, 2004)

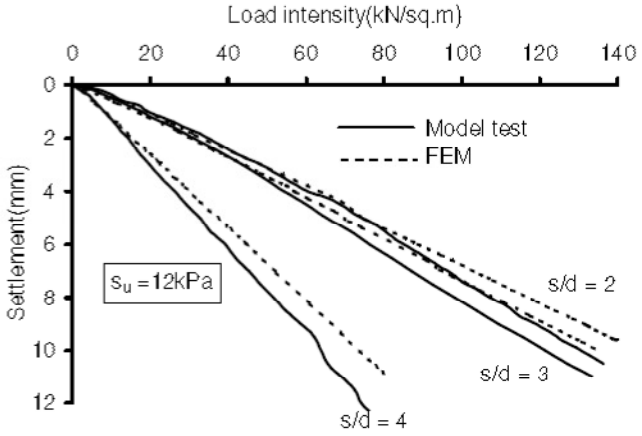

Figure 2.66 Load – settlement curves for different s/d ratios; entire area loaded (Ambily, 2004)

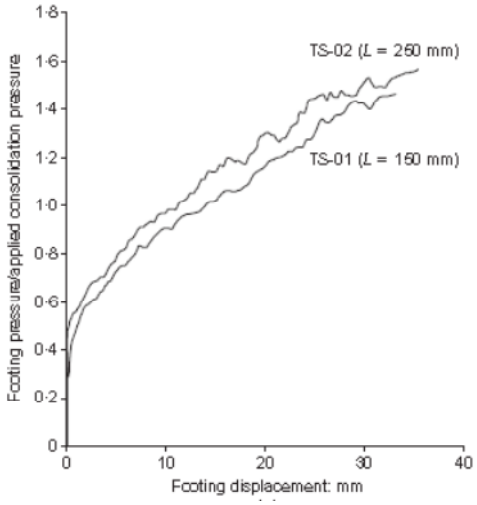

Figure 2.67 Normalized load-displacement relationships for circular footings supported on small groups of sand columns (transparent material tests) (McKelvey, 2004)

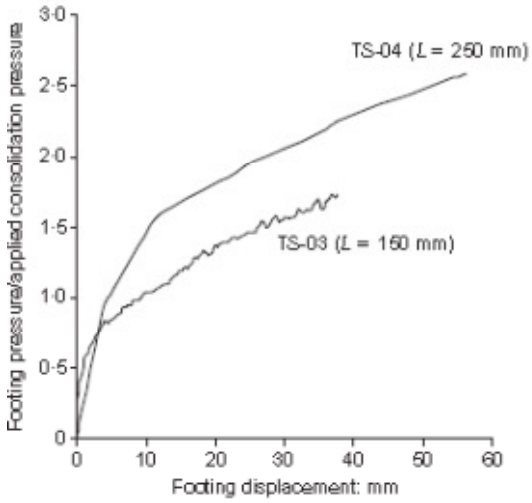

Figure 2.68 Normalized load-displacement relationships for strip footings supported on small groups of sand columns (transparent material tests) (McKelvey, 2004)

The deformation characteristics are illustrated in Figures 2.69 and 2.70. McKelvey (2004) discusses that as the L/d ratio increased from 6 to 10, the load carrying capacity of the composite ground also increases, however the bottom parts of the columns show little deformation. Moreover, McKelvey (2004) suggests the optimum column length to diameter ratio to be between 6 and 10. No considerable increase in the load carrying capacity suggested to be obtained beyond a L/d ratio than 10.

McKelvey (2004) implies that shorter columns ($L/d > 6$) give sufficient load carrying capacity, whereas longer columns may be needed for settlement control.

Figure 2.71 shows the normalized load –footing displacement relationships for pad footings supported on a small group of granular columns (Mc Kelvey, 2004).

Figure 2.72 shows the load settlement behaviour of the stone columns studied by Christoulas (2000).

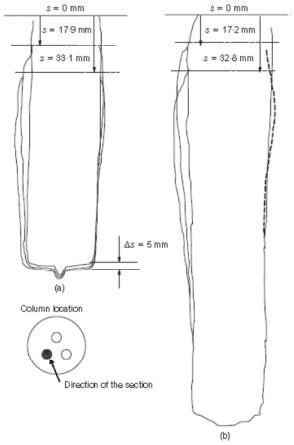

Figure 2.69 Outlines of sand columns during foundation loading process, circular footing (a) TS-01, column length 150mm; (b) column length 250 mm (McKelvey, 2004)

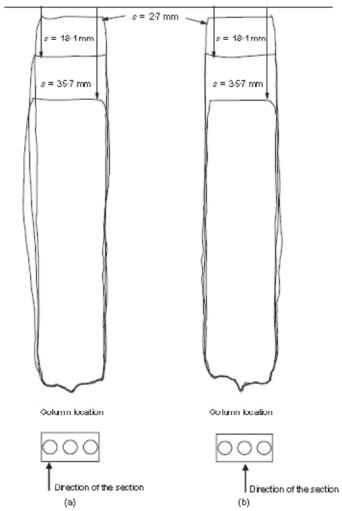

Figure 2.70 Outlines of sand columns during foundation loading process, strip footing, column length 150 mm, TS-03: (a) edge column; (b) centre column (McKelvey, 2004)

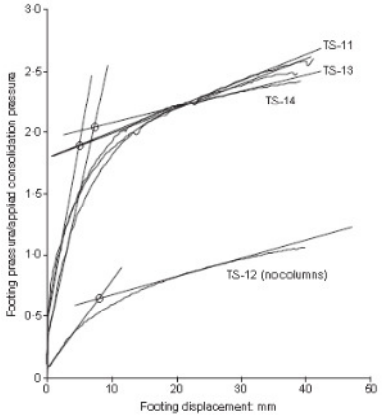

Figure 2.71 Normalized load-displacement relationships for pad footings supported on a small group of granular columns (kaolin tests TS-11, TS-12, TS-13 and TS-14) (McKelvey, 2004)

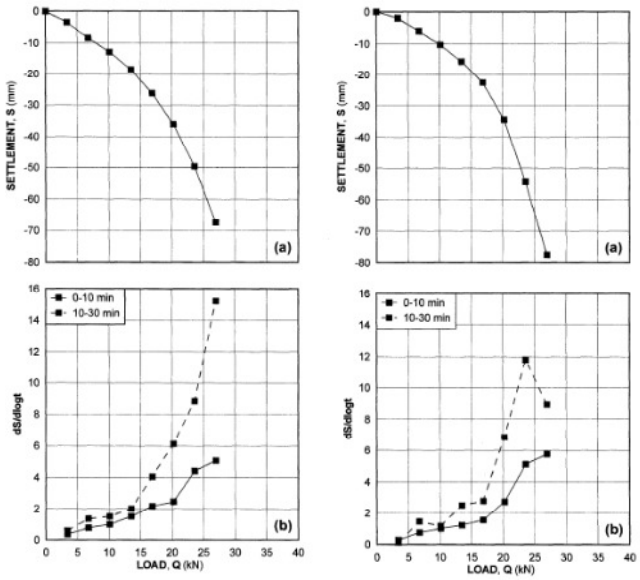

Figure 2.72 Vertical load and settlement measurements for stone column 1 and stone column 2 (a) load-settlement relation (b) logarithmic time rate of settlement (Christoulas, 2000)

CHAPTER 3

EXPERIMENTAL SETUP AND TEST PROCEDURE

3.1 General

Despite the developments in the last decade, there are still unclear points in the settlement reduction effect of floating types of stone columns.

A testing programme was planned with floating type stone columns of varying lengths and end bearing columns to determine both the footing settlements. Settlements at predefined depths are measured to estimate the settlement behaviour of the stone column treated ground and their settlement reduction effects.

3.2 Materials

3.2.1 Commercial Kaolinite Type of Clay

Commercially available kaolinite type of clay was preferred to simulate clay behaviour due to its less expansive character.

The mineralogical and chemical properties of the kaolinite published by the manufacturer are given in Tables 3.1 and 3.2. The plastic limit (PL) of kaolinite was 33% and the liquid limit (LL) was 48%, thus the plasticity index is calculated to be 15%. The specific gravity of the clay was found as $G_s = 2.62$. Material

characteristics of the kaolinite used to represent soft clay are represented in Table 3.3, and the hydrometer results are given in Figure 3.1. Table 3.4 shows the coefficient of volume compressibility, m_v values with respect to the given stress intervals and Figure 3.2 represents the void ratio-effective stress relationship of the clay.

At the end of consolidation stage, prior to stone column installation, vane shear tests were done to clay. In addition to this, at the end of the loading test unconfined compression tests were conducted in order to determine the undrained shear strength, c_u of clay. Undrained shear strength values obtained by vane shear test range between 25-32 kPa, whereas the values obtained from unconfined compression test range between 29-38 kPa.

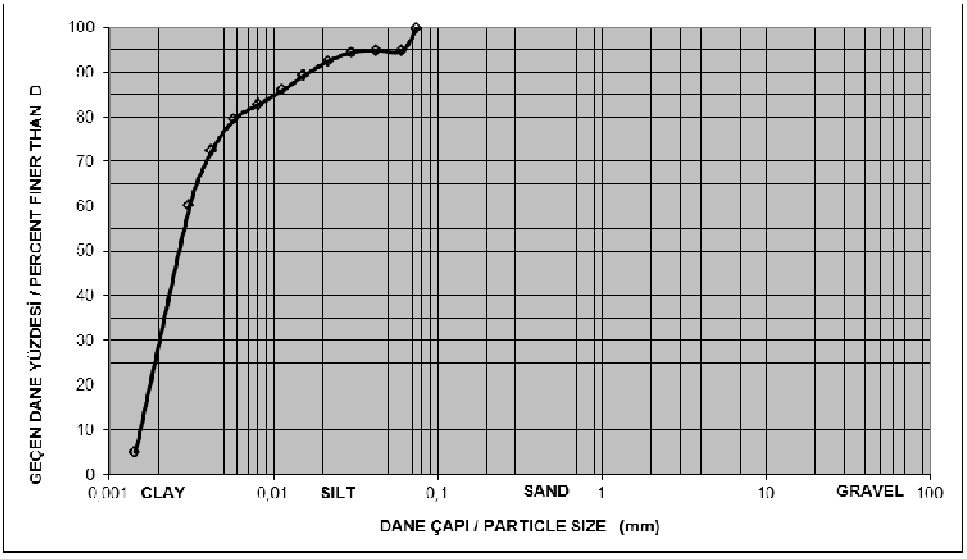

Figure 3.1 Hydrometer results of the kaolin clay

Table 3.1 Mineralogical composition of the kaolinite used in model tests (given by the manufacturer)

Type of Mineral	Volumetric content (%)
Clay Mineral	90,97
Sodium Feldspar	0,08
Potassium Feldspar	2,31
Free Quartz	4,45

Table 3.2 Chemical composition of the kaolinite used in model tests (given by the manufacturer)

Chemical Analysis	%
Loss on Ignition	12,77
SiO_2	48,56
Al_2O_3	36,62
TiO_2	0,64
Fe_2O_3	0,35
CaO	0,38
MgO	0,1
Na_2O	0,01
K_2O	0,39

The kaolin which was bought in sacks from Kale Maden Company in Çanakkale, was first dried in the oven for one day and then ground into a powder form (Figure 3.3).

The kaolin clay is prepared at a moisture content of 40% in order to achieve a desired consistency, and then the prepared slurry was left in the moisture room for at least 3 days for homogeneity of the moisture.

Table 3.3 Material properties of the kaolinite used in model tests

Property	**Value**
Liquid Limit	48 %
Plastic Limit	33%
Plasticity Index	15 %
Undrained Shear Strength, c_u after 1-D consolidation under 40 kPa	25-32 kPa
Undrained Shear Strength, c_u after loading test	29-38 kPa
Compression Index, C_c	0.213
Expansion Index, C_e	0.050

Table 3.4 Coefficient of volume compressibility, m_v, values of clay

Stress Interval (kPa)	m_v(m^2/kN)
25-50	0.00140
50-100	0.00054
100-200	0.00035
200-400	0.00021
400-800	0.00011
800-1600	0.00008
1600-400	0.00003
400-100	0.00014
100-25	0.00043

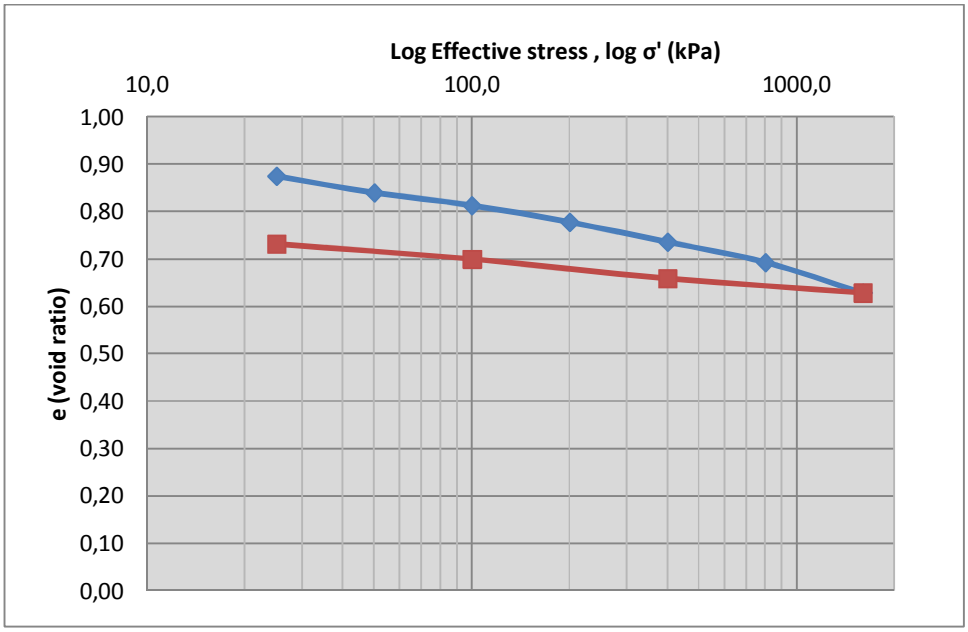

Figure 3.2 Void ratio-effective stress relationship of the clay used in the experiments

Figure 3.3 Kaolitine type of clay in powdered form

3.2.2 Sand

As mentioned in the literature review section before, Shahu and Reddy (2011) state that stone columns are usually constructed with particle sizes of $D = 25 - 50$ mm and have diameters varying between $d = 0{,}6 - 1.0\ m$. Wood et al (2000) emphasizes that d/D ratio varies between 12-40. The particle sizes of the sand used for granular column installation in the model tests were kept between 2 mm and 300 µm, which leads to d/D ratios of 10-67. The sand sample constituting the granular columns was wet sieved through the #200 sieve in order to have a sand sample with no fines. Than sand particles passing the #10 sieve and retained on the #50 sieve were used. Sieve analysis of the sand used for stone column construction is given on Figure 3.4.

A relative density, D_R of 65% was used for the granular columns, since Shahu and Reddy (2011) emphasize that uniformity of the stone column diameter may not be certified after compaction to relative density of 80%.

The specific gravity, G_s was found as 2.71. Minimum void ratio, e_{min} and the maximum void ratio, e_{max} were calculated as 0.60 and 1.32 respectively. Material properties of the sand are summarized in Table 3.5.

The stress-strain relationships of the sand for cell pressures of, $\sigma_3 = 20$, 40, 60 kPa obtained from triaxial tests are represented in Figures 3.5, 3.6, 3.7, and Mohr circles were given in Figure 3.8.

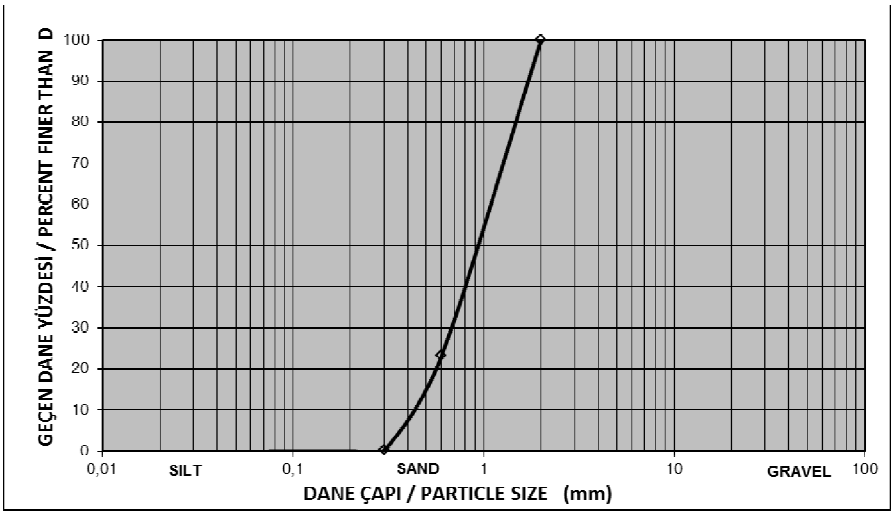

Figure 3.4 Sieve analysis of the sand used for granular column

Table 3.5 Material properties of the sand used in model tests

Property	Value
Particle size	0.30 mm-2.00 mm
Friction angle, φ	47°
Minimum void ratio, e_min	0.60
Maximum void ratio, e_max	1.32
Dry density, ρ for D_R= 65%	1.46 g/cm^3
Coefficient of uniformity, C_U	2.33
Coefficient of curvature, C_Z	1.14

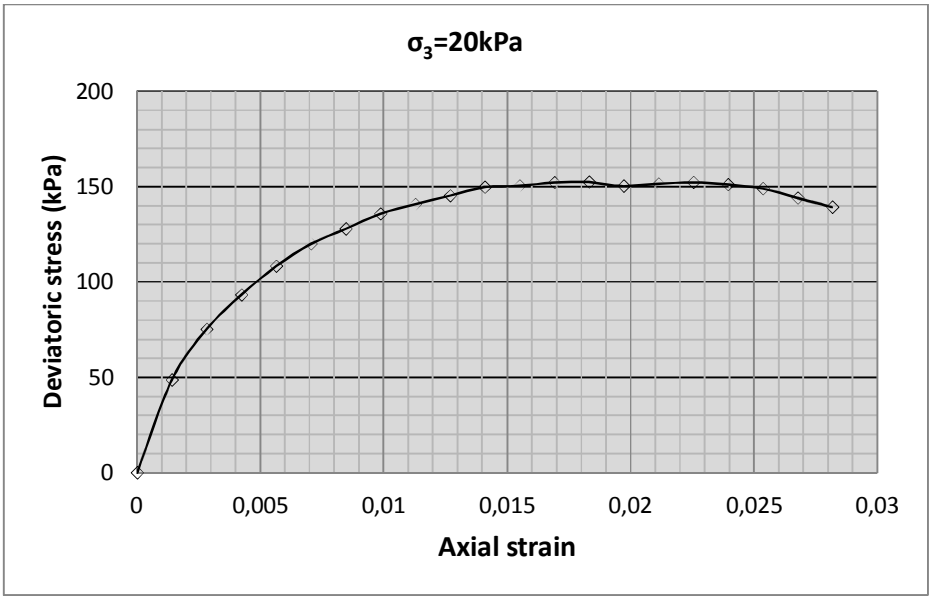

Figure 3.5 Stress-strain graph of sand obtained by triaxial test; cell pressure, σ_3=20 kPa

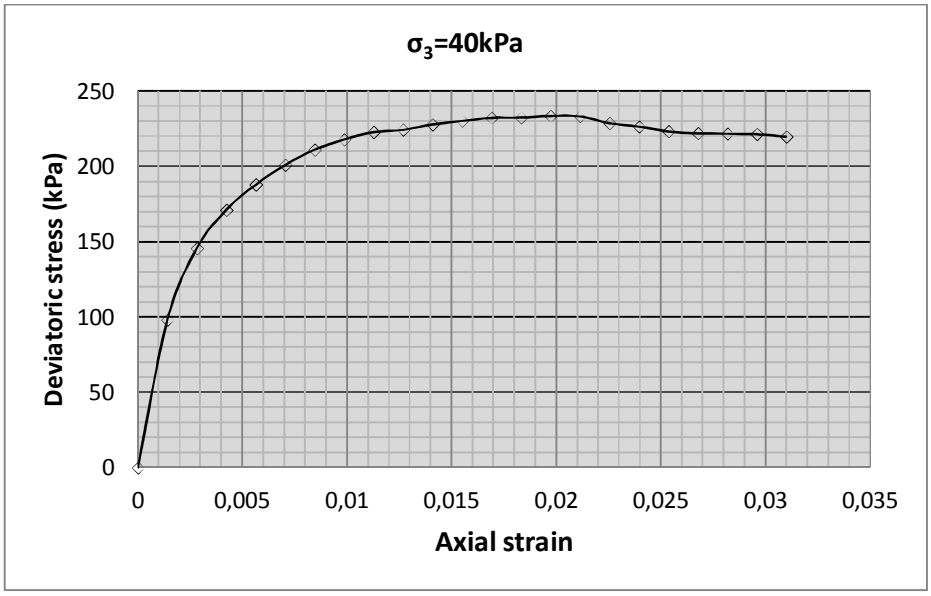

Figure 3.6 Stress-strain graph of sand obtained by triaxial test; cell pressure, σ_3=40 kPa

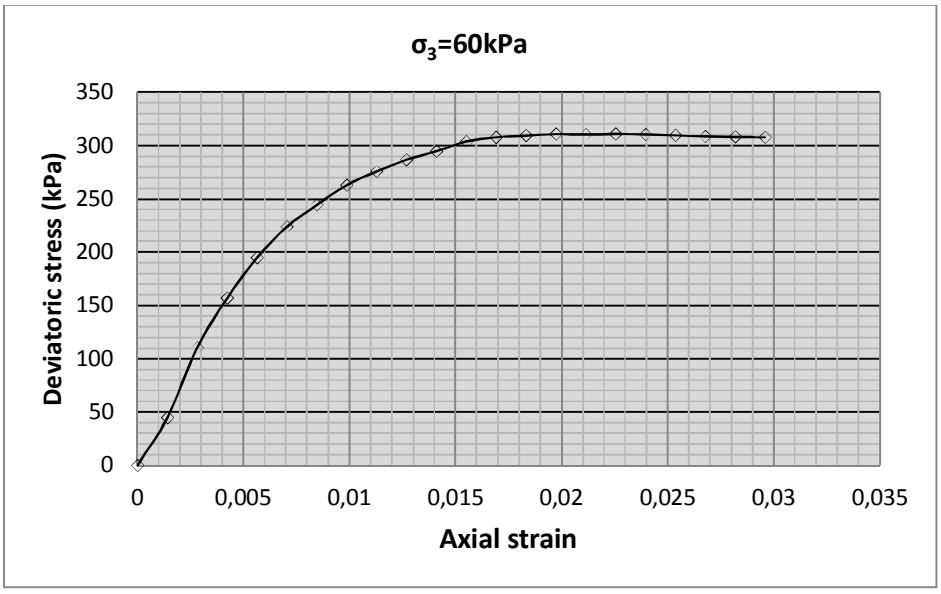

Figure 3.7 Stress-strain graph of sand obtained by triaxial test; cell pressure, σ_3=40 kPa

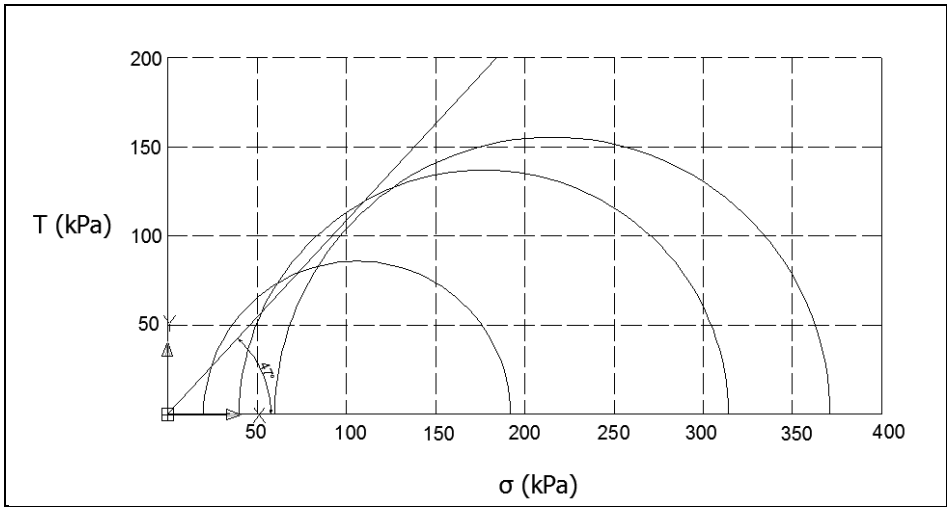

Figure 3.8 Mohr circles for sand

3.3 Experimental Set-Up

The system used in this experimental study consists of the following elements;

- Plexiglas model box
- Extension of the plexiglas model box
- Model footing
- Geotextile
- Air jack system with load frame for the application of constant consolidation pressure
- Loading hanger
- Mini plates for settlement measurement
- Dial gauges

Schematic and plan views of the test setup are illustrated in Figures 3.9-3.15.

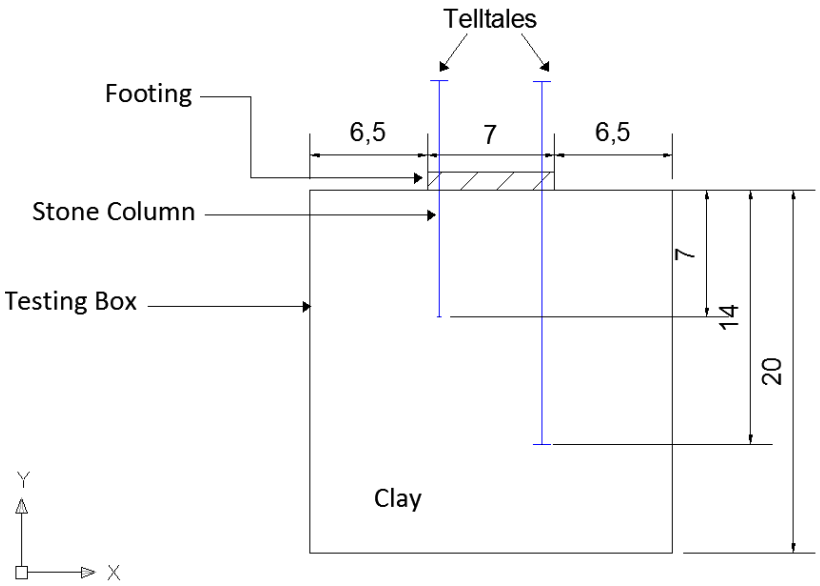

Figure 3.9 Schematic view of the test setup; no improvement *(Dimensions are in cm)*

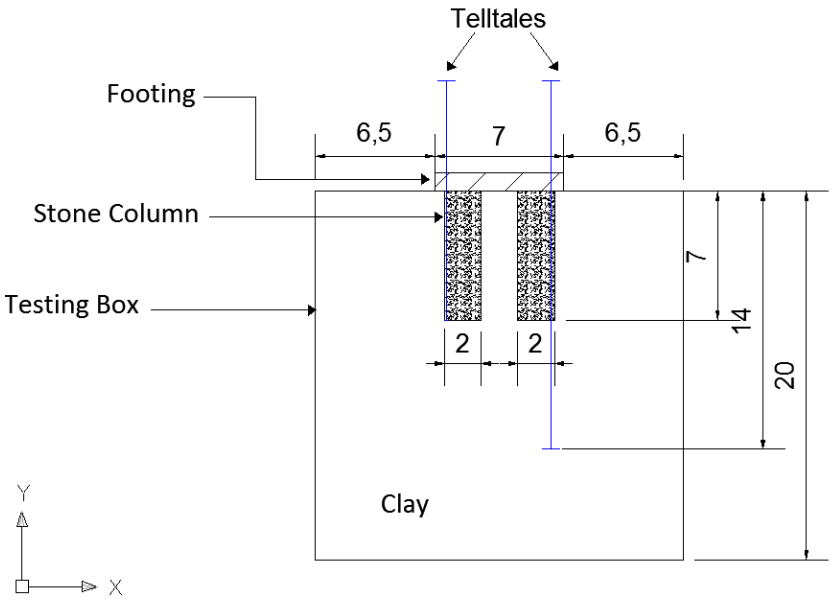

Figure 3.10 Schematic view of the test setup; L/B= 1.00 *(Dimensions are in cm)*

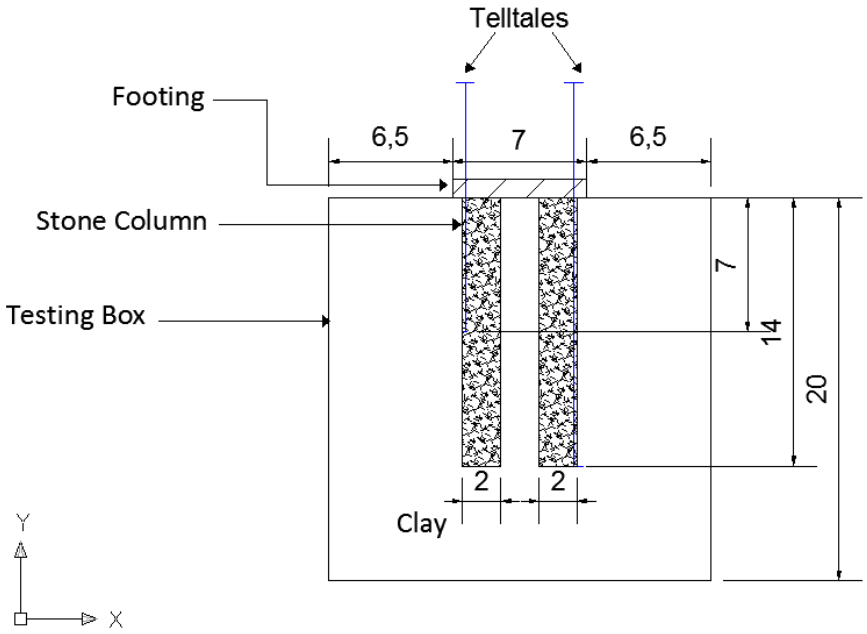

Figure 3.11 Schematic view of the test setup; L/B= 2.00 *(Dimensions are in cm)*

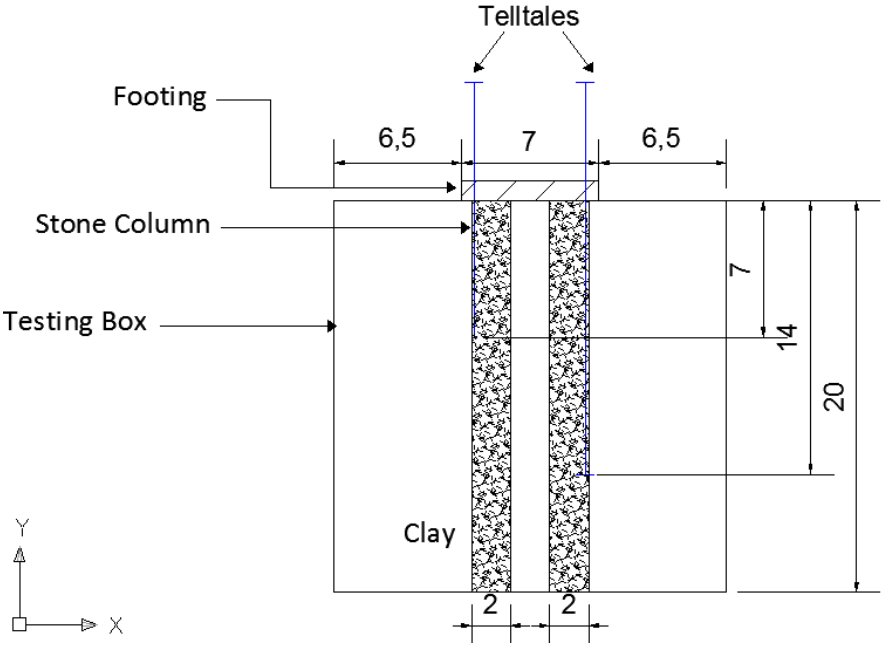

Figure 3.12 Schematic view of the test setup; L/B= 2.86 *(Dimensions are in cm)*

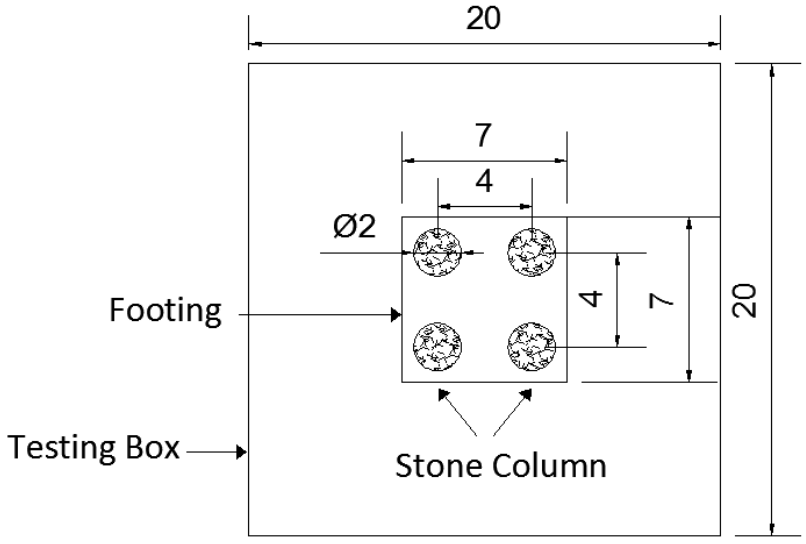

Figure 3.13 Plan view of the test setup *(Dimensions are in cm)*

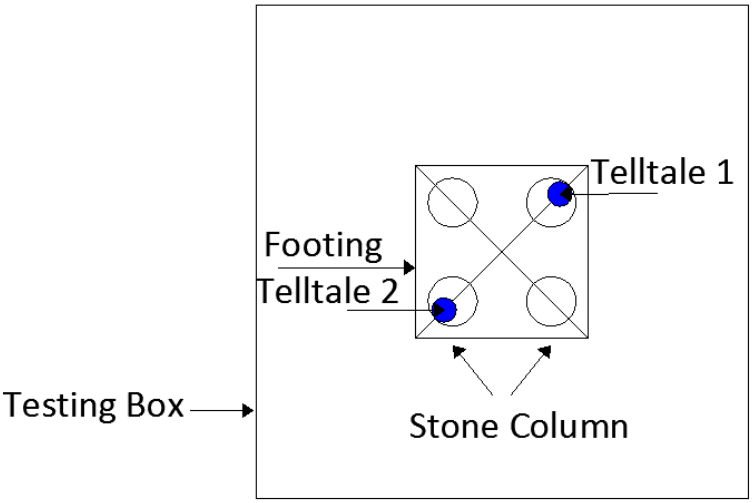

Figure 3.14 Plan view of telltales (TS1, TS2, TS3, TS4)

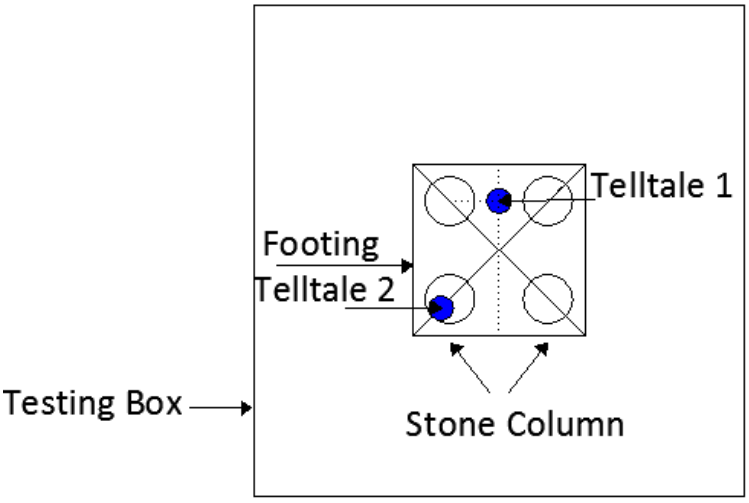

Figure 3.15 Plan view of telltales (TS2')

3.3.1 Testing Box

Tests were conducted on 200 mm* 200 mm* 200 mm cubic loading tanks (Fig. 3.16) with 50 mm*200 mm* 200 mm extensions (Fig. 3.17). Both the extension and the model box has 10 mm wall thickness. The extension is removed and 50 mm top portion of the clay is trimmed after the consolidation period fulfilled.

Figure 3.16 Plexiglas Model Box

Figure 3.17 Plexiglass Extension

3.3.2 Model Footing

A square plexiglas piece with 70 mm* 70 mm dimensions is used as a model footing (Fig. 3.18). The thickness of the footing is 10 mm.

It is known that vertical effective pressure distributions extend down to 2B and a zone around the footing should be 2.5-3 times of the footing width. Thus, in order to form a medium like an elastic half space above mentioned dimensions were chosen.

Figure 3.18 Plexiglas Model Footing

3.3.3 Geotextile

Two pieces of geotextile (Fig. 3.19) were cut and placed in the test box in order to allow the drainage and to prevent drying of the clay foundation.

Figure 3.19 Geotextile

3.3.4 Air Jack System

Air jack with load frame (Figs 3.20, 21) was used to apply the constant consolidation pressure. 40kPa of consolidation pressure was applied for at least 28 days to the specimens for the completion of consolidation stage. Air pressure regulators (Fig. 3.22) were used to adjust the pressure to be applied.

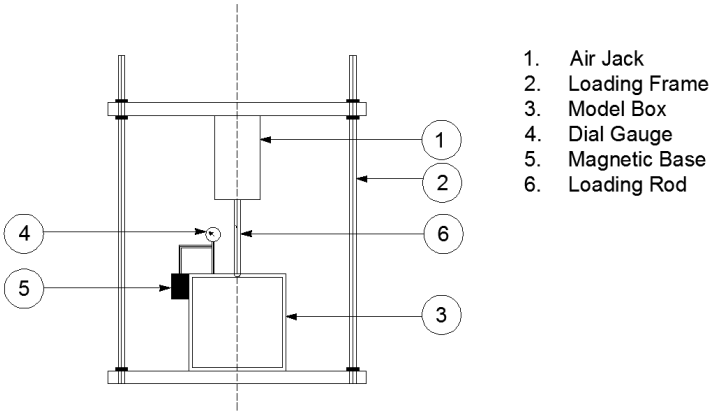

Figure 3.20 Schematic view of the air jack system

Figure 3.21 Air jack system

Figure 3.22 Air pressure regulators

3.3.5 Loading Hanger

A loading hanger (Figs. 3.23, 24) was used to apply constant footing pressure during the test.

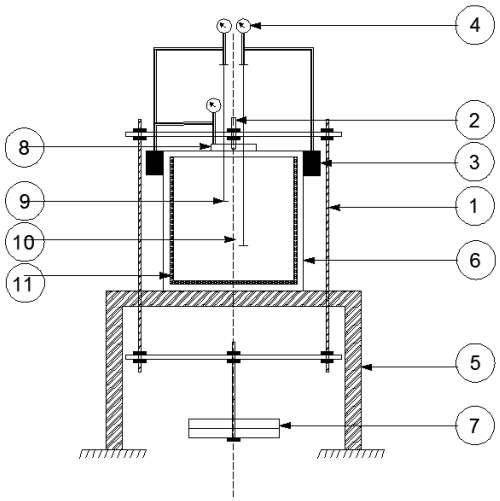

1. Loading Frame
2. Loading Rod
3. Magnetic Base
4. Dial Gauges
5. Steel Frame
6. Model Box
7. Load
8. Model Footing
9. Telltale 1 (at depth7cm)
10. Telltale 2 (at depth 14cm)
11. Geotextile

Figure 3.23 Schematic view of loading hanger

Figure 3.24 Loading Hanger System

3.3.6 Dial Gauges

50 mm, 30 mm, 20 mm and 10 mm capacity mechanical dial gauges (Fig. 3.25) with a sensitivity of 0.01 mm were used to determine the vertical displacements of both footings and the telltales. One dial gauge was needed for the sample at consolidation stage, for the determination of whether the consolidation is completed or not, and three dial gauges were needed at footing loading stage, one of which to be placed on the footing, and two of which to be placed on the telltales to determine the vertical displacements.

Figure 3.25 Dial Gauges

3.3.7 Telltales for Subsurface Settlement Measurement

Telltales (Fig. 3.26) were placed at different levels of sand columns to measure the subsoil settlements. Two telltales were used for each model test, one placed at 70 mm depth and the second placed at 140 mm depth.

Figure 3.26 Telltales for subsurface settlement measurement

3.4 Procedures

3.4.1 Specimen Preparation

Firstly, the purchased kaolin sample was dried in oven for 24 hours. After drying, it was powdered by a grinder. Powdered form of kaolin clay was then mixed with water in order to have a water content value of 40 % with the aid of mechanical mixer (Fig. 3.27). The prepared slurry was then placed in nylon bags and was left in the moisture room for at least 3 days prior to placing in the model box in order to make a homogeneous clay slurry.

Figure 3.27 Mechanical Mixer

3.4.2 Stone Column Construction

In this experimental work granular columns of 20 mm diameter were used. In order to drill boreholes, a hand auger (Fig. 3.28) and a guide plates (Fig. 3.29) were used. Rammers (Fig. 3.30) were used for the densification of sand to obtain the desired relative density of 65 %.

For the each length of stone column to be installed, the required weight of sand is calculated according to the dry density,ρ value to obtain the desired relative density value,D_R of 65%. Calculation procedure is summarized as follows;

$$D_R = \frac{e_{max} - e}{e_{max} - e_{min}}$$

The required void ratio ,e for D_R=65% is calculated to be 0,85 for;

e_{max}=1.32 and e_{min}=0,60

$$\rho_d = \frac{G_s}{1+e} * \rho_w$$

Where;

G_s=2.71 and e=0.85

Dry density of sand required for the dry density, D_R of 65% is calculated to be;

$$\rho_d = 1.465 \frac{g}{cm^3}$$

According to the dry density value obtained the required mass of sand per column are shown in Table 3.6.

Table 3.6 The required mass of sand per each column for varying lengths

Stone column length, L (mm)	**Mass of sand needed per column, M (g)**	**Relative Density, D_R (%)**
70	32.20	65
140	64.40	65
200	92.00	65

Figure 3.28 Auger

Figure 3.29 Guide plates

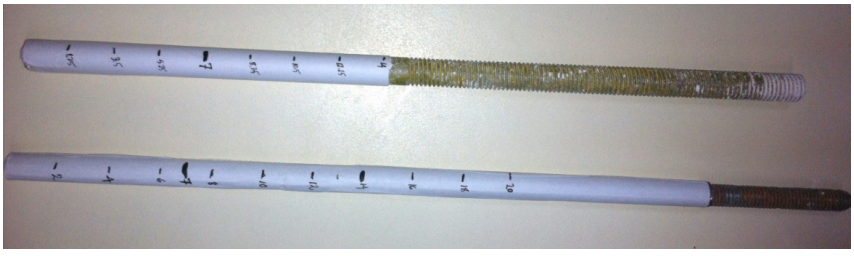

Figure 3.30 Rammers for Sand Densification

3.4.3 Testing Procedure

The testing procedure is as follows;

1. The model testing box was covered inside with geotextile.
2. The prepared clay sample was placed in the model box layer by layer by hand. (Fig. 3.31)

Figure 3.31 Placement of the prepared slurry in the model box

3. The model testing box was then placed to the jack system for the application of consolidation procedure. (Fig. 3.32)

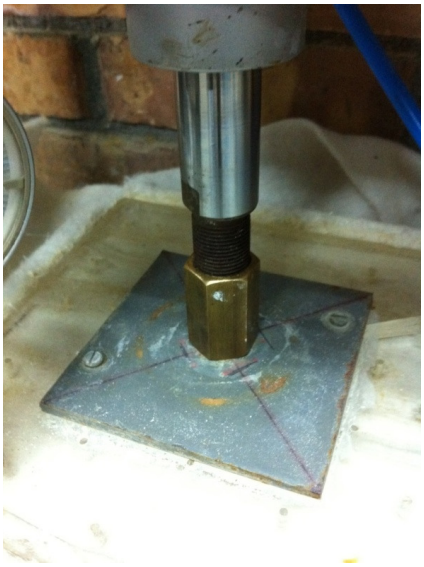

Figure 3.32 Application of consolidation pressure (40kPa) with the jack system

4. 40 kPa of consolidation pressure was applied. Consolidation time is about 3 to 4 weeks. Asaoka Method was used to check whether the consolidation stage was completed or not.

5. After the completion of consolidation, the specimen was unloaded and left to heave for 2-3 hours. Afterwards, the plexiglas extension of 50 mm height was removed and the top portion of clay was trimmed and flattened (Figs. 3.33, 34).

Figure 3.33 Removal of the 50 mm top portion and flattening the surface

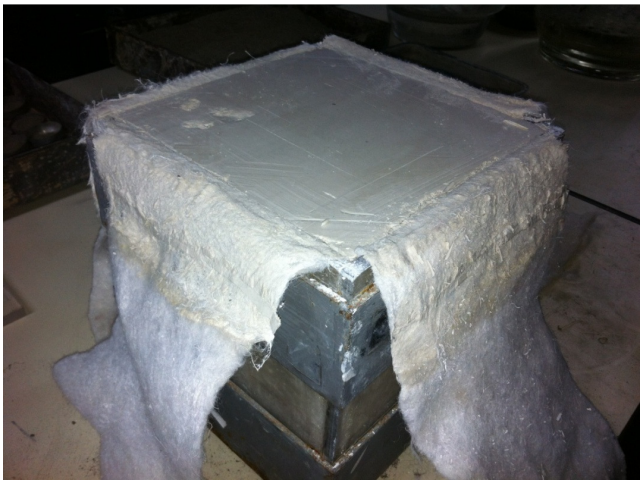

Figure 3.34 Flattened surface

6. After flattening the surface, laboratory vane shear tests were done for shear strength determination of the consolidated sample. (Fig. 3.35)

Figure 3.35 Vane shear test

7. Guide plates with an area replacement ratio, a_s= 25.65% was placed on the surface (Fig. 3.36). An auger (Fig. 3.37) with a diameter of 20 mm was used to prepare the boreholes of desired depth (70 mm, 140 mm, and 200 mm).

Figure 3.36 Placement of the guide plates

Figure 3.37 Drilling the specimen

8. Samples for water content determination were taken from the soil that came out of the holes.

9. The boreholes were filled with the predetermined mass of sand. For each column, the length and the sand mass required are divided equally, and

the granular material is rammed until the desired densification of each layer is achieved. The corresponding masses of granular material required for 65% relative density is given in Table 3.5 for varying column lengths. (Figs. 3.38, 39, 40, 41)

Figure 3.38 Sand used for stone column construction

Figure 3.39 Equally weighed sand samples

Figure 3.40 Filling the boreholes

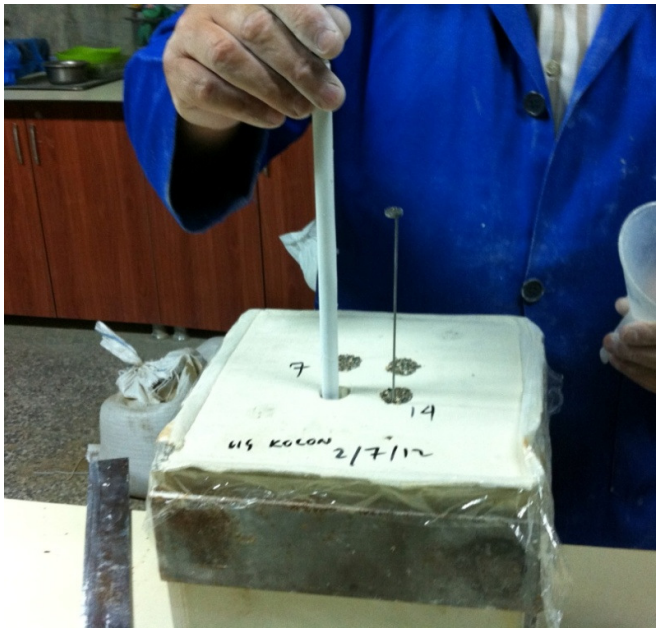

Figure 3.41 Ramming for the densification of the sand

10. Telltales which were used for measuring subsurface settlements, were placed at the 70 mm and 140 mm depths (Fig. 3.42). Prior to placement of the telltales, rods were covered with shredded plastic pipe in order to eliminate the friction between the sand and the rods.

Figure 3.42 Placement of telltales

11. After the sand column installation model footing was placed on the surface (Fig. 3.43).

Figure 3.43 Placement of the model footing

12. Three dial gauges were placed one on the footing and the other two on telltales for vertical subsurface settlement measurements. (Fig. 3.44)

Figure 3.44 Placement of dial gauges

13. The reference (t=0) dial gauge readings were taken prior to the loading stage.

14. Then a pressure of 75 kPa was applied to the footing by the loading hanger (Figure 3.45).

Figure 3.45 Application of 75 kPa vertical pressure with loading hanger

15. Daily dial gauge readings were taken for the footing and telltales.

16. After the completion of the test unconfined compression tests were done to the specimens taken from the model box for undrained shear strength determination. (Figure 3.46)

Figure 3.46 Unconfined compression test

CHAPTER 4

PRESENTATION OF TEST RESULTS

4.1 Introduction

In this study, a total number of 4 test series were conducted. For the improved ground, tests were carried out with four granular columns of 20 mm diameter, an area replacement ratio, a_s of 25.65 %, and relative density, D_R of 65 %. 75 kPa of pressure was applied to the model footing of dimensions 70mm*70mm for all the test series.

During these tests, vertical displacements of the model footing and telltales were measured by dial gauges with a sensitivity of 0,01 mm.

In these tests, stone columns were both floating and end bearing type. The only variable in the test series is the column length. Moreover, reference tests were conducted in order to simulate the untreated soil behavior, and to estimate the settlement reduction effect of granular columns installed. Table 4.1 summarizes the testing schedule.

Table 4.1 Testing schedule

Test Series	Number of Stone Columns	Column Diameter, D (mm)	Column Length, L (mm)	Area Replacement Ratio, a_s (%)	Model Footing Dimensions (mm*mm)	Pressure Applied (kPa)	Relative Density of Stone Column (%)
TS1	-	-	-	-	70*70	75	-
TS2&TS2'	4	20	70	25.65	70*70	75	65
TS3	4	20	140	25.65	70*70	75	65
TS4	4	20	200	25.65	70*70	75	65

4.2 Tests on Unimproved Soil

In the beginning of the model study, several tests on unimproved clay were conducted in order to estimate the untreated soil behavior. Table 4.2 shows the total settlements (footing settlements) of the unimproved ground for various tests. Total five untreated tests were performed in order check the consistency of the results and to obtain a mean value. The subsurface settlements of the unimproved ground obtained from telltales and average values are shown in Table 4.3 and Table 4.4, respectively.

Figure 4.1 illustrates the average vertical displacement-time behavior of footing, telltale 1 and telltale 2, moreover Figure 4.2 shows the settlement values with respect to depth.

Table 4.2 Footing settlements of the unimproved ground (TS1)

Test Number	Footing Settlement, $S_{t(unt)}$ (mm)
1	11.93
2	9.85
3	10.85
4	11.82
5	9.92

Table 4.3 Subsurface settlements of the unimproved ground (TS1)

Test Number	Subsoil Settlements (mm)	
	7 cm Depth	14 cm Depth
1	4.04	1.50
2	2.91	1.16
3	2.44	1.01
4	3.65	1.23
5	2.37	0.89

Table 4.4 Average subsurface settlements of the unimproved ground (TS1)

Depth (cm)	Settlements (mm)
0	10.87
7	3.08
14	1.16

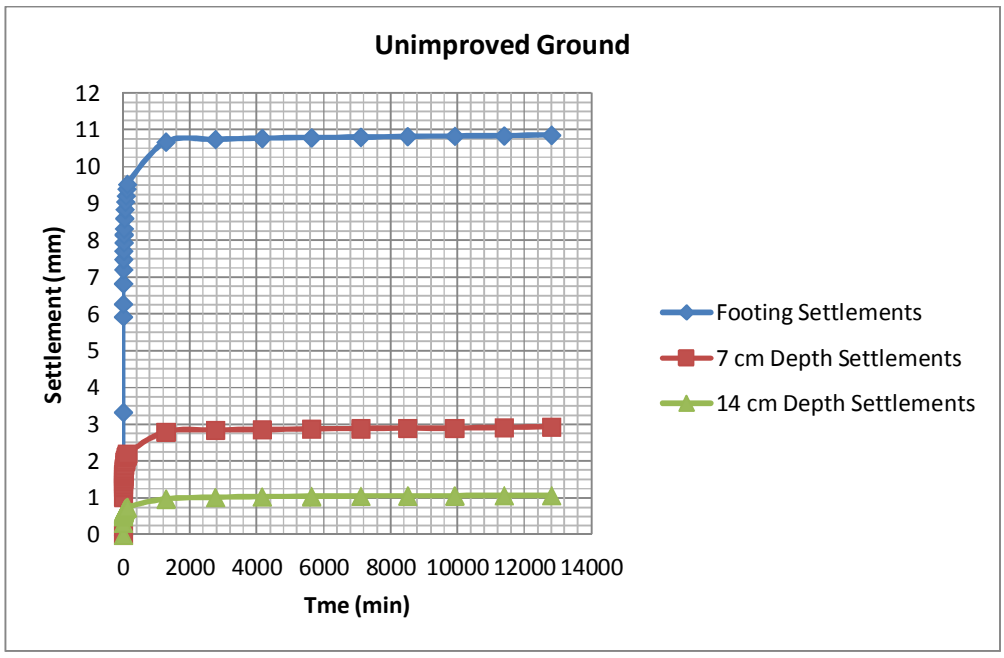

Figure 4.1 Average total and subsurface settlements, $S_{t(unimp)}$ of the unimproved ground (TS1)

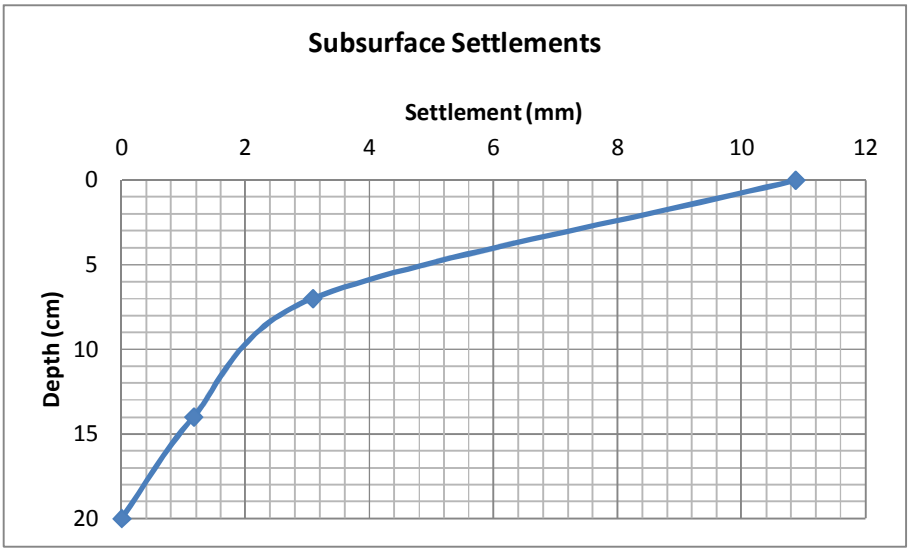

Figure 4.2 Average subsurface settlements, S_z of the unimproved ground (TS1)

4.3 Tests on Improved Soil With L=B

For the second test series, 7 cm length stone column treated soil was examined. The length of the column equals the footing width (B). Table 4.5 shows the total settlements (footing settlements) of the improved ground, $L = B$ for different tests. Table 4.6 shows the subsurface settlements of the composite ground obtained from telltales, whereas table 4.7 shows average values (TS2).

However, the measured settlement values at depth 7 cm were come out to be higher than the ones obtained from the unimproved tests. In order to check the consistency of the results, another test series (TS2') consisting of another 4 tests were conducted by placing the first telltale directly in soft clay at depth 7cm (B), rather than placing it under the stone column (Figure 3.15). Although the settlements measured at footing level and at depth 14 cm $(2B)$ were consistent for test series TS2 and TS2', the measured subsurface settlements at 7 cm depth differ from each other. The subsurface settlements measured at 7 cm (B) depth came out to be lower than that of the unimproved tests, which seems to be more closer to the expected behavior. This point forward settlement values obtained from test series TS2' were taken into consideration for the improved ground, $L = B$ behavior. The corresponding settlement values of test series TS2' are tabulated in Table 4.8 and Table 4.9, whereas Table 4.10 shows average values.

Figure 4.3 illustrates the average vertical displacement-time behavior of footing, telltale 1 and telltale 2, moreover Figure 4.4 shows the settlement values with respect to depth for test series TS2'.

Table 4.5 Footing settlements of the improved ground, $L = B$ (TS2)

Test Number	Footing Settlement (mm)
1	7.43
2	6.69
3	7.88
4	5.91

Table 4.6 Subsurface settlements of the improved ground, $L = B$ (TS2)

Test Number	Subsoil Settlements (mm)	
	7 cm Depth	14 cm Depth
1	3.68	0.59
2	3.93	1.00
3	4.57	0.89
4	4.04	1.16

Table 4.7 Average subsurface settlements of the improved ground, $L = B$ (TS2)

Depth (cm)	Settlements (mm)
0	6.96
7	4.05
14	0.91

Table 4.8 Footing settlements of the improved ground, $L = B$ (TS2')

Test Number	Footing Settlement (mm)
1	7.22
2	6.64
3	6.73
4	6.20

Table 4.9 Subsurface settlements of the improved ground, $L = B$ (TS2')

Test Number	Subsoil Settlements (mm)	
	7 cm Depth	14 cm Depth
1	2.42	0.76
2	2.18	1.01
3	2.46	0.83
4	2.12	0.95

Table 4.10 Average subsurface settlements of the improved ground, $L = B$ (TS2')

Depth (cm)	Settlements (mm)
0	6.70
7	2.30
14	0.89

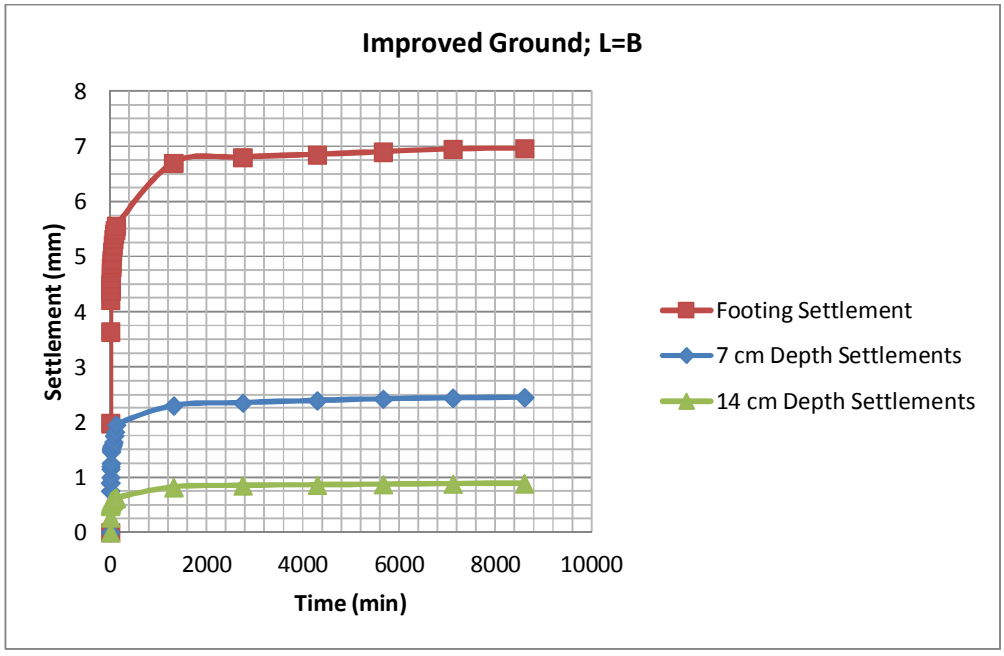

Figure 4.3 Average total and subsurface settlements, $S_{(L=B)}$ of the improved ground, $L = B$ (TS2')

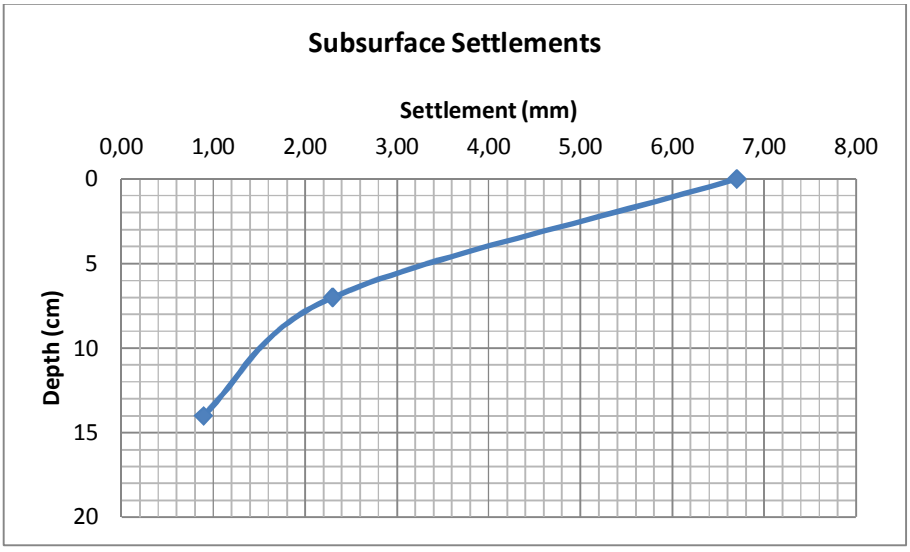

Figure 4.4 Average subsurface settlements, $S_{z(L=B)}$ of the improved ground, $L = B$ (TS2')

4.4 Tests on Improved Soil With L=2B

For the third test series, 14 cm length stone column treated soil was examined. The length of the column equals two times the footing width $(2B)$. Table 4.11 shows the total settlements (footing settlements) of the improved ground, $L = 2B$ for different tests. Total number of 4 tests were conducted for the consistency of the results. The subsurface settlements of the improved ground obtained from telltales and average values are shown in Table 4.12 and Table 4.13, respectively.

Figure 4.5 illustrates the average vertical displacement-time behavior of footing, telltale 1 and telltale 2, moreover Figure 4.6 shows the settlement values with respect to depth.

Table 4.11 Footing settlements of the improved ground; $L = 2B$ (TS3)

Test Number	Footing Settlement (mm)
1	3.29
2	3.31
3	3.39
4	3.74

Table 4.12 Subsurface settlements of the improved ground, $L = 2B$ (TS3)

Test Number	Subsoil Settlements (mm)	
	7 cm Depth	14 cm Depth
1	1.98	0.76
2	2.13	0.63
3	1.59	0.64
4	1.90	0.87

Table 4.13 Average subsurface settlements of the improved ground, $L = 2B$ (TS3)

Depth (cm)	Settlements (mm)
0	3.43
7	1.90
14	0.73

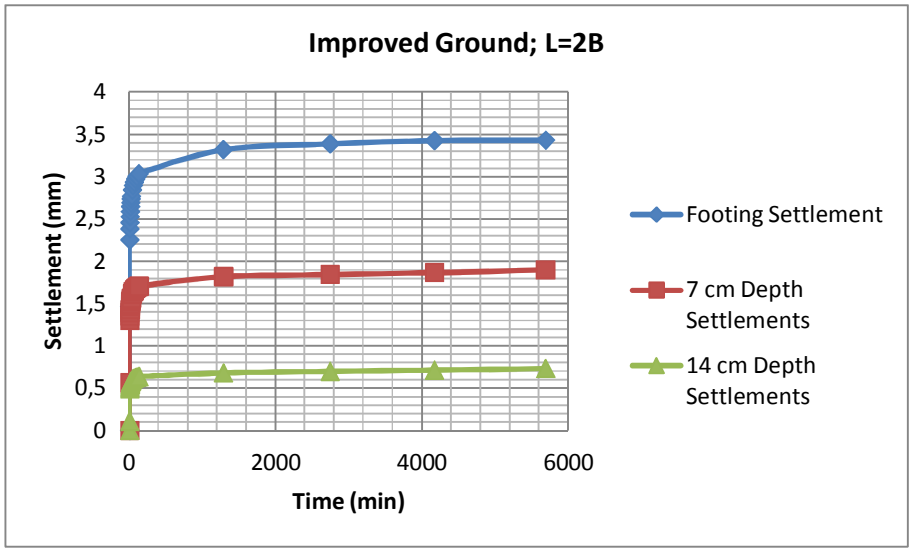

Figure 4.5 Average total and subsurface settlements, $S_{(L=2B)}$ of the improved ground, $L = 2B$ (TS3)

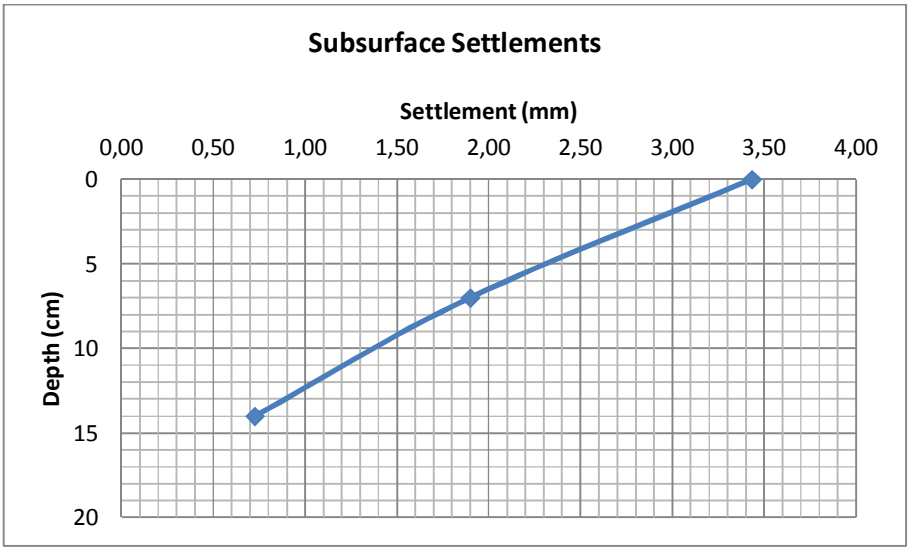

Figure 4.6 Average subsurface settlements, $S_{z(L=2B)}$ of the improved ground, $L = 2B$ (TS3)

4.5 Tests on Improved Soil With End Bearing Stone Column

For the fourth test series, 20 cm length (end bearing) stone column treated soil was examined. Table 4.14 shows the total settlements (footing settlements) of the improved ground, $L = 2.86B$ for different tests. Total number of 3 tests were conducted for the consistency of the results. The subsurface settlements of the improved ground obtained from telltales and average values are shown in Table 4.15 and Table 4.16, respectively.

Figure 4.7 illustrates the average vertical displacement-time behavior of footing, telltale 1 and telltale 2, moreover Figure 4.8 shows the settlement values with respect to depth.

Table 4.14 Footing settlements of the improved ground; End bearing (TS4)

Test Number	Footing Settlement (mm)
1	3.01
2	2.83
3	2.94

Table 4.15 Subsurface settlements of the improved ground; End bearing (TS4)

Test Number	Subsoil Settlements (mm)	
	7 cm Depth	14 cm Depth
1	1.73	0.66
2	1.62	0.64
3	1.54	0.57

Table 4.16 Average subsurface settlements of the improved ground, End bearing (TS4)

Depth (cm)	Settlements (mm)
0	2.93
7	1.63
14	0.62

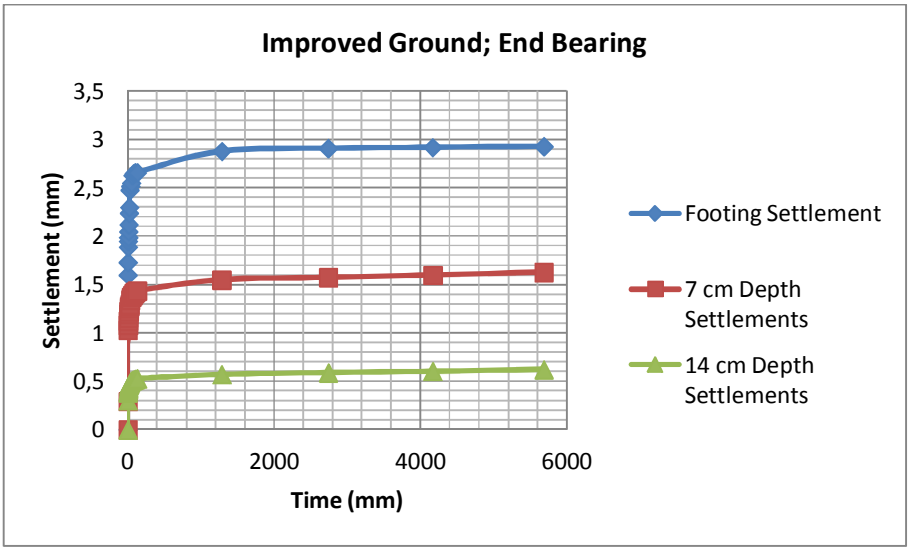

Figure 4.7 Average total and subsurface settlements, $S_{(end\ bearing)}$ of the improved ground, end bearing stone column (TS4)

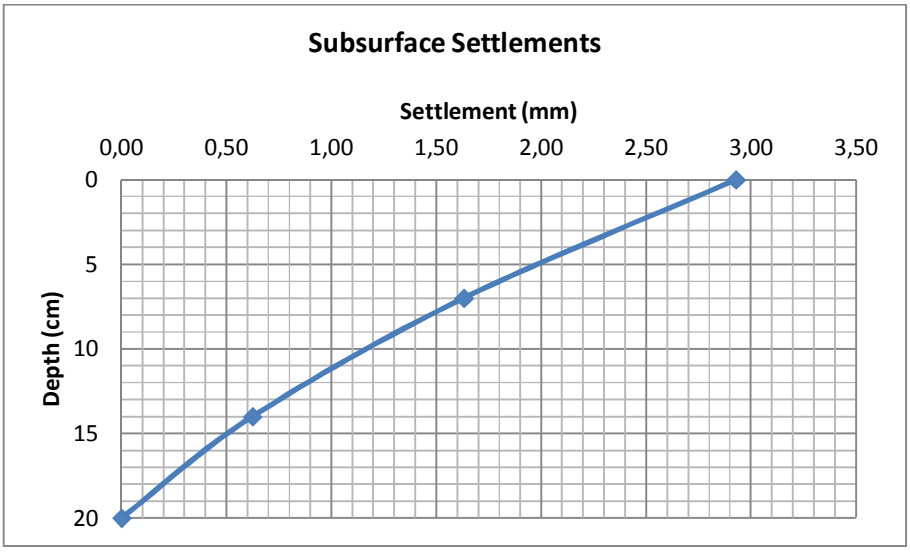

Figure 4.8 Average subsurface settlements, $S_{z(end\ bearing)}$ of the improved ground, end bearing stone column (TS4)

4.6 Individual Settlements of Layers

By placing two telltales at depths 7 cm and 14 cm, individual settlements of three layers can be determined. First and second layer have a height of 7 cm, whereas the third layer has a height of 6 cm (Figure 4.9). The vertical displacement of the third layer equals the vertical displacement of the telltale placed at 14 cm depth, on the other hand the settlement of the second layer plus the settlement of the third layer equals the vertical displacement of the telltale placed at 7 cm depth. Settlement of the first layer is obtained by subtracting the vertical displacement of the telltale placed at 7 cm depth from the total vertical displacement which equals to the settlement of the footing. These settlement calculations can be formulated as:

$$\delta_{layer\,1} = \delta_{total} - \delta_{telltale\,(7\,cm)} \tag{4.1}$$

$$\delta_{layer\,2} = \delta_{telltale\,(7\,cm)} - \delta_{telltale\,(14\,cm)} \tag{4.2}$$

$$\delta_{layer\,3} = \delta_{telltale\,(14\,cm)} \tag{4.3}$$

Where;

$\delta_{layer\,1}$: Settlement of the first layer,

$\delta_{layer\,2}$: Settlement of the second layer,

$\delta_{layer\,3}$: Settlement of the third layer,

δ_{total}: Total settlement (Footing settlement),

$\delta_{telltale\,(7\,cm)}$: Vertical displacement of the telltale placed at 7 cm depth,

$\delta_{telltale\,(14\,cm)}$: Vertical displacement of the telltale placed at 14 cm depth.

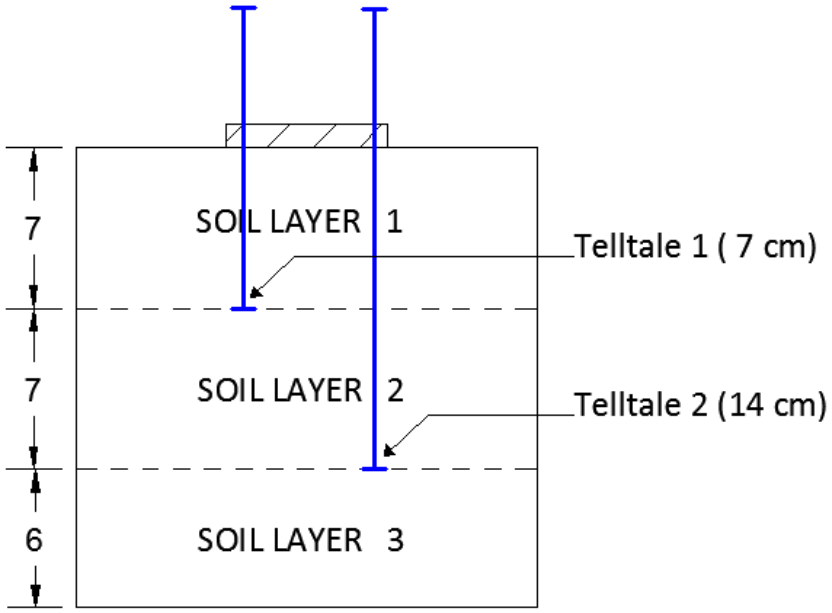

Figure 4.9 Representation of soil layers *(Dimensions are in cm)*

4.6.1 Layer Settlements of the Unimproved Ground

Table 4.17 shows soil layer settlements of the unimproved ground calculated by equations 4.1, 4.2, 4.3, whereas Figure 4.10 illustrates the settlement-time behaviour of the soil layers.

Table 4.17 Average layer settlements of the unimproved ground

Layer	Settlement (mm)
1	7.79
2	1.92
3	1.16

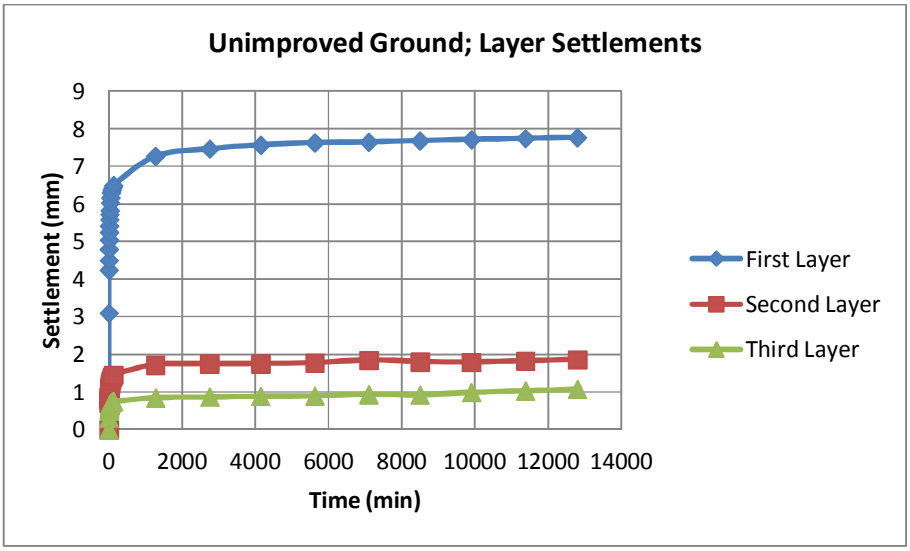

Figure 4.10 Unimproved ground; settlement-time graphs

4.6.2 Layer Settlements of the Improved Ground; L=B

Table 4.18 shows soil layer settlements of the improved ground, $L = B$, which were calculated by equations 4.1, 4.2, 4.3, whereas Figure 4.11 illustrates the settlement-time behaviour of the soil layers.

Table 4.18 Average layer settlements of the improved ground; $L = B$

Layer	Settlement (mm)
1	4.40
2	1.41
3	0.89

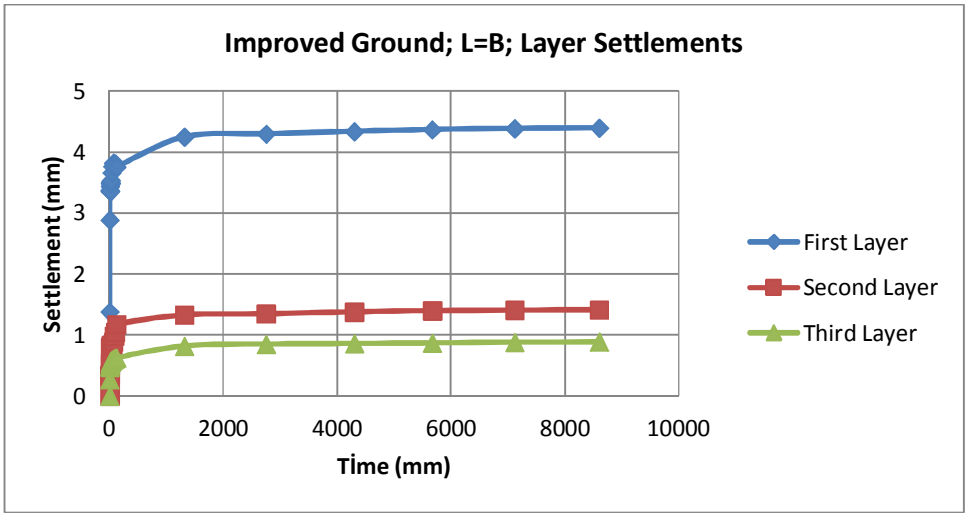

Figure 4.11 Improved ground; $L = B$; settlement-time graphs

4.6.3 Layer Settlements of the Improved Ground; L=2B

Table 4.19 shows soil layer settlements of the improved ground, $L = 2B$, which were calculated by equations 4.1, 4.2, 4.3, whereas Figure 4.12 illustrates the settlement-time behaviour of the soil layers.

Table 4.19 Average layer settlements of the improved ground, $L = 2B$

Layer	Settlement (mm)
1	1.53
2	1.17
3	0.73

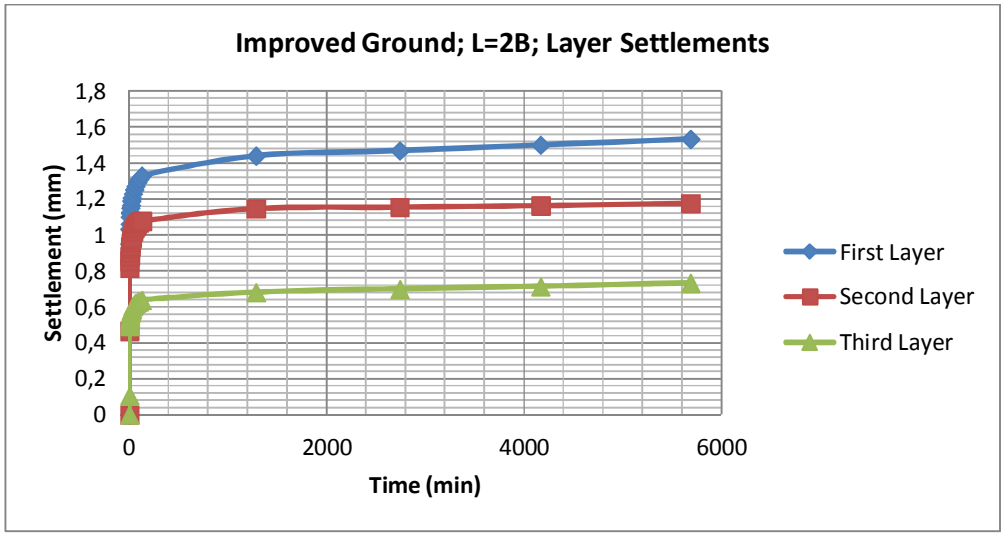

Figure 4.12 Improved ground; $L = 2B$; settlement-time graphs

4.6.4 Layer Settlements of the Improved Ground; End Bearing

Table 4.20 shows soil layer settlements of the improved ground, $L = 2.86B$ which were calculated by equations 4.1, 4.2, 4.3, whereas Figure 4.13 illustrates the settlement-time behaviour of the soil layers.

Table 4.20 Average layer settlements of the improved ground, end bearing stone column

Layer	Settlement (mm)
1	1.37
2	1.01
3	0.62

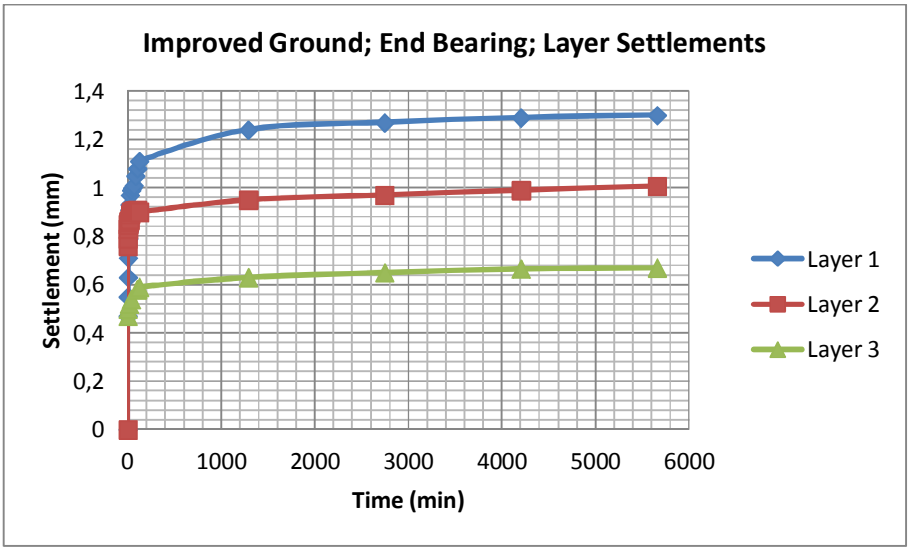

Figure 4.13 Improved ground; end bearing stone column; settlement-time graphs

Figure 4.14 summarizes the settlement profiles of individual layers.

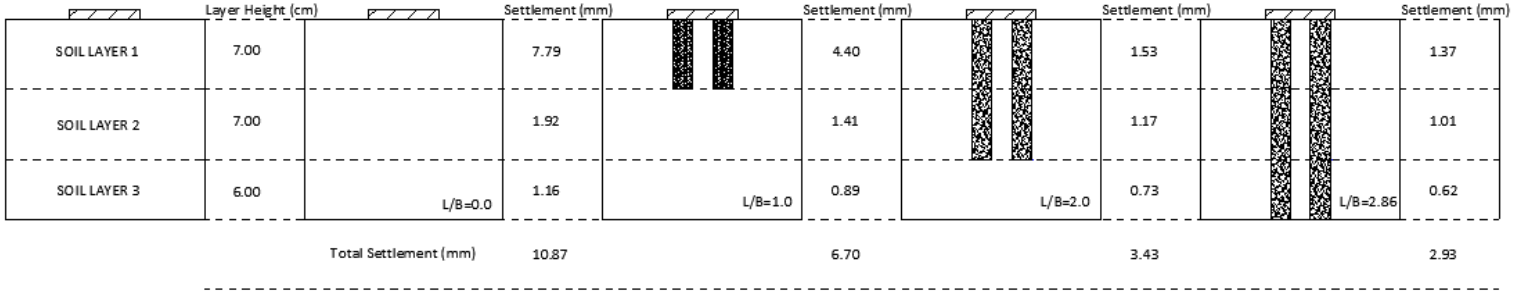

Figure 4.14 Settlement profiles of individual soil layers

CHAPTER 5

DISCUSSION OF RESULTS

5.1 Introduction

As mentioned before the only variable in model tests carried out was the stone column length (L). Tests were done with constant values of area replacement ratio, footing dimensions, relative density of granular material, stone column diameter, consolidation pressure and footing pressure. Behaviour of floating stone columns with two different lengths ($L = B$, and $L = 2B$) and end bearing stone columns $(L = 2.86\,B)$ were aimed to be determined. Unimproved soil tests were conducted to determine settlement reduction ratios (β) for comparison.

Table 5.1 represents dimensionless parameters used for comparison.

Table 5.1 Dimensionless parameters

L (cm)	$L_{treated}/L_{sample}$	L/D	L/B
0*	0.00	0.0	0.00
7	0.35	3.5	1.00
14	0.70	7.0	2.00
20**	1.00	10.0	2.86

**Unimproved soil, ** End bearing stone column*

Where;

L= Stone column length

B= Footing width

D= Stone column diameter

5.2 Column Lengths versus Settlements

Table 5.2 and Figure 5.1 show average settlement values obtained from improved soils and unimproved soils with different lengths of granular columns. As it is seen, as the length of the stone column increases total settlements decrease considerably. Similarly, this behaviour is also valid for subsurface settlements. As the column length increases both telltale 1 and telltale 2 settlements decrease. Depth-settlement curves of the reinforced soil and unimproved soil diverge from each other as going upwards in the interval of 0-7 cm (Figure 5.1), however corresponding curves of soil improved with $L = 2B$ columns, and soil improved with end bearing columns are almost parallel. For the depth interval of 7-14 cm $(B - 2B)$ all curves corresponding telltale settlements seem to be parallel to each other.

Variation of settlements normalized with footing width (δ/B) with respect to stone column lengths normalized with footing width (L/B) are tabulated in Table 5.3. As seen on Figure 5.2, as the L/B ratio increases, δ_t/B ratio decreases. However, for the L/B interval of 0.00-2.00, a linear decrease with a higher slope in the δ_t/B ratio takes place, whereas for the L/B interval 2.00-2.86 the slope seems to diminish. It can be concluded that increasing L/B ratio beyond 2.00, presents little improvement.

Table 5.2 Variation of settlements with respect to stone column lengths

L (cm)	Total Settlements (mm)	Telltale 1 Settlements at depth 7 cm (mm)	Telltale 2 Settlements at depth 14 cm (mm)
0	10.87	3.08	1.16
7	6.70	2.30	0.89
14	3.43	1.90	0.73
20	2.93	1.63	0.62

Table 5.3 Variation of settlements normalized with footing width with respect to stone column lengths normalized with footing width

L (cm)	L/B	Total Settlements (mm)	$(\delta_t/B) * 10^2$
0.00	0.00	10.87	15.53
7.00	1.00	6.70	9.57
14.00	2.00	3.43	4.90
20.00	2.86	2.93	4.18

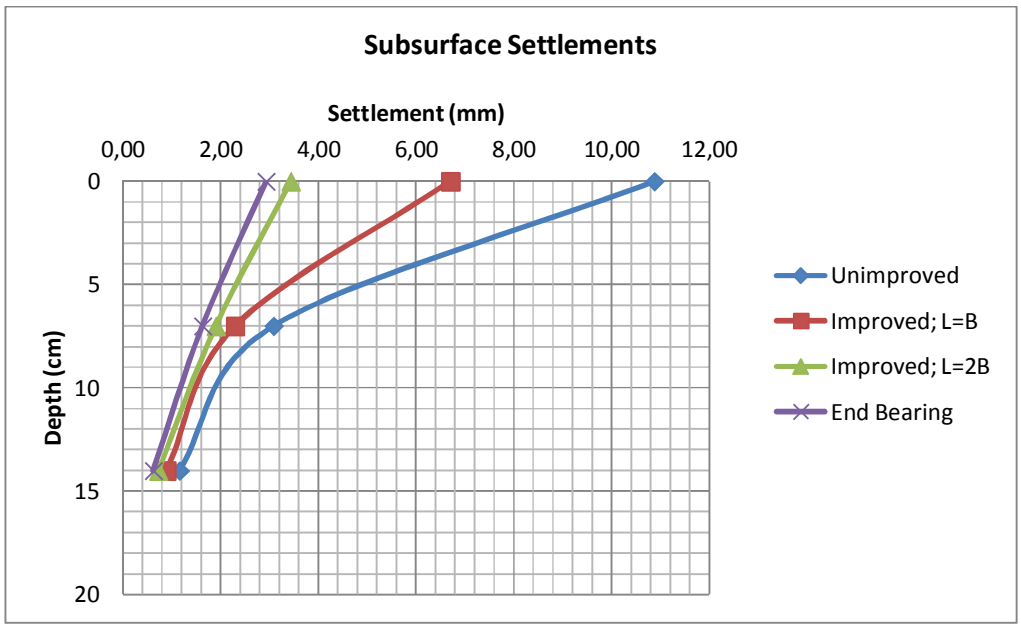

Figure 5.1 Subsurface settlements of the unimproved, improved; $L = B$, improved; $L = 2B$, improved; end bearing

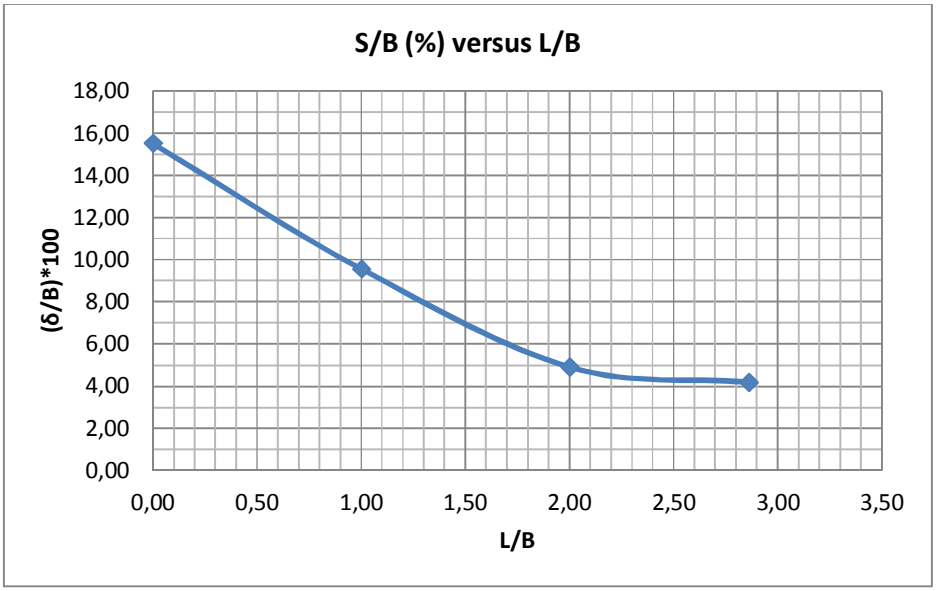

Figure 5.2 $\delta_t/B - L/B$ relation of model tests

5.3 Settlement Reduction Ratios (β)

As mentioned before settlement reduction ratio (β), which is widely used for improvement gradation can be described as the ratio of settlement of the improved ground to the settlement of the unimproved ground. For this purpose unimproved ground tests were performed.

$$\beta = \frac{\delta_t}{\delta_0} \tag{5.1}$$

Where:

β: Settlement reduction ratio

δ_t: Settlement of the composite ground (Stone column-soil)

δ_0: Settlement of the unimproved ground

5.3.1 Settlement Reduction Ratios (β) for Total Settlements

Table 5.4 summarizes average settlement reduction ratios of footing settlements for different column lengths. From Figure 5.3, it is evident that as normalized column length (L/B) increases, settlement reduction ratio decreases, which indicates better improvement. Similarly, for interval L/B=1.00-2.00, rate of decrease in the settlement reduction factor is apparently higher than that for the interval beyond the limiting value of L/B=2.00.

Table 5.4 Settlement reduction ratios (β) at footing level

L (cm)	$L_{treated}/L_{sample}$	L/D	L/B	Settlement Reduction Ratio (β)
7	0.35	3.5	1.00	0.62
14	0.70	7.0	2.00	0.32
20	1.00	10.0	2.86	0.27

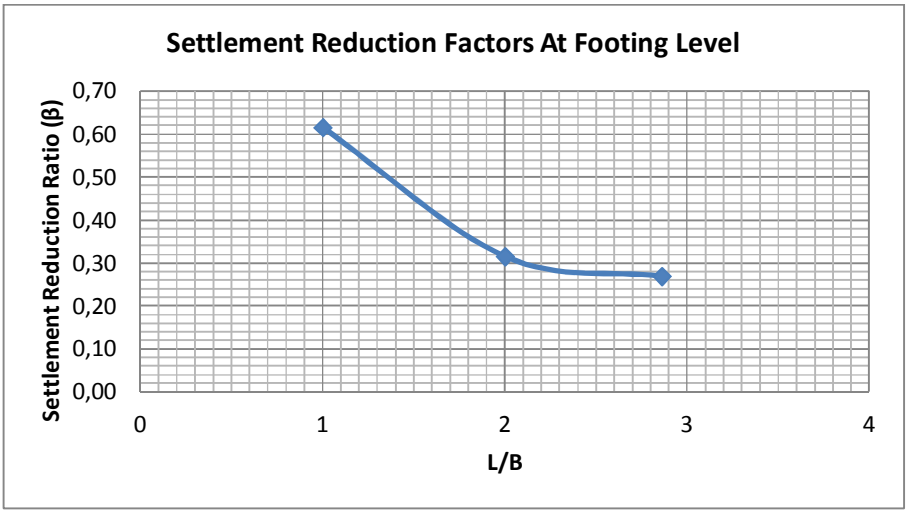

Figure 5.3 $\beta - L/B$ relationship of model tests

Figures 5.4 and 5.5 represent the settlement reduction ratio-normalized column length (L/D and L/B) relationships of different experimental studies. As seen on Figure 5.4, settlement reduction ratios are higher than the ones obtained by Akdoğan (2001) and Tekin (2005) with respect to column lengths normalized with footing width. In Figure 5.5 it is seen that settlement reduction ratios are again higher than the ones obtained by Tekin (2005), Black et. Al. (2011), however they are lower than the ones obtained by Akdoğan (2001). This diversity in ratios may arise from the variability of the parameters such as area

replacement ratio (a_s) and relative density of granular material (D_R), column spacing (s), the stress concentration ratio (n), number of columns beneath the footing, stiffness of the granular column, stiffness of surrounding soil and method of installation. Area replacement ratios of corresponding model studies are 22% for Tekin (2005) and 17% for Black et. Al. (2011). Moreover, Tekin (2005) used granular columns of 80% relative density.

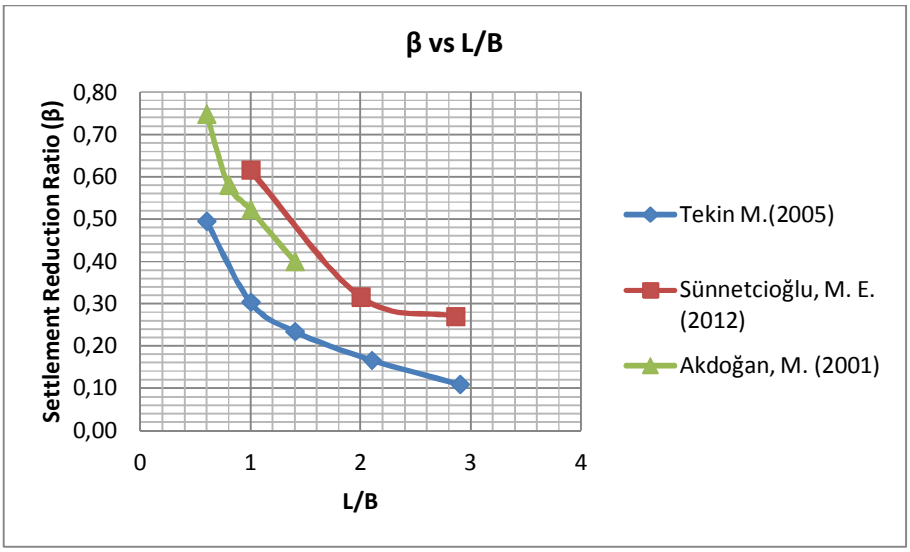

Figure 5.4 Comparison of settlement Reduction Ratio (β)- normalized stone column length (L/B) relationships in the literature

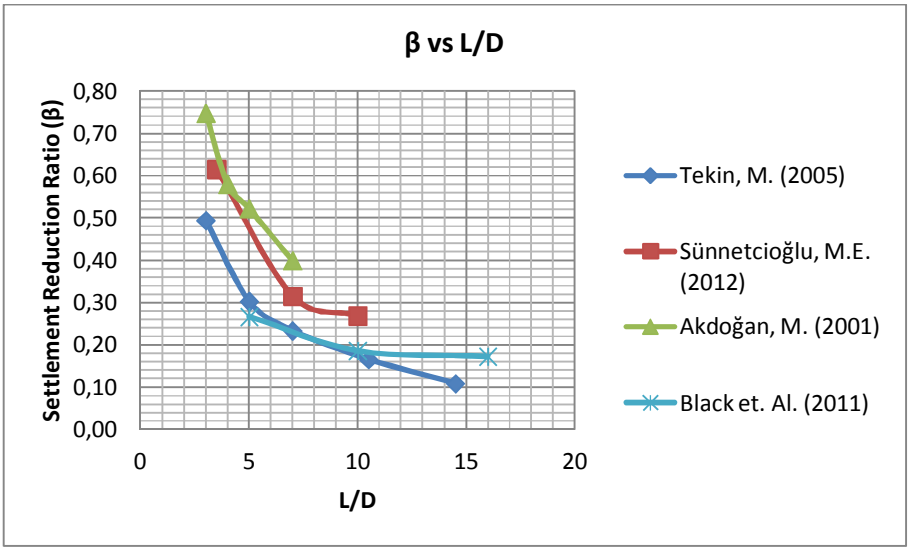

Figure 5.5 Comparison of settlement reduction ratio (β) - normalized stone column length (L/D) relationships in the literature

Table 5.5 and Figure 5.6 represents the settlement reduction ratios (β) obtained from model tests and literature for end bearing column improved ground. It is seen that the settlement reduction ratio obtained from this experimental study is lower than the ones obtained from the charts proposed by Priebe (1995) and Van Impe and De Beer (1983). In other words settlement improvement is underestimated.

Table 5.5 Settlement reduction ratios (β) obtained from model tests and literature for end bearing column improved ground

Setttlement Reduction Ratio (β)	Sünnetcioğlu (2012)	Priebe (1995)	Van Impe and De Beer (1983)
	0.27	0.38	0.54

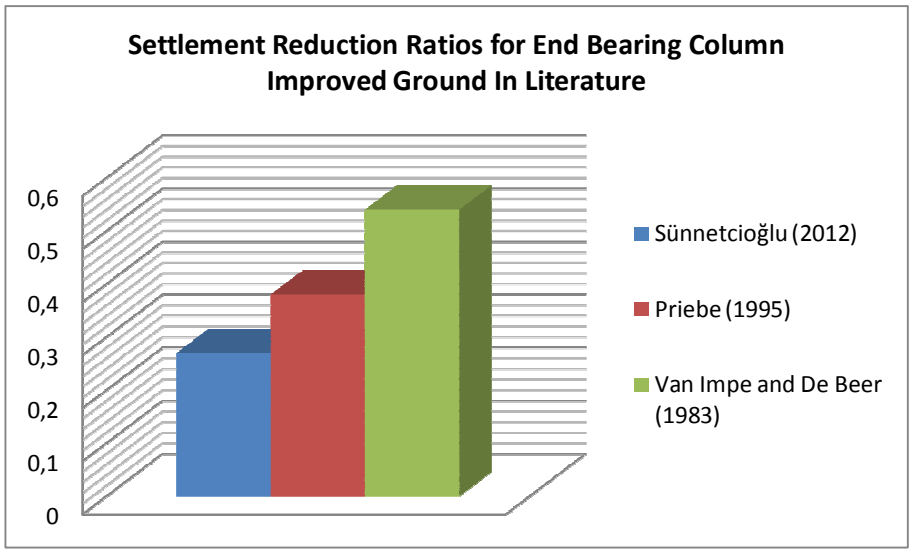

Figure 5.6 Settlement reduction ratios (β) obtained from model tests and literature for end bearing column improved ground

5.3.2 Settlement Reduction Ratios (β) Beneath the Surface

Table 5.6 and Figure 5.7 represent the variation of settlement reduction ratios with respect to depth. The reduction ratio values were calculated by the following formulations:

$$\beta_{7cm} = \frac{\delta_{telltale\ 1(improved)}}{\delta_{telltale\ 1(unimproved)}} \quad (5.2)$$

$$\beta_{14cm} = \frac{\delta_{telltale\ 2(improved)}}{\delta_{telltale\ 2(unimproved)}} \quad (5.3)$$

Where:

β_{7cm}: Settlement reduction ratio at depth 7cm

β_{14cm}: Settlement reduction ratio at depth 14cm

$\delta_{telltale\ 1(improved)}$: Telltale 1 settlement of the composite ground

$\delta_{telltale\ 1(unimproved)}$: Telltale 1 settlement of the unimproved ground

$\delta_{telltale\ 2(improved)}$: Telltale 2 settlement of the composite ground

$\delta_{telltale\ 2(unimproved)}$: Telltale 2 settlement of the unimproved ground

Figure 5.8 indicates that subsurface settlement reduction ratios decrease as the normalized column length (L/B) increases. There appears to be a slight reduction in the rate of decrease of settlement reduction ratios as the normalized column length is increased from L/B=2.00 to L/B= 2.86. It can be assumed that a linear decrease of settlement reduction ratio occurs as normalized column length increases from $L = B$ to $L = 2.86\,B$ at both depths B and $2B$. It is also noticeable from Figure 5.8 that, for the same normalized column length, subsurface settlement reduction ratios at depth B are slightly lower than those at depth $2B$.

Table 5.6 Settlement reduction ratios at depths 0, 7 cm (B), and 14 cm ($2B$)

Depth (cm)	Settlement Reduction Ratio (β)		
	$L = B$	$L = 2B$	End Bearing
0	0.62	0.32	0.27
7	0.74	0.62	0.53
14	0.77	0.63	0.54

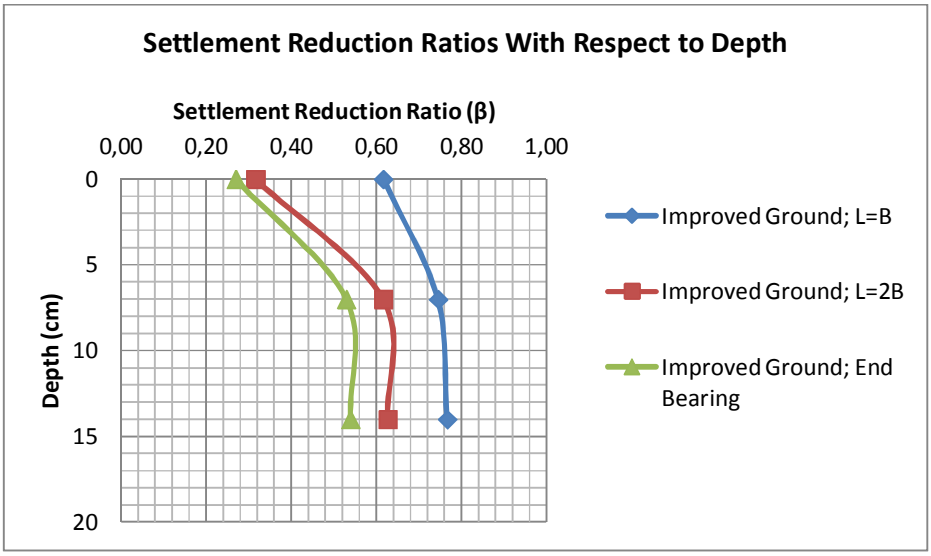

Figure 5.7 Settlement Reduction Ratio (β) - depth relationship

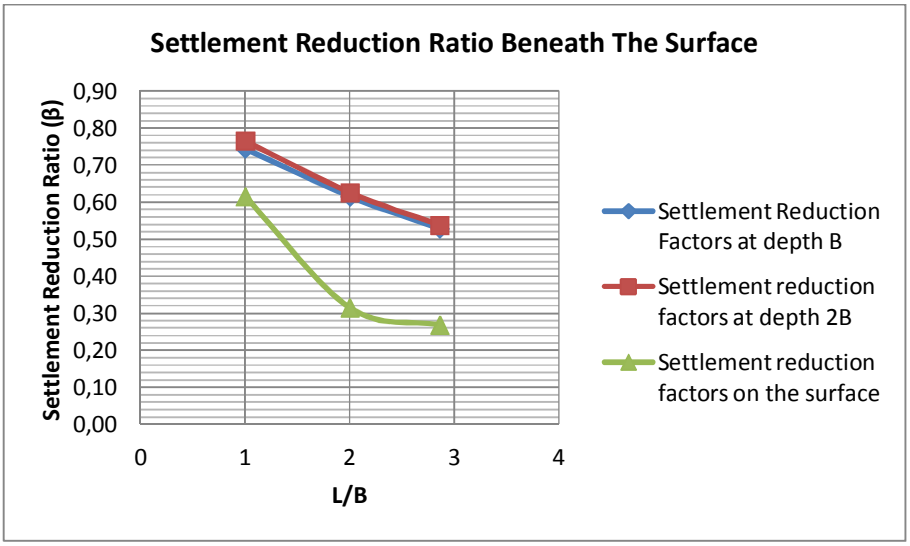

Figure 5.8 Subsurface settlement reduction ratio (β) - normalized column length (L/B) relationship

5.3.3 Settlement Reduction Ratios (β) for Individual Soil Layers

Settlement reduction factors for layers 1, 2, and 3 were calculated according to the aforementioned equations in section 4 (4.1, 4.2 & 4.3), and with the following equations:

$$\beta_{layer\ 1} = \delta_{layer\ 1(improved)}/\delta_{layer\ 1(unimproved)} \quad (5.4)$$

$$\beta_{layer\ 2} = \delta_{layer\ 2(improved)}/\delta_{layer\ 2(unimproved)} \quad (5.5)$$

$$\beta_{layer\ 2} = \delta_{layer\ 3(improved)}/\delta_{layer\ 3(unimproved)} \quad (5.6)$$

Where:

$\beta_{layer\ 1}$: Settlement reduction ratio of the first layer

$\beta_{layer\ 2}$: Settlement reduction ratio of the second layer

$\beta_{layer\ 3}$: Settlement reduction ratio of the third layer

$\delta_{layer\ 1(improved)}$: First layer settlement of the composite ground *(Calculated by the equation 4.1)*

$\delta_{layer\ 1(unimproved)}$: First layer settlement of the unimproved ground *(Calculated by the equation 4.1)*

$\delta_{layer\ 2(improved)}$: Second layer settlement of the composite ground *(Calculated by the equation 4.2)*

$\delta_{layer\ 2(unimproved)}$: Second layer settlement of the unimproved ground *(Calculated by the equation 4.2)*

$\delta_{layer\ 3(improved)}$: Third layer settlement of the composite ground *(Calculated by the equation 4.3)*

$\delta_{layer\ 3(unimproved)}$: Third layer settlement of the unimproved ground *(Calculated by the equation 4.3)*

Table 5.7, and Figure 5.9 illustrate the settlement reduction ratios of individual layers corresponding to the different normalized column lengths. It is evident that as the stone column length increases, the settlement reduction ratios decrease for all the three layers. As seen on Figure 5.9, rate of decrease of settlement reduction ratio for the interval L/B =1.00-2.00 is nearly the same for the second and third layers, whereas it is much higher for the first layer. However, for the interval L/B =2.00-2.86, rate of decrease is considerably lower

for the first layer, whereas for the second and third layers the rate of decrease in the settlement reduction ratios seems to slightly diminish. Also it is valid for all normalized column lengths that the settlement reduction ratio value is the highest in the first layer. The settlement reduction ratios for the same normalized column length don't seem to differ from each other for the second and the third layers.

Table 5.7 Settlement improvement factors for layers 1, 2, and 3

$L_{treated}/L_{sample}$	L/D	L/B	Settlement Reduction Ratio (β)		
			Layer 1	Layer 2	Layer 3
0.35	3.5	1.00	0.56	0.73	0.77
0.70	7.0	2.00	0.20	0.61	0.63
1.00	10.0	2.86	0.18	0.52	0.54

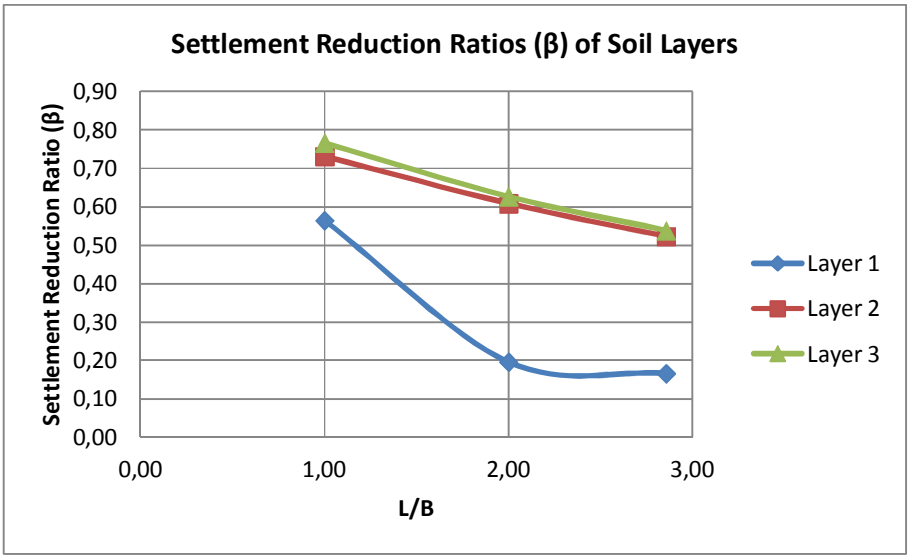

Figure 5.9 β- L/B relationships of layers 1, 2, and 3

5.4 Settlement and Settlement Reduction Ratio Comparison of the Treated and Untreated Zones of Floating Stone Columns

5.4.1 Settlement Comparison of Treated and Untreated Zones

In the experimental study conducted floating columns with two different lengths were examined ($L = B, \& L = 2B$). Tables 5.8-5.9 and Figure 5.10 represent the settlements in the treated and untreated zones. The corresponding settlement values were calculated by the following equations:

$$\delta_{treated\ (L=B)} = \delta_{layer\ 1\ (L=B)} \tag{5.7}$$

$$\delta_{treated\ (L=2B)} = \delta_{layer\ 1\ (L=2B)} + \delta_{layer\ 2(L=2B)} \tag{5.8}$$

$$\delta_{untreated\ (L=B)} = \delta_{layer\ 2\ (L=B)} + \delta_{layer\ 3\ (L=B)} \tag{5.9}$$

$$\delta_{untreated\ (L=2B)} = \delta_{layer\ 3\ (L=2B)} \tag{5.10}$$

Where:

$\delta_{treated\ (L=B)}$: Settlement of the treated zone of composite ground; L=B

$\delta_{treated\ (L=2B)}$: Settlement of the treated zone of composite ground; L=2B

$\delta_{untreated\ (L=B)}$: Settlement of the untreated zone of composite ground; L=B

$\delta_{untreated\ (L=2B)}$: Settlement of the untreated zone of composite ground; L=2B.

$\delta_{layer\ 1\ (L=B)}$: Settlement of the first layer of the composite ground; L=B

$\delta_{layer\ 2\ (L=B)}$: Settlement of the second layer of the composite ground; L=B

$\delta_{layer\ 3\ (L=B)}$: Settlement of the third layer of the composite ground; L=B

$\delta_{layer\ 1\ (L=2B)}$: Settlement of the first layer of the composite ground; L=2B

$\delta_{layer\ 2(L=2B)}$: Settlement of the second layer of the composite ground; L=2B

$\delta_{layer\ 3(L=2B)}$: Settlement of the third layer of the composite ground; L=2B

It is evident that as the normalized column length (L/B) increases both the normalized settlements (S/B) for the treated and untreated zones decrease. Settlements in the untreated layers are lower than those in the treated layers. However, for more healthy comparison, settlement reduction ratios should be examined (Figure 5.9).

Table 5.8 Normalized settlements for untreated layers of floating columns

L/B	$L_{treated}/L_{untreated}$	Untreated Layers	Settlement of The Untreated Zone (mm)	δ/B
1.00	0.50	Layer 2, Layer 3	2.30	0.33
2.00	2.33	Layer 3	0.73	0.10

Table 5.9 Normalized settlements for treated layers of floating columns

L/B	$L_{treated}/L_{untreated}$	Treated Layers	Settlement of The Treated Zone (mm)	δ/B
1.00	0.50	Layer 1	4.40	0.63
2.00	2.33	Layer 1, Layer 2	2.71	0.39

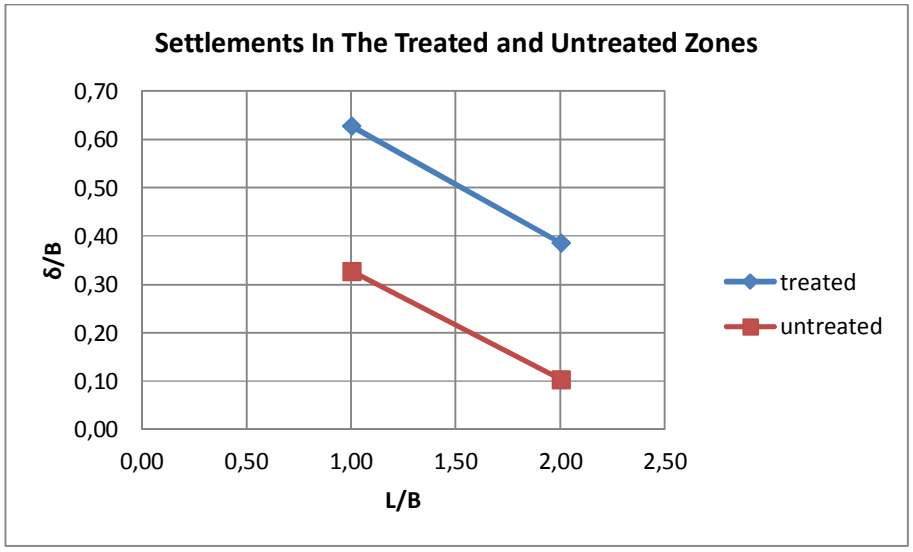

Figure 5.10 $(\delta/B)-(L/B)$ relationships of the treated and untreated zones

5.4.2 Settlement Reduction Ratio Comparison of Treated and Untreated Zones

Table 5.10 and Figure 5.11 represent the settlement reduction ratios of the treated and untreated zones for the floating type of stone columns. The corresponding settlement reduction ratios were calculated by the following equations:

$$\beta_{untreated(L=B)} = \frac{\delta_{layer\ 2(L=B)} + \delta_{layer\ 3(L=B)}}{\delta_{layer\ 2(unimproved)} + \delta_{layer\ 3(unimproved)}} \quad (5.11)$$

$$\beta_{untreated(L=2B)} = \frac{\delta_{layer\ 3(L=2B)}}{\delta_{layer\ 3(unimproved)}} \quad (5.12)$$

$$\beta_{treated(L=B)} = \frac{\delta_{layer\ 1(L=B)}}{\delta_{layer\ 1(unimproved)}} \quad (5.13)$$

$$\beta_{treated(L=2B)} = \frac{\delta_{layer\ 1(L=2B)} + \delta_{layer\ 2(L=2B)}}{\delta_{layer\ 1(unimproved)} + \delta_{layer\ 2(unimproved)}} \quad (5.14)$$

Where:

$\beta_{untreated(L=B)}$: Settlement reduction ratio of the untreated zone of the composite ground; $L = B$

$\beta_{untreated(L=2B)}$: Settlement reduction ratio of the untreated zone of the composite ground; $L = 2B$

$\beta_{treated(L=B)}$: Settlement reduction ratio of the treated zone of the composite ground; $L = B$

$\beta_{treated(L=2B)}$: Settlement reduction ratio of the treated zone of the composite ground; $L = 2B$

$\delta_{layer\ 1(unimproved)}$: First layer settlement of the unimproved ground

$\delta_{layer\ 2(unimproved)}$: Second layer settlement of the unimproved ground

$\delta_{layer\ 3(unimproved)}$: Second layer settlement of the unimproved ground

For both the treated and untreated zones settlement reduction ratios decrease as the normalized column length (L/B) increases (Figure 5.11). Rate of decrease in the settlement reduction ratio for the treated zone is considerably higher than that for the untreated zone. Moreover, for the same normalized column length (L/B), settlement reduction ratio is lower in the treated zone. Akdoğan (2001) states that the settlement reduction ratios along the column was found relatively smaller than the ones measured at the footing level, which is consistent within

this experimental study. Tekin (2005) also emphasizes that the settlement reduction ratios beneath the treated zone are similar to footing settlement reduction ratios, however this conflicts with the results in this study and, settlement reduction ratios of untreated zones are found to be considerably larger than the ones obtained at footing level. Factors responsible for this difference are mentioned in Section 5.3.1.

Figure 5.12 illustrates settlement profiles of treated and untreated zones for floating stone columns.

Table 5.10 Settlement reduction ratios of the treated and untreated zones

L/B	$L_{treated}/L_{untreated}$	$\beta_{untreated}$	$\beta_{treated}$	$\beta_{(total\ settlement)}$
1.00	0.50	0.74	0.56	0.62
2.00	2.33	0.63	0.28	0.32

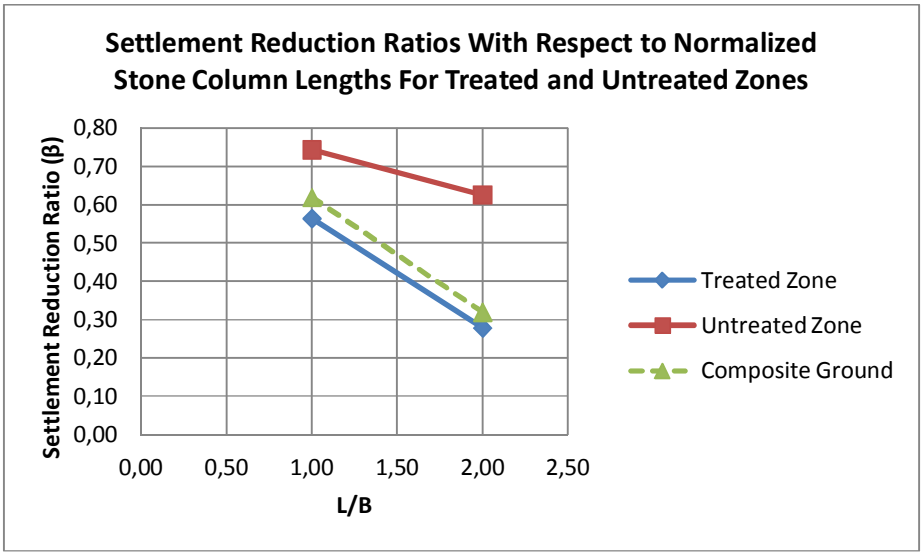

Figure 5.11 $\beta-(L/B)$ relationships of the treated and untreated zones

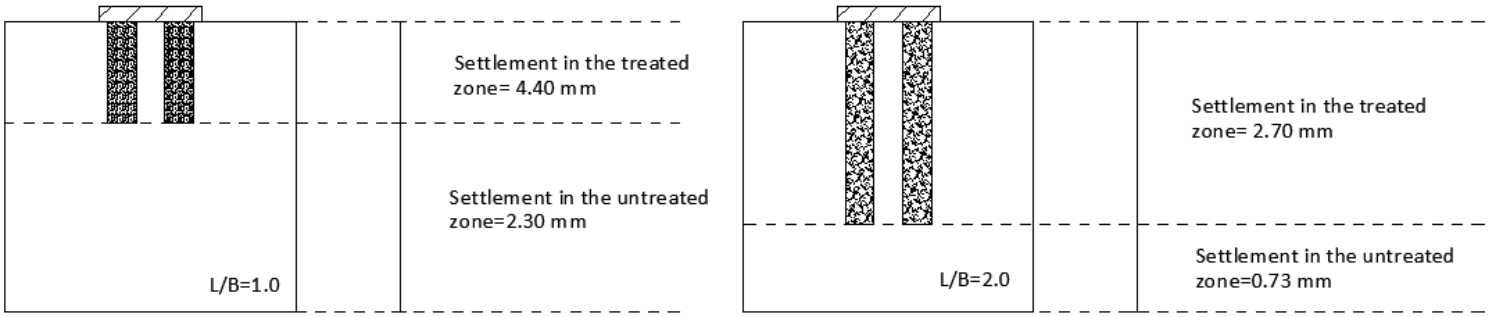

Figure 5.12 Settlement profiles of treated and untreated zones for floating stone columns; $L = B$, and $L = 2B$

5.5 Strain Mechanisms of Stone Columns

By the placement of two telltales for subsurface settlement determination, the strain behaviour of the three depth intervals can be examined. The strain values of each three depth intervals are tabulated in Table 5.11 and illustrated in Figure 5.13. Moreover, Figure 5.14 represents the strain – normalized stone column length (L/B) relationship. By the inspection of this figure, it can be seen that, as the normalized column length increases, strain decreases for all depth intervals. However for the 0-7cm $(0 - B)$ depth interval, for values smaller than the threshold value of L/B=2.00, the rate of decrease in strain values is much higher than the remaining two depth intervals. Beyond the threshold value of L/B=2.00 there exists a dramatic change in the slope. The curves corresponding to depth intervals of 7-14 cm $(B - 2B)$ and 14-20 cm $(2B - 2.86B)$ are nearly parallel, and the slope of the both curves decrease as the L/B ratio increases. However, Tekin (2005) states that the normalized column length, $L/B = 1.4$ may be a sufficient column length in settlement reduction, since the strains along the column decrease.

Table 5.11 Strain (%) values varying with depth

Depth Interval (cm)	Strain (%)			
	Unimproved	$L = B$	$L = 2B$	End Bearing
0-7	11.13	6.29	2.19	1.85
7-14	2.75	2.01	1.67	1.44
14-20	1.93	1.48	1.21	1.04

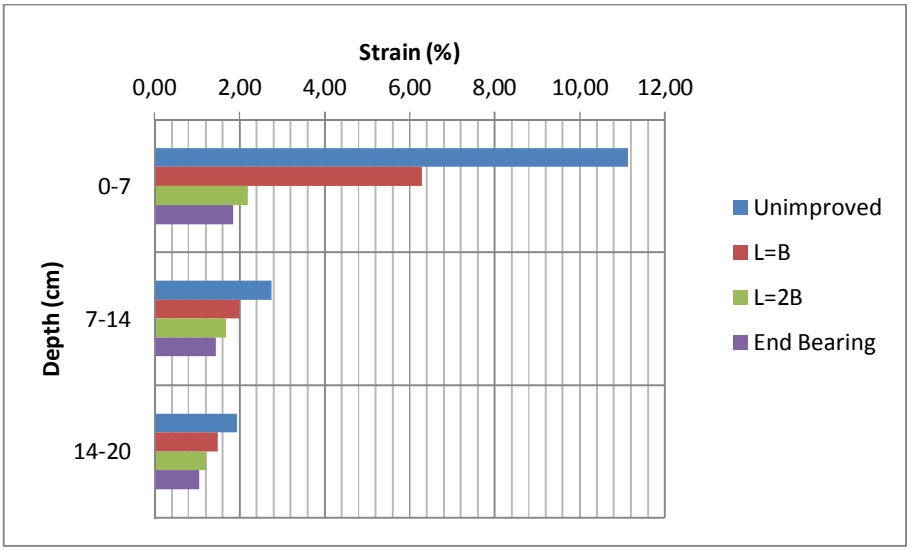

Figure 5.13 Depth interval – strain (%) relationship

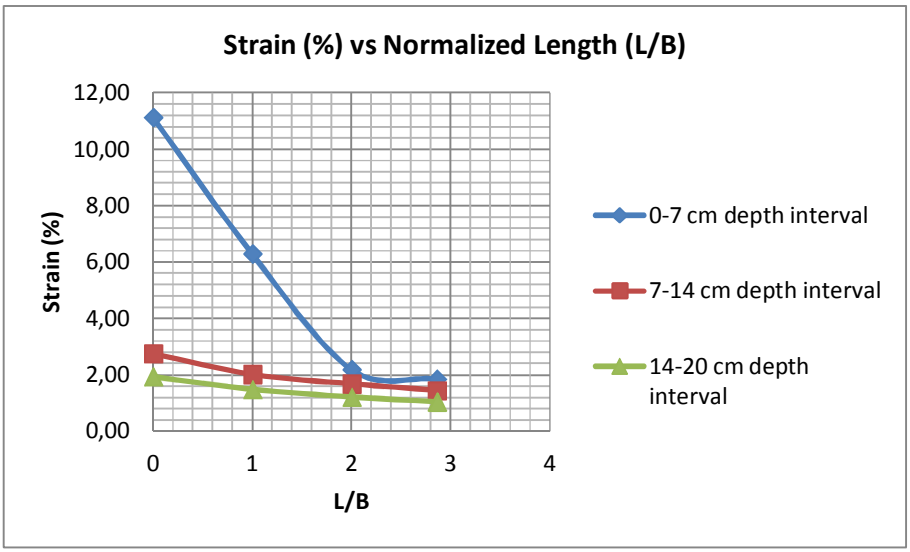

Figure 5.14 Strain (%)- normalized stone column length (L/B) relationship

CHAPTER 6

CONCLUSION

6.1 General

This experimental study conducted discusses the effect of stone column length on the settlement reduction of the footing lying on soft clay. For this purpose, the settlements of composite grounds reinforced with stone columns of lengths $L = B$, $L = 2B$, and $L = 2.86B$ (end bearing) were examined. In order to determine the settlement reduction effects of varying lengths of columns, unimproved soil tests were also conducted.

By the experimental studies conducted it is aimed to determine the effective length of stone columns which supplies significant settlement reduction. For this purpose, settlements at surface and subsurface were measured, and the corresponding settlement reduction ratios were determined both for surface and subsurface. By the placement of telltales at depths equal to B, and $2B$, the soil under the footing was considered to be divided to three layers. The settlement reduction ratios for these individual layers were also calculated for the determination of subsoil improvement effects of the variable column lengths. Similarly, the strains along the depth of the composite and unimproved soil were examined.

6.2 Influence of Stone Column Length on Total Settlement

By the assessment of the results acquired, it is apparent that the settlement reduction ratio decreases as the length of the column increases.

A considerable reduction of settlement is obtained at footing level by lengthening the column from $L = B$ to $L = 2B$. However, the rate of decrease of the settlement reduction ratio is significantly decreased when the column length is increased from $L = 2B$ to $L = 2.86B$ (end bearing), which implies that there appears to be a threshold value of normalized column length, $L = 2B$ for settlement reduction effect of total settlement.

6.3 Influence of Column Length on Subsurface Settlements

The evaluation of subsurface settlement reduction ratios indicates that as the normalized column length (L/B) increases subsurface settlement reduction ratio decreases. Rate of decrease of subsurface settlement reduction ratio slightly diminishes with increasing the column length from $L = 2B$ to $L = 2.86B$ (end bearing) at depths B and $2B$. Thus, one can assume that the slope between normalized column lengths $L = B$ and $L = 2.86B$ to be constant. Another remarkable point is that subsurface reduction ratios at depth B is slightly smaller than those at depth $2B$ for column lengths of $L = B$, $L = 2B$, and $L = 2.86B$.

6.4 Influence of Column Length on Settlements of Individual Layers

Similar to the footing settlement behaviour, as the column length increases, settlement reduction ratios decrease. However, first layer demonstrates altering

behaviour when the normalized column length value is lower and higher than $L/B = 2.00$. For values higher than the threshold normalized length of $L/B = 2.00$, the first layer exhibits smaller improvement. In other words rate of decrease of settlement reduction ratio considerably decreases for the interval between $L = 2B$ and $L = 2.86B$ (end bearing). Conversely, second and third layers demonstrates nearly constant rate of decrease between values $L/B = 1.00$ and $L/B = 2.86$. Moreover, there appears to be a minor difference between the settlement reduction ratios of the second and third layers.

6.5 Influence of Column Length on the Treated and Untreated Zones

By the inspection of the settlement reduction ratios in the treated and untreated zones, it is found out that the rate of decrease of settlement reduction ratio with respect to normalized column length of the treated zone, is significantly higher than that of the untreated zone. In other words, increasing the column length from $L = B$ to $L = 2B$ leads to better improvement in the treated zone than in the untreated zone.

Composite ground settlement reduction ratios (settlement reduction ratios of the footing settlements) lie between the settlement reduction ratios of the treated and untreated zone which are higher than the ones in the treated zone, and lower than the ones in the untreated zone.

6.6 Influence of Column Length on Strain Mechanisms of Stone Columns

By the evaluation of the results obtained, it is seen that even for the normalized column length $L/B = 1.00$, strain values under the treated zone decrease. However, there again exists a threshold value of $L/B = 2.00$ for the strain mechanism of 0-7 cm $(0 - B)$ depth interval. By increasing the length from $L/B = 1.00$ to $L/B = 2.00$, the strain values diminish significantly for the 0-7cm $(0 - B)$ depth interval. The normalized column length, $L/B = 1.00$ also demonstrates considerable improvement in the first zone. However, for normalized column length values greater than the threshold value of $L/B = 2.00$, the rate of decrease of the strain values significantly diminishes. On the other hand, increasing the normalized column lengths from $L/B = 0$ to $L/B = 2.86$ demonstrates relatively smaller strain improvement in 7-14 cm and 14-20 cm depth intervals.

6.7 Future Research

Further experimental test series and/or 3-D finite element analysis should be conducted in order to estimate the effects of the area replacement ratio, column spacing, number of columns, relative density of granular material on the settlement reduction ratio. A more detailed subsurface settlement measurement program is recommended. It would be better to perform another test series to estimate stress concentration factors of floating columns with varying column lengths.

BIBLIOGRAPHY

ABOSHI, H., ICHIMOTO, E., ENOKI, M., HARADA, K. (1979). The Compozer-a Method to Improve Characteristics of Soft Clays by Inclusion of Large Diameter Sand Columns. Proceedings *of International Conference on Soil Reinforcement.* Reinforced Earth and Other Techniques, Paris Vol.1, pp.211-216

AKDOĞAN, M. (2005). Settlement Behaviour of a Model Footing on Floating Sand Columns , *P.H.D. Thesis in Civil Engineering*, METU, TURKEY

AMBILIY, P.A., GANDHI, R.S. (2004). Experimental and Theoretical Evaluation of Stone Column in Soft Clay. *International Conference on Geosynthetics and Geo-environmental Engineering*. ICGGE-2004 held at IIT Bombay during December 2004. pp 201-206

AMBILIY, P.A., GANDHI, R.S. (2007). Behavior of Stone Columns Based on Experimental and FEM Analysis. *Journal of Geotechnical and Geoenvironmental Engineering*. ASCE, Vol.133. No. 4, pp.405-415

BALAAM, N.P., BOOKER, J.R. (1981). Analysis of Rigid Rafts Supported by Granular Piles. *International Journal of Numerical and Analysis Methods in Geomechanics*. Vol 5, pp. 379-403

BARKSDALE R. D., BACHUS R.C. (1983). Design and Construction of Stone Columns. *Federal Highway Administration Technical Report*, School of Civil Engineering Georgia Institute of Technology. Vol.1

BERGADO, D.T., RANTUCCI, G., WIDODO, S. (1984). Full Scale Load Test of Granular Piles and Sand Drains in the Soft Bangkok Clay. *Proceedings of the International Conference on " In-Situ Soil and Rock Reinforcement"*. Paris. pp. 111-118

BERGADO, D.T., ALFARO, M.C., CHAI, J.C. (1991). The Granular Pile: Its Present State and Future Prospects for Improvement of Soft Bangkok Clay. *Journal of South Asian Society of Soil Engineering. Geotechnical Engineering*. Vol. 22. pp. 143-171

BLACK J.A., SIVAKUMAR V. & BELL A. (2011). The settlement performance of stone column foundations, *Géotechnique*, 61(11), 909-922.

CHRISTOULAS, S. S., BOUCKOVALAS, G. G., & GIANNAROS, C. C. (2000). An Experimental Study on Model Stone Columns. *Soils And Foundations -Tokyo-, 4011-22*.

CRAIG, W. H., AL-KHAFAJI, Z.A., 1997. Reduction of Soft Clay Settlement by Compacted Sand Columns. *Ground Improvement*. *Geosystems Densification and Reinforcement*. *Proceedings of 3rd International Conference on Ground Improvement Geosystems*, Thomas Telford Publication. London, pp. 218-224

DATYE, K. R. (1982). Settlement and Bearing Capacity of Foundation System with Stone Columns. *Symposium on Recent Developments in Ground Improvement Techniques,* 29 Nov- 3 Dec. Bangkok, pp. 85-103

GOUGHNOUR, R.R. (1983). Settlement of Vertically Loaded Stone Columns in Soft Ground. *Proceedings of 8th ECSMFE*. Helsinki, Vol.1, pp. 235-240

GREENWOOD, D.A. (1970). Mechanical Improvement of Soils Below Ground Surface. *Proceedings of the Conference on Ground Engineering.* London, ICE

JURAN, I., RICCOBONO, O. (1991). Reinforcing Soft Soils With Artificially Cemented Compacted –Sand Column. ASCE, *Journal of Geotechnical Engineering Division*. Vol. 117, pp. 1042-1060

MALARVIZHI S.N. & ILAMPARUTHI K. (2004). Load versus Settlement of Claybed stabilized with Stone & Reinforced Stone Columns. *Proceedings of the 3rd Asian Regional Conference on Geosynthetics*, GEOASIA. Seoul, Korea. pp. 322-329

MATTES, N.S., POULOS, H.G. (1969). Settlement of a Single Compressible Pile. *ASCE Journal of Soil Mechanics and Foundations Division*, S.M.1, January, pp. 189-207

MCKELVEY, D. D., SIVAKUMAR, V. V., Bell, A. A., & Graham, J. J. (2004). Modelling vibrated stone columns in soft clay. *Geotechnical Engineering*, 157(3), 137-149.

MOSELEY M. P. & KIRSCH K. (2004). Ground Improvement. New York: Spon Press

MUNFAKH, G. A., ABRAMSON, L. W., BARKSDALE, R. D., JURAN, I. (1987). In-Situ Ground Reinforcement. *Conference Proceeding of Soil Improvement- A Ten Year Update*. ASCE Special Publication No:12, pp. 1-15

PRIEBE, H.J. (1993). Design Criteria for Ground Improvement by Stone Columns. *4th National Conference*. *Ground Improvement*. January 18-19. Lahore. Pakistan

PRIEBE, H.J. (1995). "The Design of Vibro-replacement", *Ground Engineering*. Vol. 28, No. 10

PRIEBE, H.J. (2005). Design of Vibro Replacement, The Application of Priebe's Method to Extremely Soft Soils , Floating Foundations and Proof Against Slope or Embankment Failure. *Ground Engineering*.

SHAHU, J.T., MADHAV, M.R., HAYASHI S. (2000). Analysis of Soft Ground-Granular Pile-Granular Mat System. *Computers and Geotechnics*. 27, pp 45-62.

SHAHU, J. T., & REDDY, Y. R. (2011). Clayey Soil Reinforced with Stone Column Group: Model Tests and Analyses. *Journal Of Geotechnical & Geoenvironmental Engineering*. 137(12), pp. 1265-1274.

TEKIN M., 2005. Model Study on Settlement Behavior of Granular Columns Under Compression Loading, *P.H.D. Thesis in Civil Engineering*, METU, Ankara, Turkey

VAN IMPE W.F. (1989). Soil Improvement Techniques and Their Evolution. Rotterdam: A. A. Balkema.

VAN IMPE W. F., DE BEER E. (1983). Improvement of Settlement Behavior of Soft Layers by means of Stone Columns. *Proceedings of 8th European Conference on Soil Mechanics and Foundation Engineering*. Helsinki, pp. 309-312

WOOD, D. M., HU, W. & NASH, D. F. T. (2000). Group effects In Stone Column Foundations: Model Tests. *Geotechnique* 50, No. 6, 689–698